

# CLEVER – A THREE WHEEL VEHICLE WITH A PASSIVE SAFETY COMPARABLE TO CONVENTIONAL CARS

**Lars Hollmotz**

**Steffen Sohr**

TAKATA-PETRI Aschaffenburg/Berlin/Ulm

Germany

**Heiko Johannsen**

Technical University Berlin

Germany

Paper Number 05-0160

## ABSTRACT

The alternative vehicle called CLEVER (Compact Low Emission Vehicle for Urban Transport) is conceived as a small, three-wheel vehicle with minimal demands on urban space, both in terms of traffic and parking. Furthermore, energy consumption, exhaust and noise emissions are low. CLEVER is funded by the European Commission with the Growth Programme of the Fifth Framework Programme.

The CLEVER project task is to find solutions for the challenge of increasing mobility by developing a new type of a small vehicle, which could be an alternative to traditional cars.

As a result, a vehicle was designed that is classified as a three-wheeler, according to European Union directive 2002/24/EC (class of motorcycles).

The main characteristics are:

- three-wheel vehicle for two occupants with a tilting, enclosed body
- dimensions: length 3.0 m; width 1.0 m; height 1.4 m
- use of a natural gas engine
- energy storage by using specially designed removable gas cylinders

Furthermore, the requirements define that passive safety standards must be comparable to the safety level of conventional cars. In addition, the CLEVER vehicle has to meet all relevant European legal requirements.

In order to meet these requirements, the vehicle's frame structure must be very stiff and a special restraint system had to be designed. The restraint system consists of state-of-the-art components and specially designed components, which are adapted to CLEVER's requirements.

This paper includes a description of the CLEVER safety concept, i.e. of the components' character-

istics, as well as information concerning the results generated by the numerical simulation.

## INTRODUCTION

With the constantly increasing need for mobility, particularly in urban areas, various problems arise including the urban space and energy consumption. In addition, exhaust and noise emissions have to be mentioned. In order to be able to satisfy the mobility needs in the future, new solutions are required. Therefore, it is necessary to develop new concepts for individual urban transport to close the gap between conventional individual transport and public transport. Due to the increasing readiness of customers to buy a second or third vehicle, there will be a market for new, innovative vehicles for urban transport.

The project aims at improving urban transport, whilst minimising of negative environmental impacts caused by increased mobility. Within the CLEVER project, various requirements are recognised (e.g. customer requirements, environmental requirements, safety requirements etc.).

Different European companies and research institutes (e.g. BMW, TAKATA-PETRI, Technical University Berlin) are working together to meet the requirements.

Goal of the CLEVER project is to identify general conditions for new mobility concepts, and to realise a vehicle with the following characteristics:

- three-wheel vehicle with minimal requirements on urban space (for 2 occupants)
- environmental friendly, optimised for urban transport
- length = 3.0 m, width = 1.0 m
- natural gas engine
- tilting mechanism

- aluminium Frame
- CO<sub>2</sub> – emissions approx. 50 – 60 g/km in the European car driving cycle
- high level on passive safety comparable to small and micro-cars (checked by a rating-test)



Figure 1. The CLEVER vehicle.



Figure 2. Pictures of a 1:4 model of the CLEVER vehicle.

To meet the defined goals for the safety, the vehicle structure and the restraint system have to be designed and optimised in a special way. TAKATA, as the project partner responsible for the restraint system, will use optimised state-of-the-art components, as well as specially designed components concerning to the occupant body regions, which have a higher injury risk. These body regions were figured out by the accident analysis.

## CLEVER ACCIDENT ANALYSIS

The following accident analysis is based on data from the German Federal Accident Statistics (GFAS), the German In-Depth Accident Study (GIDAS) and the National Accident Sampling System (NASS).

### Statistic analysis in general

In general, the reporting period was from July 1999 to April 2004 for GIDAS and GFAS. The NASS data analysis describes the statistic period from 1996 to 2002. Additionally, for the period of time between 1985 and 1995, data of 1029 motorcycle accidents and 89 scooter accidents are available.

Because of the special design, the same accident situation as for scooters and motorcycles can be assumed for CLEVER. The driving performance and the application areas, which are mostly cities, is mostly similar with scooters and motorcycles.

Because of the fact that for CLEVER a restraint system will be used, which is comparable with state-of-the-art restraint systems for cars, the occupant kinematics during accidents and the injured body regions could be more similar to car accidents than to scooter or motorcycle accidents.

That is why, different accident data (for cars, motorcycles and scooters) were analysed.

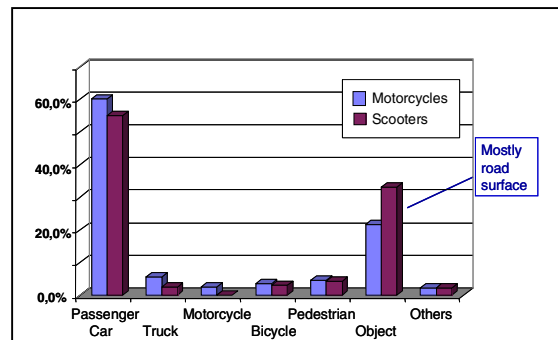
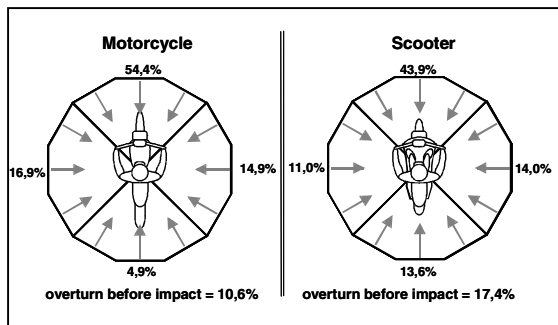


Figure 3. Collision opponents for motorcycles and scooters. [1]

Figure 3 shows the collision opponents of motorcycles and scooters. The main opponents are passenger cars, followed by the collisions of two wheelers with objects, mostly the road surface.



**Figure 4. Directions of impact for motorcycles and scooters. [1]**

The main impact directions for motorcycles and scooters are the frontal directions (figure 4), followed by side impact and overturn. Similar impact directions can be assumed for CLEVER because of similar vehicle width.

#### Accident analysis for the driver

The following figure shows the body regions, which are affected in accidents with a two wheel vehicle.

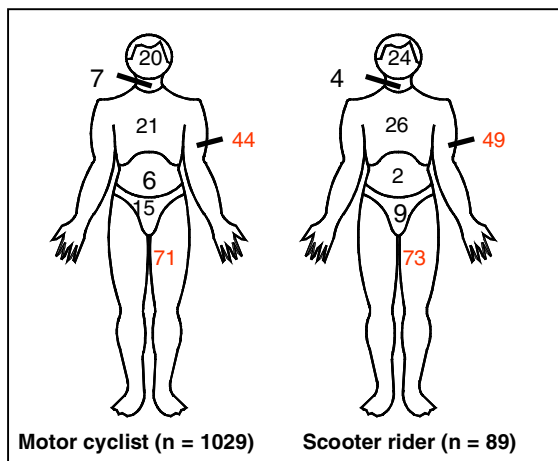


**Figure 5. Affected body regions of persons involved in two-wheel vehicle accidents. [1]**

As result, the body regions (most injured) are arms and legs. The most fatal or severe injuries result from head injuries, followed by thorax injuries. It has to be stated that in 95 % of all cases, helmets were used.

These data only show the figures for riders, due to the fact that the figures for passengers are extremely low.

The closing speed in accidents is far lower for scooters than for motorcycles. More than 95 % of all registered accidents are covered with a closing speed of 50 kph (figure 6). In addition, the closing speed of accidents with the “Smart” (built by DaimlerChrysler for the European market) was figured out and evaluated. These data are also

available in the GIDAS database. This closing speed is nearly similar to the closing speed of scooters. The low number of 28 reported accidents with an involved “Smart” is not very representative. But it gives an idea about the tendency for small and micro car accidents.

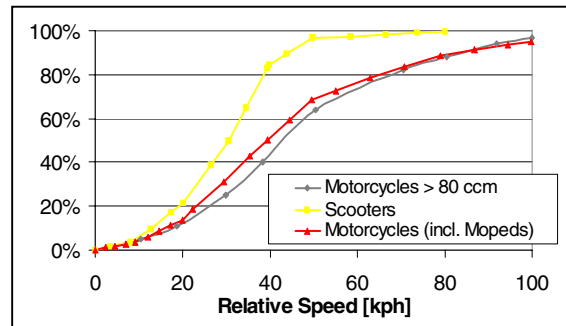


**Figure 6. Accident closing speed of two-wheelers. [1]**

The concept of the BMW C1, a two-wheel vehicle equipped with seat belts, load limiter and energy absorbing elements, is partly similar to the CEVER concept. In several EU member states, it is allowed to drive the C1 without wearing a helmet.

The main results of accident analysis by BMW are illustrated with two examples, which describe the real world accident performance of the C1.



**Figure 7: The BMW C1. [2]**

In frontal collision with a velocity of about 50 kph of the C1, and approximately 20 kph of the collision opponent (car), the belted driver (without helmet protection) had a AIS 1 injury-severity. Furthermore, a few injuries like cuts and contusions at the upper and lower extremities were reported.

In a side collision between a C1 and a middle class car, the belted C1 driver had lacerations and contusions of his left leg and abrasions at his left forearm and hand.

These results should be typical for the C1 accident situation taking account to the low number of reported accidents. [2]

It seems that the most endangered body parts of the C1 driver are the extremities.

### Passenger statistic analysis

In order to determine the most affected body regions of passengers, a statistic analysis of the accidents with car occupants in the second or third row will be used. The database for this analysis includes traffic fatalities, sampled by GIDAS and NASS.

The GIDAS database gives the information that for a number of 347 traffic fatalities, 195 of the occupants were car passengers. Out of these 195 passengers, 22 did not use the first row and 12 of them were seated in the second row during a frontal crash.

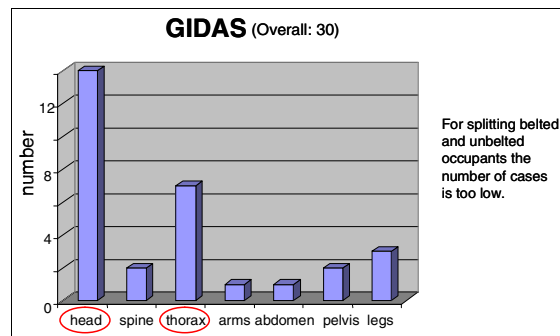


Figure 8. Passenger injured body regions from the database GIDAS. [3]

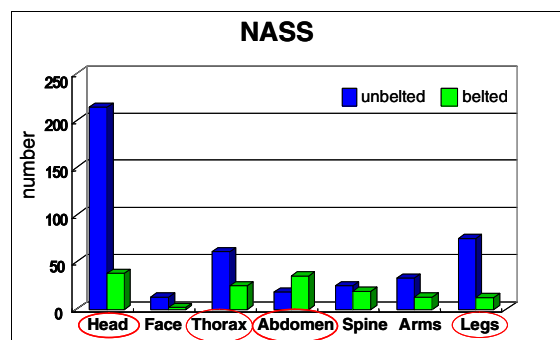


Figure 9. Passenger injured body regions from the database NASS. [4]

These figures show that the most affected body regions with AIS3+ injuries are the head and thorax of passengers. This applies to Europe as well as to the US.

Other results of the investigation for passengers are that the occupant position is quite regular. The closing speed for these accidents is between 20 kph and 60 kph.

The reasons for the accidents were mostly DWI (driving while intoxicated) and speed. About 50 %

of the accidents occur without involving other road users.

### Result of the accident investigation

As result of this accident investigation, the following scenarios must be in the centre of frontal restraint system development.

Main collision opponents will be conventional cars. The main impact type will be frontal impact. Another important accident type is single collision by hitting an object.

As to the injuries regarding body regions, the frequency of head, thorax and pelvis injuries can be reduced significantly by use of conventional restraint systems.

The open passenger compartment of the BMW C1 does not give enough protection for the upper and lower extremities of the occupants. The absolute number could be reduced, compared to the injury figures for the upper and lower extremities for riders of two-wheelers.

### CLEVER SAFETY REQUIREMENTS

The main safety requirements for the CLEVER vehicle are listed below:

- Meeting all legal requirements
- No obligation to wear a helmet (similar to the BMW C1)
- High level of passive safety comparable to the level of conventional cars

### Legal Requirements

For a three-wheel vehicle like CLEVER, no legal requirements exist concerning passive safety for the approval of motorcycles. To attain an operating license, the European regulation 97/24/EG has to be met. This regulation specifies constructive characteristics of vehicle parts, windshields and the seat belts with their connections to the vehicle, if included.

The obligation to use crash helmets is compulsory (in European countries) for riders and passengers of motorcycles without a full-lining. However, different exemptions exist in EU member states.

For Germany, exemptions are defined by the vehicle type approval or by legislation, like the C1. For example, the German law allows for two-wheel vehicles to be ridden without wearing a helmet, if the following requirements are fulfilled:

- The belt system must be state of the art and comply with Directive 97/24/EC.

- A light signal for a clear warning, if the rider is not wearing a belt, is required, as per Directive 78/316/EEC.
- The requirements for windows must be fulfilled, amongst others the minimum radii have to be complied with European Union Directive 97/24/EC.
- Crash tests against a motorcar have to be performed (according to ISO 13232, which defines relevant impact scenarios for two-wheelers) – the values for the HPC criterion have to be lower than 1000
- Lateral fall tests without head contact to the road surface and roof indentation tests (FMVSS 216) have to be fulfilled.

On the basis of this directive, the exemption to wear a helmet applies to other European countries. [2]

### **Additional safety requirements for CLEVER**

However, to meet the requirements for accepting CLEVER for the ACEA CO<sub>2</sub>-Agreement [5], the vehicle “should demonstrate passive and active safety appropriated to it’s intent to use”. To be able to assess these requirements, the CLEVER consortium defined a test procedure called “CLEVER-CAP”. This procedure should allow comparing the passive safety level of CLEVER to conventional cars. Therefore, it is reasonable to use similar or nearly similar test procedures as in consumer rating programmes.

The most important consumer test for Europe is the EuroNCAP, while the US-NCAP is the state-of-the-art consumer test for the United States. CLEVER is mainly designed to cope with European requirements. Therefore, the EuroNCAP test procedure should be favoured.

However, due special design properties of CLEVER, it does not seem to be realistic to follow the test procedure completely.

### **Frontal Impact**

EuroNCAP defined a 40%-offset crash configuration against a deformable barrier for the frontal impact test. Because of the shape and width of the CLEVER vehicle, an offset crash seems not to be a suitable test to simulate real-world accidents. Data analysis revealed that frontal impacts were the main type of impacts for motorcycles. In addition, it is nearly impossible to conduct a 40%-offset crash with CLEVER, because 40 % of the front structure width is about 100 mm and the vehicle width is increasing from front to rear. Vehicle motions following a crash would not take place in a reproducible manner.

As a result of these conditions, a crash test configuration with impacting a rigid wall without an offset barrier is usable and should give a realistic output concerning to the anticipated accident situation.

For frontal impact, the test configuration of the US-NCAP is useful. This means a frontal impact with 56 kph against the rigid wall. For comparing the CLEVER safety level with the safety level of European conventional cars, the EuroNCAP Star-rating is used.

In addition, chest acceleration will be measured. This allows a verification of the test results according to the US-NCAP rating. It seems possible to meet US-NCAP rating without major problems.

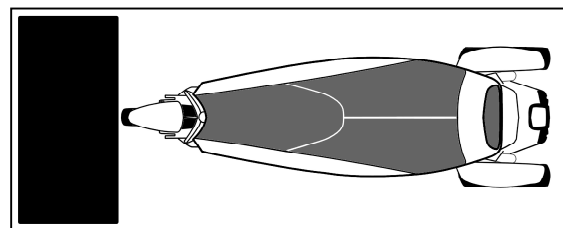


**Figure 10. CLEVER frontal test configuration. [1]**

This paper focuses mainly on the frontal impact, because this configuration was the most challenging one.

### **Side Impact**

For lateral impact testing, the EuroNCAP is the most suitable test procedure. Therefore, this procedure is selected for CLEVER.

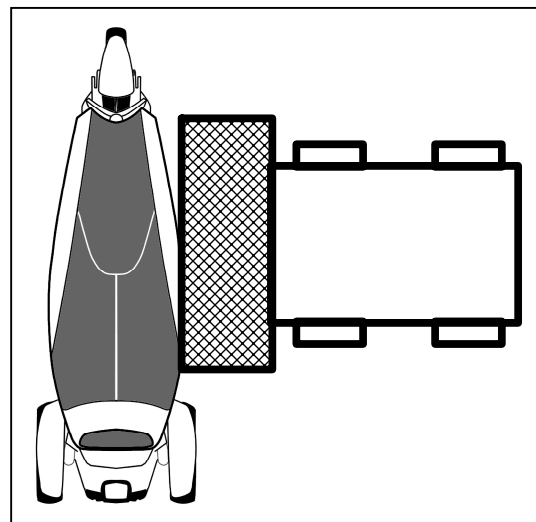


**Figure 11. CLEVER side test configuration. [1]**

### **Roll-over**

For CLEVER, the impact after an overturn is likely the most realistic scenario for the roll-over impact.

The safety cell will be tested by a static structure test procedure. The safety cell should resist a static force impact of about 22,2 kN.

### Pedestrian Safety

The pedestrian safety level of the CLEVER vehicle will be checked by numerical simulation. Frontal impact to pedestrians with a velocity of 40 kph will be simulated. The assessment of criteria will comprise the mechanical loads to head, neck, and legs.

## **CLEVER VEHICLE STRUCTURE AND CRASH PULSE**

The level of passive safety depends on different parameters. One important parameter is the characteristic of the crash pulse, mainly influenced by the crash velocity and the vehicle's structure.

In conventional cars, the crash structure influencing the accident performance is composed of a bumper, crash boxes and long members. Due to the CLEVER design with one wheel in the front, this conventional way of energy absorption is not possible. Therefore, a new approach was necessary. Special effort was needed to avoid any intrusion into the cabin, as the driver's feet are located directly behind the front wheel.

The crash structure of the CLEVER vehicle consists of the front wheel, the swing arms (front wheel suspension) and special designed crash elements. While conventional car wheels are stiff, motorcycle wheels normally brake in accidents. The CLEVER front wheel is designed to deform under crash loads. This is important to use as much as possible deformation length without injuring the legs of the driver on the one hand and for compatibility reasons in a side impact, when CLEVER hits a conventional car, on the other hand.

The stiffness of the swing arms is quite high, resulting in small deformations of this part. However, the swing arms are designed to route the crash forces to the crash elements, which connects the swing arms with the stiff frame. These deformable elements allow the front wheel to move backwards together with the suspension, which absorbs energy. The cabin frame itself offers appropriated stiffness to avoid dangerous intrusions in frontal impacts. The body panels are made of laminated synthetic materials. The influence of the body panels to the crash behaviour should be negligible small.

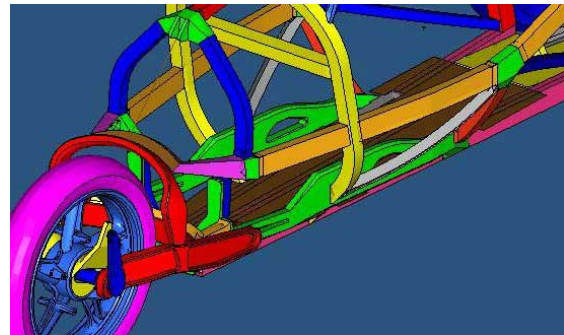


**Figure 12. CLEVER – front frame structure.**

Based on finite element simulations the above described measures lead to the pulse shown in the following figure.

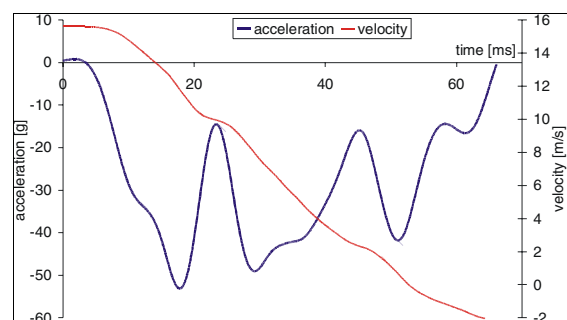


**Figure 13. CLEVER crash pulse.**

The order of magnitude of these accelerations agrees with the documented test results of micro-cars.

A picture of the expected deformation is shown in figure 14.

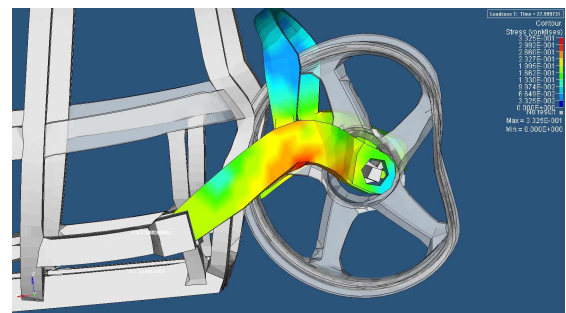


**Figure 14. CLEVER deformation characteristic.**

Concerning the lateral impact, the introduced cross beams lead to appropriated cabin stiffness. The expected intrusion and intrusion velocity will not exceed 130 mm or 7,8 m/s, respectively figure 15.

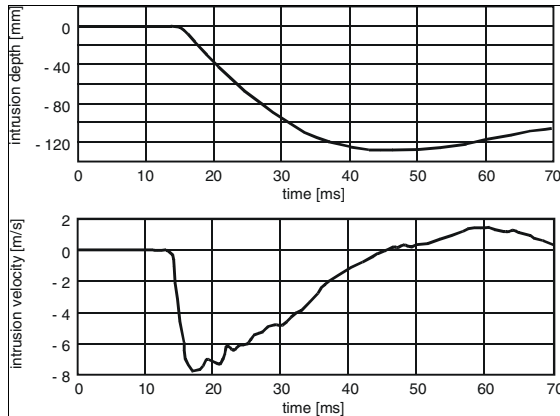


**Figure 15. Lateral impact characteristics in 50 kph MDB test.**

The deformation of the structure is shown in the figure below.

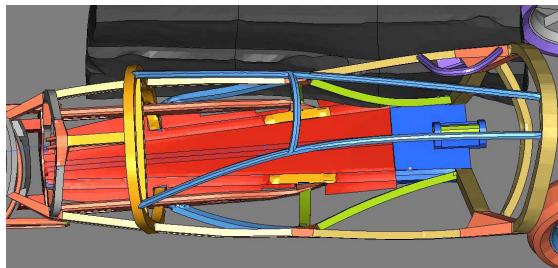


**Figure 16. Maximum deformation in EuroNCAP lateral impact.**

The special designed rear seat will introduce additional lateral stiffness, which will result in lower intrusion and intrusion velocity.

The knowledge about the structural behaviour of the vehicle allows the design of the restraint system.

## **CLEVER FRONTAL RESTRAINT SYSTEM**

CLEVER's frontal restraint system will be specially designed. The package conditions are not similar to conventional cars.

To reduce the engineering and production costs for CLEVER, standard components for the restraint system were used wherever possible. However, due to the challenging restraint requirements caused by the small vehicle and the high pulse, it was necessary to adopt and modify existing components and design special components for CLEVER.

### **MADYMO-Simulation of the CLEVER Vehicle**

The performance of the restraint system was checked by using numerical simulation tools. Furthermore, the components for the restraint

system were also adjusted by numerical simulation too.

The computer programme MADYMO was chosen for the simulation. With this solver, it is possible to combine the capabilities of multi-body and finite element techniques.

In a first step, a very simple simulation model was built up, which presented the known vehicle characteristic at the beginning of the project. It was used for preliminary investigations. With this model, it was possible to see that the requirements could be met.

When the project progressed, more detailed characteristics for the vehicle were defined. A better simulation model was built. Consequently, more exactly investigations could be carried out. The effect of different components like pretensioner or load limiters, separate or in combination with other components, were analysed. In addition, the safety level for different occupants (5%-HIII, 50%-HIII, 95%-HIII) was checked.

As main output of this development step, the necessity of a combination of driver airbag, pretensioner and load limiter for reaching a three star ranking with the 50%-HIII was shown. For the 5%-HIII and the 95%-HIII, the same configuration of the restraint system will lead to best results.

These investigations started by using a synthetic generated crash-pulse. Within the ongoing development, a more realistic crash pulse (figure 13) generated by the structural simulation was used and, consequently, more realistic results could be generated.

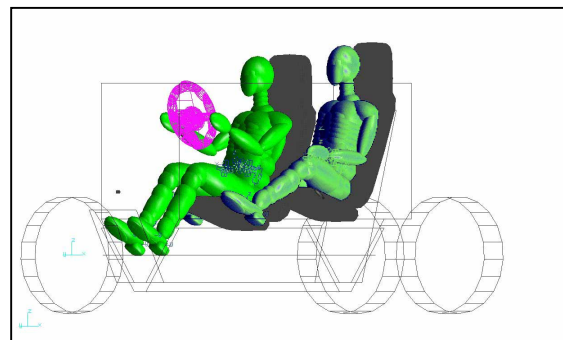


**Figure 17. More detailed simulation model.**

In the next development step, a final model was built. This model included all defined geometries, shapes, material characteristics and well known, validated components.

This final simulation model was consequently built with multi-body parts (dummy, steering wheel) and finite element parts (seat, airbag, and belt).

The complete results for the driver and passenger will be shown below. Because of the imprecision of

the simulation model, it is nearly impossible (at the moment) to generate realistic results for the lower extremities. For example, the design of the knee contact area of the dashboard and the footrest (with the mounted pedals) is not yet finished. It should be kept in mind that this could influence the overall performance rating compared with the currently existing results based on numerical simulations.

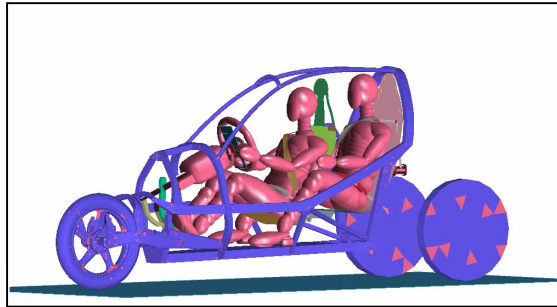


**Figure 18. Final CLEVER numerical simulation model.**

### Driver Restraint System

The current CLEVER results for the driver and the passenger are shown in the following table. The limits are comparable to the CLEVER-CAP limits. For the driver, the difference between a restraint system with deformable steering column and with stiff steering column is additionally shown.

**Table 1. Calculated results for the CLEVER driver**

		Limits	18.02.2005	18.02.2005
		50% HIIII CLEVER- Requirements 2003	Driver 50% HIIII	Driver 50% HIIII
EuroNCAP -Criteria- 50% HIIII			CLEVER-Plus (final)	CLEVER-Plus (final)
Simulation	seat rest	-	-	-
	Airbag	-	60 l coated	60 l coated
	AOE Steering column	-	2 x 30 mm stiff	2 x 30 mm deformable
Head	HIC <sub>35</sub>	<b>883</b>	658	412
	HIC <sub>15</sub>	-	-	-
	a <sub>3ms</sub> [g]	<b>83</b>	58	43
	-	-	-	-
Neck	My+ (max. Flexion) [Nm]	-	80	55
	My- (max. Extension) [Nm]	<b>52</b>	14	14
	Fx+/ (max. Shearforce) [kN]	<b>2,7</b>	1,0	0,7
	Fz+ (max. Force) [kN]	<b>3,1</b>	1,3	1,1
	Fz- (max. Force) [kN]	<b>3,1</b>	0,2	0,2
Thorax	a <sub>3ms</sub> [g]	-	59	58
	a <sub>max</sub> [g]	-	-	-
	s <sub>max</sub> [mm]	<b>41</b>	40	39
	VC [m/s]	<b>0,83</b>	0,22	0,22
Pelvis	a <sub>3ms</sub> [g]	-	92	92
Femur	Fz left [kN]	<b>7,3</b>	5,1	5,1
	Fz right [kN]	<b>7,3</b>	7,1	7,1

The limits, defined by the CLEVER-CAP for the frontal impact, were partially below target. In comparison to the US-NCAP, a three-star rating could be possible.

These results come from a comparison of different components for the driver restraint system by numerical simulation. The most effective system

consists of a deformable steering column, a driver airbag with two chambers, a pretensioner, and a dual stage load limiter. The system is shown in the figure 19.

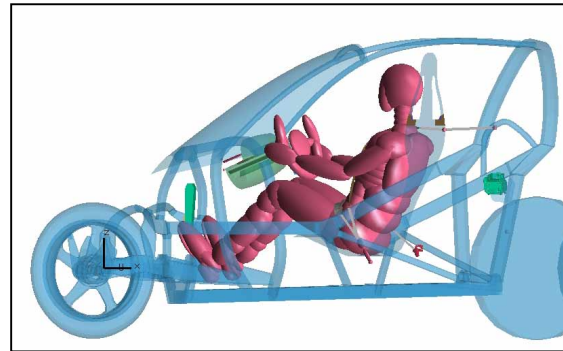


**Figure 19. CLEVER driver restraint system.**

The steering column is an existing one, used in conventional cars out of the series production.

The difference between restraint systems with a deformable and non-deformable steering column is significant. That is why the decision was made, to include a deformable steering column.

In the following figure, the difference of the energy application of the airbag from a restraint system with deformable and non-deformable steering column is shown. In a restraint system without deformable steering column, the kinetic energy of the head and partly of the thorax will be absorbed by the airbag, and the deformation of the steering wheel. If a deformable steering column is used, the airbag has to absorb about 1/3 less energy. This 1/3 will be absorbed by the deformable steering column. So the diameter of the airbag vents can be increased. That is why the airbag will be much softer. This will result in lower values of the assessment criteria.

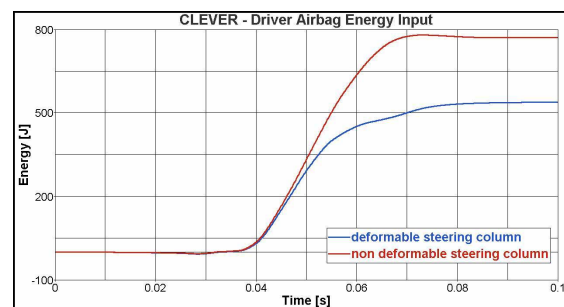


**Figure 20. Application of energy by the airbag.**

The steering wheel is a modified steering wheel from serial production. Some styling and design modifications will be necessary. The deformation characteristics are well known.

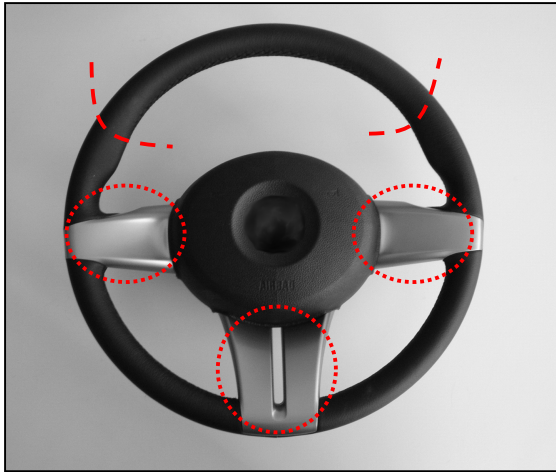


**Figure 21. Possible modifications of a series steering wheel for CLEVER.**

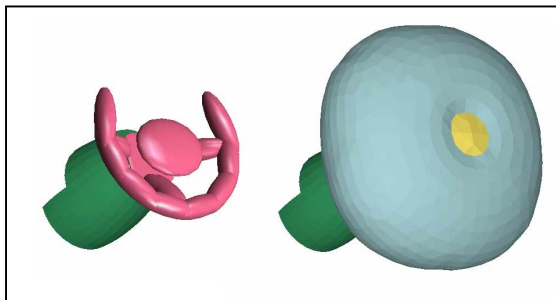


**Figure 22. Simulation model of the steering column, steering wheel and driver airbag.**

The airbag system is consisting of a dual-stage inflator in combination with a 60 l two-chamber airbag. There are two venting holes with a diameter of about 30 mm each. This provides excellent performance for head protection in combination with lower impact force to the sternum. The positioning of the airbag will be better than with a conventional one chamber airbag.

In the case of a restraint system without driver airbag, the head of the driver would touch the steering wheel. High values for head acceleration and the HIC would follow. To avoid these effects, the decision to use a driver airbag was taken.

The belt system is fitted with a retractor mounted pretensioner. A dual-stage load limiter will be used. The load limiter will switch after a defined time from stage 1 to stage 2. The shoulder belt force will not exceed a maximum force of about 4,5 kN for stage 1 and 2,5 kN for stage 2.

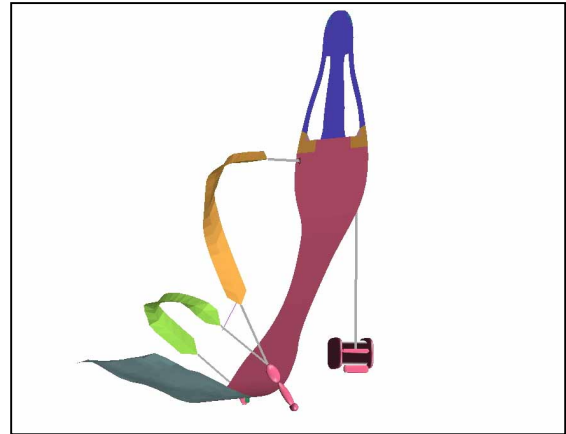


**Figure 23. Driver seat belt system.**

Furthermore, optimal connection points of the seat belt system with the vehicle frame were found by the simulation. The value of chest deflection is influenced by the seat belt geometry. This geometry is determined by the connection points of the d-ring with the vehicle frame and the seat belt guiding on the seat rest.

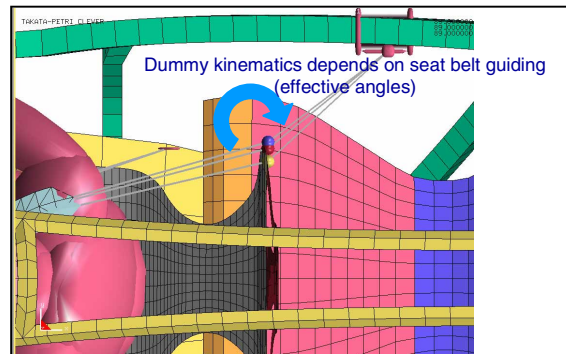


**Figure 24. Seat belt guiding by the seat.**

The retractor has to be connected with the vehicle frame because of the high level of the reacting forces.

For checking the seat characteristic for the case that the seat belt system is mounted on the seat, a static force load of about 2 kN was directed on the connection points at the seat rest. The results of the numerical simulation showed that the seat collapsed and, in result, the protection of the occupants could not be guaranteed. The calculation was made twice, at first with a steel seat with a thickness of 5 mm, second by a steel seat with a thickness of about 10 mm.

Please remind, the real value of the belt forces at the shoulder are from 2,5 kN up to 5 kN.

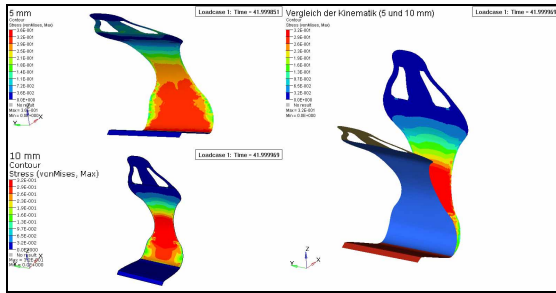


Figure 25. Seat characteristic under force influence in x-direction.

### Passenger Restraint System

For the passenger side, the requirements could not be met for a system with stiff seat rest. The decision was to design a deformable seat rest. The thickness and the material characteristics were defined based on validation tests.

Table 2:  
Calculated results for the CLEVER passenger

TAKATA		Limits 50% HII CLEVER- Requirements 2003	18.02.2005 Passenger 50% HII	18.02.2005 Passenger 50% HII
EuroNCAP -Criteria- 50% HII			CLEVER-Plus Fmg	CLEVER-Plus Fmg
Simulation	seat rest	-	stiff	deformable
	Airbag	-	-	-
	AOE	-	-	-
	Steering column	-	-	-
Head	HIC <sub>36</sub>	883	7743	548
	HIC <sub>15</sub>	-	-	-
	a <sub>3ms</sub> [g]	83	218	64
Neck	My+ (max. Flexion) [Nm]	-	-	-
	My- (max. Extension) [Nm]	52	113	53
	Fx+/- (max. Shearforce) [kN]	2,7	3,9	1,4
	Fz+ (max. Force) [kN]	3,1	-3,7	0,0
	Fz- (max. Force) [kN]	3,1	1,0	3,3
Thorax	a <sub>3ms</sub> [g]	-	80	59
	a <sub>max</sub> [g]	-	-	-
	s <sub>max</sub> [mm]	41	36	44
	VC [m/s]	0,83	0,31	0,32
Pelvis	a <sub>3ms</sub> [g]	-	111	113
Femur	Fz left [kN]	7,3	5,6	5,7
	Fz right [kN]	7,3	5,5	5,6

The passenger restraint system basically consists of a seat belt system. In addition, a head protection bolster is integrated. The front seat is designed with a deformable head rest. After the passenger's head hits the head rest of the front seat, energy will be absorbed by the deformation of the bolster and by the deformation of the head rest, too.

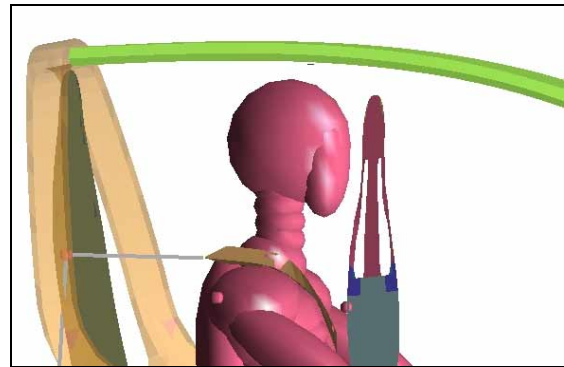


Figure 26. Position of contact between passenger head and seat rest.

The validation of the head to seat contact will be made by head impactor tests. Therefore, a head impactor with a mass of about 4,8 kg will be shot with a defined velocity of 5,3 m/s on the head rest, similar to the head impacting velocity of the CLEVER passenger. The accelerations will be measured and different bolster thicknesses have to be checked.

The expected bolster thickness by the calculated head impacting velocity is of about 20 to 50 mm, depending on the deformation characteristics and the stiffness of the seat rest.

The best performance - lowest head impactor acceleration by acceptable deformation of the back rest and a realisable thickness of the bolster – will be found with the described test procedure and be used for the CLEVER vehicle.

The seat belt system is similar to the seat belt system for the driver. The time, when the load limiter switches from level 1 to level 2, is different.

## CONCLUSIONS

CLEVER is an alternative vehicle concept, which is characterised by innovative solutions such as its fuel concept, the propulsion system, or the safety concept.

The safety concept is specially designed for real world accident scenarios. The advantages and disadvantages of conventional protection systems for two-wheeled and three-wheeled vehicles could be identified.

With the support of numerical simulation, the entire restraint system could be optimised. The exact application of different components was done.

The performance has to be verified by real crash tests.

To improve the safety level of two-wheel and three-wheel vehicles, occupants should be prevented from ejection during an accident. This will be realised by using a seat belt system.

It is possible to develop a small three-wheel vehicle with an occupant safety level comparable with conventional cars. The calculated values for the

assessment criteria are equal or below the defined limits of the CLEVER-CAP, which was developed specifically for CLEVER.

Furthermore, it is possible to adapt conventionally used restraint system components to alternative vehicles. A few changes have to be made, e.g. belt load limits, or the time to fire.

## ACKNOWLEDGEMENT

The CLEVER project is funded by the European Commission (GROWTH Programme, 5<sup>th</sup> FWP) under the Contract no. G3RD-CT-2002-00815. Additional information concerning the CLEVER project is available at [www.clever-project.net](http://www.clever-project.net).

## REFERENCES

- [1] H. Johannsen, L. Lasek, S. Sohr, P. Krams: "Safety Concept for Narrow Track Urban Vehicles;"; Innovativer Kfz-Insassen- und Partnerschutz - Fahrzeugsicherheit 2010, VDI-Konferenz Berlin, 20./21.11.2003
- [2] Osendorfer, H; Rauscher, S.: "The development of a new class of two-wheeler vehicles"; 17<sup>th</sup> Int. ESV-conference Amsterdam, June 4-7, 2001; Proceedings
- [3] Internal Investigation of TAKATA-PETRI by using the actual Database of the GIDAS – German In Depth Accident Study
- [4] Internal Investigation of TAKATA-PETRI by using the actual Database of the NASS – National Automotive Sampling System –look at: <http://www-nrd.nhtsa.dot.gov/departments/nrd-30/ncsa/NASS.html>
- [5] Monitoring of ACEA's Commitment on CO2 Emission Reduction from Passenger Cars; Final Report, Commission of the European Communities, 2002  
[www.acea.be/ACEA/20040317PublicationEmissions.pdf](http://www.acea.be/ACEA/20040317PublicationEmissions.pdf)

## DAYTIME RUNNING LIGHTS FOR MOTORCYCLES

**Michael Paine**

**David Paine**

Vehicle Design and Research

**Jack Haley**

National Roads and Motorists Association

**Samantha Cockfield**

Transport Accident Commission of Victoria

Australia

Abstract ID 05-0178)



---

### ABSTRACT

The daytime use of motorcycle headlights has had mixed success in various countries. Dedicated lights that are optimised for use as daytime running lights (DRLs) can be far more effective and energy-efficient than low beam headlights.

A difficulty with motorcycles is a lack of space for fitting extra lights at the front. In the USA many General Motors cars use bright yellow front turn signals as DRLs. The feasibility of applying this approach to motorcycles is examined. Initial research suggests that bright yellow DRLs could be highly cost effective for preventing motorcycle accidents. Technology improvements such as Light Emitting Diodes and ambient light sensors would make them even more effective.

### INTRODUCTION

#### Motorcycle accidents

Motorcycle riders make up about 17% of vehicle operator fatalities in Australia. Per kilometre travelled, motorcycle riders are 29 times more likely to be killed than operators of other vehicles. Motorcycle operators in the 17 to 25 age range have almost 100 times greater risk to operators of other vehicles (ATSB 2002).

About two-thirds of Australian motorcycle accidents occur in daylight and 65% involve more than one vehicle. It was reported that in 21% of daytime multi-vehicle collisions the driver of the other vehicle claims to have not seen the motorcycle (Hendtlass 1992).

More recently, an in-depth study of motorcycle crashes in Europe found that in 37% of all cases the primary contributing factor was the failure of another vehicle operator to detect the motorcycle (ACEM

2004). 73% of accidents occurred in daylight and a further 8% at dawn or dusk. It is notable, however, that the headlights were in use in 69% of these accidents. Unfortunately any link between detection failure and lack of headlights is not reported by the authors but it is evident that many cases involve motorcycles with illuminated headlights that are not seen by other motorists.

#### Daytime running lights

Daytime running lights (DRLs) are bright white or yellow forward-facing lights that improve the forward conspicuity of vehicles in the daytime. They are intended to increase the chance of other road users seeing the approach of the vehicle.

Four main types of DRLs are currently in use:

- a) low-beam headlights that illuminate when the vehicle is started
- b) dimmed high beam headlights - the voltage to the high-beam headlights is regulated so that they have greatly reduced intensity
- c) dedicated lights with a defined beam pattern and light intensity
- d) increased intensity yellow turn signals. These illuminate constantly until the turn signal control is activated and then they flash on one side.

In each case the vehicle is usually wired so that the DRLs illuminate whenever the engine is running. DRLs that do not utilise low-beam headlights must deactivate whenever normal headlights come on.

In the case of motorcycles DRLs are almost always low-beam headlights.

## Regulations and standards

Australian Design Rule 76/00 'Daytime Running Lamps' sets out requirements for optional lamps fitted to vehicles sold in Australia. The ADR calls up Europe (UN ECE) Regulation 87 and only allows white lamps to be used as DRLs.

SAE Recommended Practice J2087 'Daytime running lights for use on motor vehicles' is an optional standard.

Canada Motor Vehicle Safety Standard 108 specifies requirements for the mandatory fitting of DRLs to vehicles built from 1st December 1989.

Several countries require the use of DRLs (mainly low beam headlights) under traffic laws but they are not required to be 'hard wired':

In 1992 Australia introduced mandatory "hard-wired" headlights for motorcycles - low-beam headlights were required to illuminate whenever the engine was running. This requirement was rescinded in 1996, due mainly to pressure from motorcycle lobby groups: "The Motorcycle Council of NSW (MCC) counts amongst its major achievements... Convincing the Federal government in 1996 to provide an alternative to ADR 19/01 (requiring hard wired lights on for motorcycles) in the form of ADR 19/02 (which does not require hard wired headlights)" (MCC website).

## Effectiveness studies – cars

Overseas studies have generally shown that daytime running lights reduce daytime accidents by making vehicles more conspicuous to other road users. The greatest benefits are with the more severe accidents, including head-on and intersection crashes and collisions with pedestrians and cyclists.

According to a European study (Koornstra 1997) the potential savings are:

- 25% of daytime multi-vehicle fatal accidents
- 28% of daytime fatal pedestrian accidents
- 20% of daytime multi-vehicle injury accidents
- 12% of daytime multi-vehicle property accident

The large benefits to pedestrians arise from improved conspicuity of vehicles - the pedestrian is less likely to move into the path of an approaching vehicle that is equipped with DRLs. Similar benefits would apply to other vulnerable road users such as bicyclists and motorcyclists.

In Australia 64% of fatal crashes and 79% of non-fatal crashes occur during the daytime and about 3/4 of these are multi-vehicle crashes. If the savings

estimated for Europe could be achieved in Australia this would equate to savings of:

11% of all fatal accidents

15% of all other accidents

## Effectiveness studies – motorcycles

Rumar (2003) reviews the effectiveness of motorcycle DRLs. He reports that there are relatively few applicable studies. For example, Henderson and others (1983) showed that motorcycle crashes were reduced by about 5% after the introduction of the DRL legislation for motorcycles in North Carolina in 1973. Other crashes were not influenced. Williams (1996) reports an estimated 13% reduction in motorcycle crashes through the use of motorcycle DRLs (mostly headlights) in the USA.

Rumar points out that motorcycles have a significant conspicuity disadvantage due to their smaller front cross-sectional area. This also leads to speed and distance estimation errors by other drivers. Rumar notes that a single headlamp does not provide adequate distance information and he suggests that three lamps, mounted in a triangular pattern, may assist in speed and distance estimation.

This observation by Rumar, combined with the recent studies of motorcycle accidents where most motorcycles had headlights illuminated in the daytime, indicates that single low-beam headlights might not be particularly effective as motorcycle DRLs. It is therefore necessary to consider the visual ergonomics of on-road situations when accessing the functional requirements for motorcycle DRLs.

## FUNCTIONAL REQUIREMENTS OF DRLS

Vehicle signal lights need to be designed to meet the conflicting requirements of:

- providing sufficient signal range to be seen and recognised and
- avoiding undue glare that hinders the vision of other road users

This must be achieved throughout a very large range in background lighting conditions (Paine and Fisher 1996).

The luminous intensity of lights is measured in candela. Research with traffic signals found that yellow lights require three times the luminous intensity of red lights to achieve the same signal range (Fisher and Cole 1974). White light signal range lies between these extremes.

In 1993 a detailed report on DRLs was issued by the Commission Internationale de l'Eclairage (CIE) - the international authority on lighting standards. Prof Rumar was chair of the CIE committee that prepared the report. The committee recommended that dedicated DRLs be encouraged with the following features:

- Relatively high intensity: up to 1200cd along the central axis
- Two white lights mounted at the front of the vehicle
- Minimum area of illumination 40cm<sup>2</sup>.
- Motorists should be encouraged to switch to low beam headlights at dawn and dusk to minimise potential glare problems.

Paine (2003) reviewed the functional and operational issues associated with DRLs. Road design guidelines provide a benchmark for determining the required signal range for DRLs:

Table 1. Road Design Sight Distances - metres (Lay 1991)

Design Speed	Intersection sight distance	Overtaking sight distance
40km/h	80	160
60km/h	120	220
80km/h	170	340
100km/h	230	480

These required sight distances can be compared with the signal range of various colours of light under a range of background lighting conditions. With DRLs the worse case is a bright day (background luminance 10,000cd/m<sup>2</sup>).

Using the formula provided by Paine and Fisher (1996), Table 2 sets out the estimated signal range of a selection of automotive lamps on a bright day.

Table 2. Australian Requirements for Vehicle Lamps

Type of lamp	Minimum Intensity	Maximum Intensity	Estimated Range*
Front turn signal (yellow, not flashing)	175cd	700cd	110m
Rear turn signals (yellow, not flashing)	50cd	200cd	60m
Rear brake lamp (red, day/night)	40cd	100cd	70m
Rear brake lamp (red, day only)	130cd	520cd	160m
Rear fog lamp (red)	150cd	300cd	120m
Low beam (white, upper portion)	-	437.5cd	100m
Dedicated DRL (white)	400cd	800cd	140m

\*Estimated range in bright daylight with light 3° from observer's line of sight and at maximum permitted intensity.

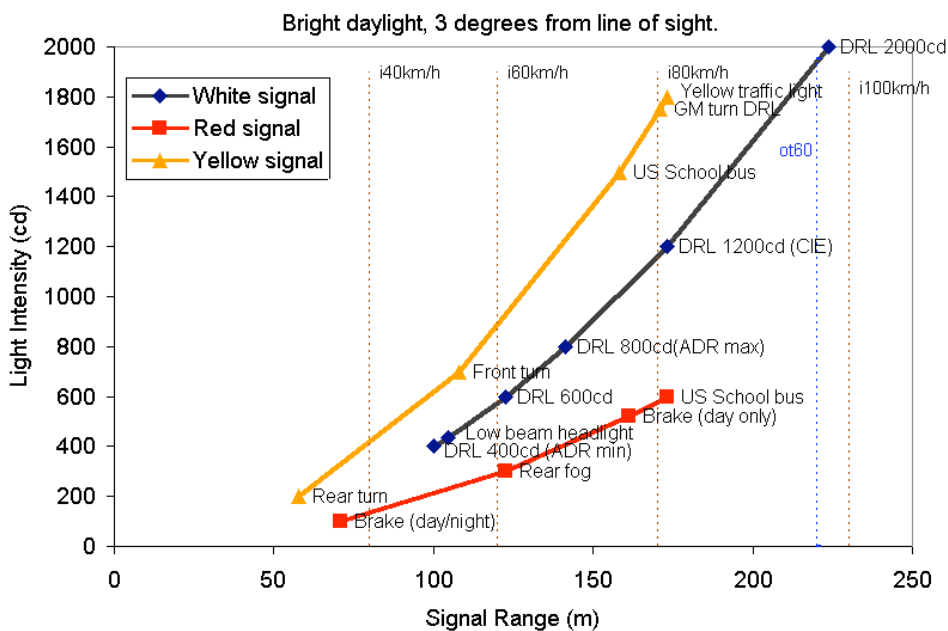


Figure 1. Light intensity and signal range for a selection of vehicle lights

These are illustrated in Figure 1, together with the sight distances from Table 1 (e.g. i40 = intersection with 40km/h traffic speeds, ot60 = overtaking with 60km/h traffic speeds).

Notable from this analysis is that *on bright days*, low-beam headlights which are at their maximum permitted intensity (437cd in the direction of other road users) are barely adequate for intersection situations where traffic is travelling at about 50km/h. They are inadequate for traffic speeds of 60km/h or higher. This outcome could go some way to explain the so-called latitude effect where DRLs have generally been found to be more effective in high latitude countries (Koonstra 1997). If this is the case then brighter DRLs can be expected to overcome this latitude effect.

On cloudy days, or near dawn or dusk, most potential DRL lights can be expected to be effective for the range of signal ranges set out in Table 1. An exception is for overtaking in traffic travelling at 80km/h or more. In this case low beam headlights (437cd) are likely to be marginally effective.

This analysis is supported by a US study reported by Thompson (2003). The effectiveness of several types of DRL now fitted as standard to GM cars was evaluated by comparing the collision rates of models built before and after DRLs became standard:

Table 3. Effectiveness of DRLs on GM cars (from Thompson 2003)

DRL Type	Change in Collision rate
Dedicated DRL (900cd)	-8.76%
Low beam headlight	-3.23%
Reduced intensity low beam	-2.31%
Reduced intensity high beam*	-4.86%
Yellow turn signal #	-12.4%

\* Although reduced intensity high beams are bright (around 5000cd) they have a very narrow beam angle that limits their effectiveness as a DRL (CIE 1993)L

# GM uses high intensity turn signals (around 900cd).

Subject to sample size limitations, the GM study suggests that dedicated DRLs are nearly three times as effective as low beam headlights and bright turn signals are nearly four times as effective.

It is therefore important that the type of DRL be taken into account when considering DRLs for motorcycles.

## DRLS FOR MOTORCYCLES

Low beam headlights are the most popular form of DRL on motorcycles. Although these are the easiest to implement they have several disadvantages:

1. As demonstrated in the previous section, they have marginal photometric performance, even at the brightest intensity permitted by regulation. In any case, it is likely that most motorcycle headlights are well below this maximum permitted value.
2. Headlights waste energy when used as DRLs because, on low beam, they are designed to direct most light below the horizontal and away from the eyes of other road users. Tail lights and number plate lights also illuminate with the headlights but are not needed in daylight.
3. There is increased risk of a headlight bulb failure and this is a more serious night-time issue with motorcycles than cars.

Dedicated DRLs overcome these disadvantages but motorcycles generally do not have sufficient space at the front for these additional lamps.

Turn signal DRLs also overcome the disadvantages of headlight DRLs. Furthermore they do not require extra space at the front of the motorcycle. All that is required is the replacement of normal motorcycle turn signals (which are likely to have relatively poor photometric performance) with much brighter ones.

Turn signal DRLs would unambiguously indicate to other motorists that the approaching vehicle was a motorcycle and the intended direction of turn (conventional motorcycle turn signals are so close together that, sometimes, the intended direction of turn is not evident to other motorists).

Yellow DRLs are not currently permitted in Australia. There is therefore the one-off opportunity to regulate to allow optional yellow DRLs on motorcycles and ensure that these vehicles are uniquely identified to other road users. A pair of yellow DRLs will also assist other road users to judge the speed and distance of an approaching motorcycle.

## CRITICISMS OF DRLS

There are several myths and misunderstandings about DRLs that need to be addressed by policy makers.

Increased fuel consumption not an issue with energy-efficient dedicated or turn signal DRLs that send light in exactly the direction where it is most effective. Recent developments in LED technology should

mean that a pair of DRLs with excellent photometric performance will consume less than 20W.

Concern about masking of vulnerable road users has been shown to be unfounded (Williams 1996). In any case vulnerable road users benefit most from being able to see approaching vehicles with DRLs.

Masking of brake lights by tail lights (that come on with headlights) and premature failure of headlight globes are not issues with dedicated/turn signal DRLs

Glare could be a problem at dawn and dusk (Stern 2002). This is easily overcome by automatic headlights with an ambient light sensor. Many new cars now have this feature. If turn signal DRLs are to remain continuously illuminated at night then they should have reduced intensity (maximum 700cd) when the headlights are illuminated. Bright turn signals that only illuminate when they flash would not need to have reduced intensity at night and may provide increased signal effectiveness.

## CONCLUSION

Bright yellow turn signal DRLs should be encouraged for motorcycles. These should have an on-axis luminous intensity of not less than 1000cd and not more than 1800cd. Automatic headlights should also be encouraged so that a light sensor is used to switch from DRL operation to headlights. To avoid glare, bright turn signals should not be continuously illuminated at night.

In Australia bright yellow DRLs should be permitted on motorcycles but should continue to be disallowed on other vehicles. These would be far more effective as DRLs than headlights and have the potential to reduce fatal motorcycle crashes by more than 13%.

## REFERENCES

ATSB, 2002, "Motorcycle Safety", Monograph 12, Australian Transport Safety Bureau, October 2002.

Bergkvist P., 1998, "Daytime Running Lights - A North American Success Story", *Proceedings of 17th Conference on the Enhanced Safety of Vehicles*, Windsor, Canada, 1998.

CIE, 1993, "Daytime Running Lights", Commission Internationale de l'Eclairage, Technical Report 104.

DOTARS, 2002, "Australian Design Rule 76/00 Daytime Running Lamps", Dept of Transport and Regional Services, Canberra.

Elvik R., 1996, "A meta-analysis of studies concerning the safety effects of daytime running lights on cars", *Accident Analysis and Prevention*, Vol.28, No.6, 685-694.

Fisher A. and Cole B., 1974, "The photometric requirements of vehicular traffic signal lanterns", *Proceedings of 7th ARRB Conference*, 7(5), 246-265.

Henderson, R.L., Ziedman, K., Burger, W.J., and Cavey, K.E. (1983). *Motor vehicle conspicuity* (SAE Technical Paper Series 830566). Warrendale, PA: Society of Automobile Engineers.

Hentlass J., 1992 "Literature Review for Inquiry into Motorcycle Safety:", Appendix to Inquiry into Motorcycle Safety in Victoria, Parliament of Victoria, Australia, January 1992.

Koornstra M., Bijleveld F. and Hagenzieker M, 1997, "The Safety Effects of Daytime Running Lights", SWOV Institute for Road Safety, The Netherlands, R-97-36.

Lay M., 1991, "Handbook of Road Technology", Volume 2, Traffic and Transport, Gordon and Breach Science Publishers.

NHTSA, 2000, "A preliminary assessment of the crash-reducing effectiveness of passenger car daytime running lamps (DRLs)", NHTSA Technical Report DOT HS 808 645, June 2000.

Paine M. and Fisher A., 1996, "Flashing lights on school buses", *Proceedings of 16th Conference on the Enhanced Safety of Vehicles*, Melbourne. <http://www4.tpg.com.au/users/mpaine/buslight.html>

Rumar K. 2003. "Functional Requirements for Daytime Running Lights", University of Michigan Transportation Research Institute, UMTRI-2003-11, May 2003.

Schug J. and Sischka I., 2000, "Daytime running lamps - different ways of realization", SAE Paper 2000-01-0435, Society of Automotive Engineers, Warrendale.

Stern D., 2002, "Where does glare come from", Daniel Stern Lighting Consultancy, USA.

Thompson P., 2003, "Daytime Running Lamps for Pedestrian Protection", SAE paper 2003-01-2072, Society of Automotive Engineers, Warrendale.

Tofflemire T. and Whitehead P., 1997, "An evaluation of the impact of daytime running lights on traffic safety in Canada", *Journal of Safety Research*, Vol.28, No.4, 257-272.

White J., 1998, "Information on Daytime Running Lights", Transport Canada, Technical Memoranda TMSR 9801, May 1998.

Williams A. and Lancaster K., 1996, "The Projects of Daytime Running Lights for Reducing Vehicle Crashes in the United States", *Public Health*, May-June 1996, Vol.110, No.3, 233-239.

## REAL AND SIMULATED CRASHWORTHINESS TESTS ON BUSES

VINCZE-PAP Sándor

AUTÓKUT, Budapest

Hungary

CSISZÁR András

EDAG Hungary Ltd., Győr

Hungary

ID: 05-0233

### ABSTRACT

This paper discusses the design aspects of bus frontal impact behavior as one of the main subjects of bus crashworthiness and surveys conditions and results of previous full impact laboratory tests comparing the FEM simulation results carried out on a Hungarian Ikarus bus.

Clarifying the adequate background gives possibilities for checking bus passive safety solutions by computer and the best utilizable resolutions can be applied in the standardized production. This paper shows frontal impact test arrangements of a 10 tons' city bus with three different impact speeds and computer simulation versions of these real tests. It gives possibilities to compare the test results to the requirements of current bus regulations.

### BUS CRASHWORTHINESS – FRONTAL IMPACT

Design for frontal impact, side impact and rollover safety come within the crashworthiness subject.

Frontal impact of automobiles is an accurately researched and well-circled topic versus bus frontal impact behavior.

A well-designed bus structure has good deformation and energy absorbing capability. In case of frontal impact it has to meet three criteria:

*Force criterion:* the order of stability losing (crushing) of structural elements happens in pre-determined sequence; the forces due to the plastic hinges are in successive magnitude;

*Energy criterion:* the kinetic energy of the vehicle must be absorbed with deformation energy of other pre-determined elements of bus framework to avoid the damage of any protected structural element (initial condition for generating the safety bumper features)

*Kinematical deformation criterion:* during the energy absorbing process the (elastic and residual) displacement possibility of structural elements is limited and the damage-free conditions of elements can be allowed or ensured due to this.

The reality of above-mentioned goals was investigated by a test series carried out at AUTÓKUT in 80's. Dynamic impact tests on full-

scale bus, driver space, front-wall, understructure, bumper and bumper elements were accomplished.

All kinds of crashworthiness' demand claims to minimize the injury probability of vehicle driver and passengers during standard accident conditions or to maximize their survival chance.

According to the knowledge of biomechanical tolerance limits of human beings two basic premises shall be fulfilled:

– As rigid as possible driver and passenger zones shall be created for ensuring the so-called "survival space";

– Suitable energy absorbing zones shall be designed for limiting the (inertia forces) acting on the drivers and passengers for reducing the inner impact forces, which can cause fatality.

„Survival zone” of bus is defined only for rollover safety (ECE R66) and regards to the passenger area exclusively, but it is not adaptable to the frontal impact due to the primacy of driver cabin. Ensuring to keep in a prescribed space and cover the surroundings with energy absorbing materials are the two most effective tools for mitigation of injury risk of passengers (and partly of the driver). [1]

Deformations and displacements of certain vehicle equipment, accessories (dashboard, steering-wheel, seat-back,) shall not cause the dangerous reduction of „personal free space”.

Structural behavior of bumper, understructure, front-wall, driver seat anchorages, passenger seat structural strength and fixing are giving the main tasks at structural strength design.

On the analogy of automobile, the bus energy absorbing capability of a bus can be defined as follows: aim is to create such an understructure with adapted bumper which can absorb the bus impact energy by crushing of bumper elements and elastic compression of understructure due to min. 7 km/h impact into rigid wall. In this case the impact energy to be absorbed is 19 kJ for a 10-ton bus. [2] (The calculated impact energy is 25 kJ at 8 km/h impact speed.)

### REAL IMPACT TESTS [2] [3]

#### Full impact onto rigid wall

**Ikarus 411** type bus was the test vehicle (prototype of the current running IK 415 city buses). The rigid wall was a 300 tons concrete block with wooden surface in 50 mm thickness. There were 4 load transducers between the impact surface and the concrete block. Opto-gate measured the impact speed. In the passenger cabin two 50 % male dummy (Hybrid II and Ogle) were seated and the Hybrid II dummy was equipped with head and chest accelerometers and femur load transducers in

the right leg. A longitudinal accelerometer was fixed onto the floor above the CGV of the bus.

The test bus was impacted three times with three different speeds. [3]

Vehicle dimensions:

Length: 11000 mm

Width: 2500 mm

Height: 2940 mm

Axle distance: 5570 mm

Front/rear overhang: 2630/2800 mm

Measured values	Bus frontal impact onto rigid wall		
	3,6 km/h speed	6,98 km/h speed	29,76 km/h speed
Max. impact force at the left longitudinal beam [kN]	180	220	780
Max. impact force at the right longitudinal beam [kN]	160	190	390
Resultant impact force [kN]	320	390	1100
Max. acceleration on the floor above the CGV [g]	3	4	12
Max. resultant acceleration in the Hybrid II head [g]	3	10	60
Measured max. femur force in the Hybrid II dummy [kN]	1,1	1,3	1,6

**Table 1. Results of three frontal impacts**

(The IK 411 bus was equipped with the same bumper as was developed for the IK 250 type bus, **Fig. 1.a.**) The mass of bus prepared for test was: 10 080 kg.

There was only elastic deformation at the first (3,6 km/h) impact, and there was no outer damage on

the bus after the second (6,98 km/h) impact test. The detailed examination discovered the crushing destruction at left side; the bumper connecting tubes (two 60/40x2 mm tubes between the bumper surface and the longitudinal beam) have crumpled. (**Fig. 1.b-c.**)

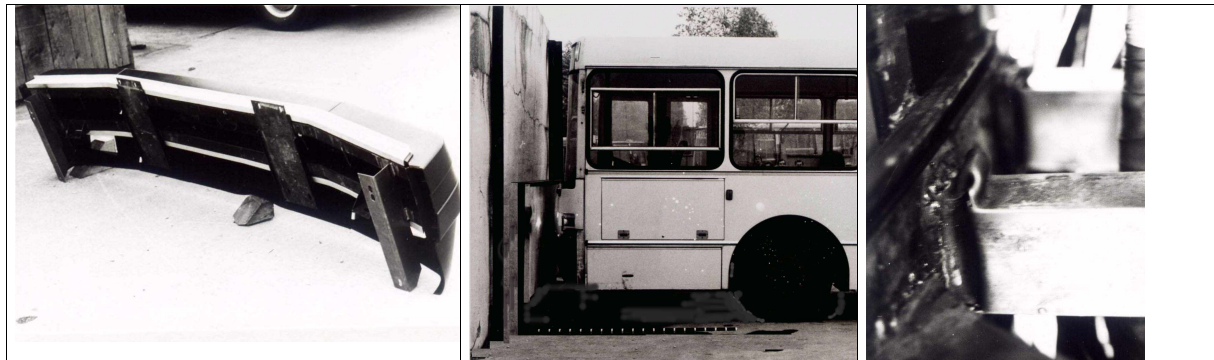


**Figure 1a-c. Pictures on the bumper and bus frontal impact test with 6,98 km/h speed**

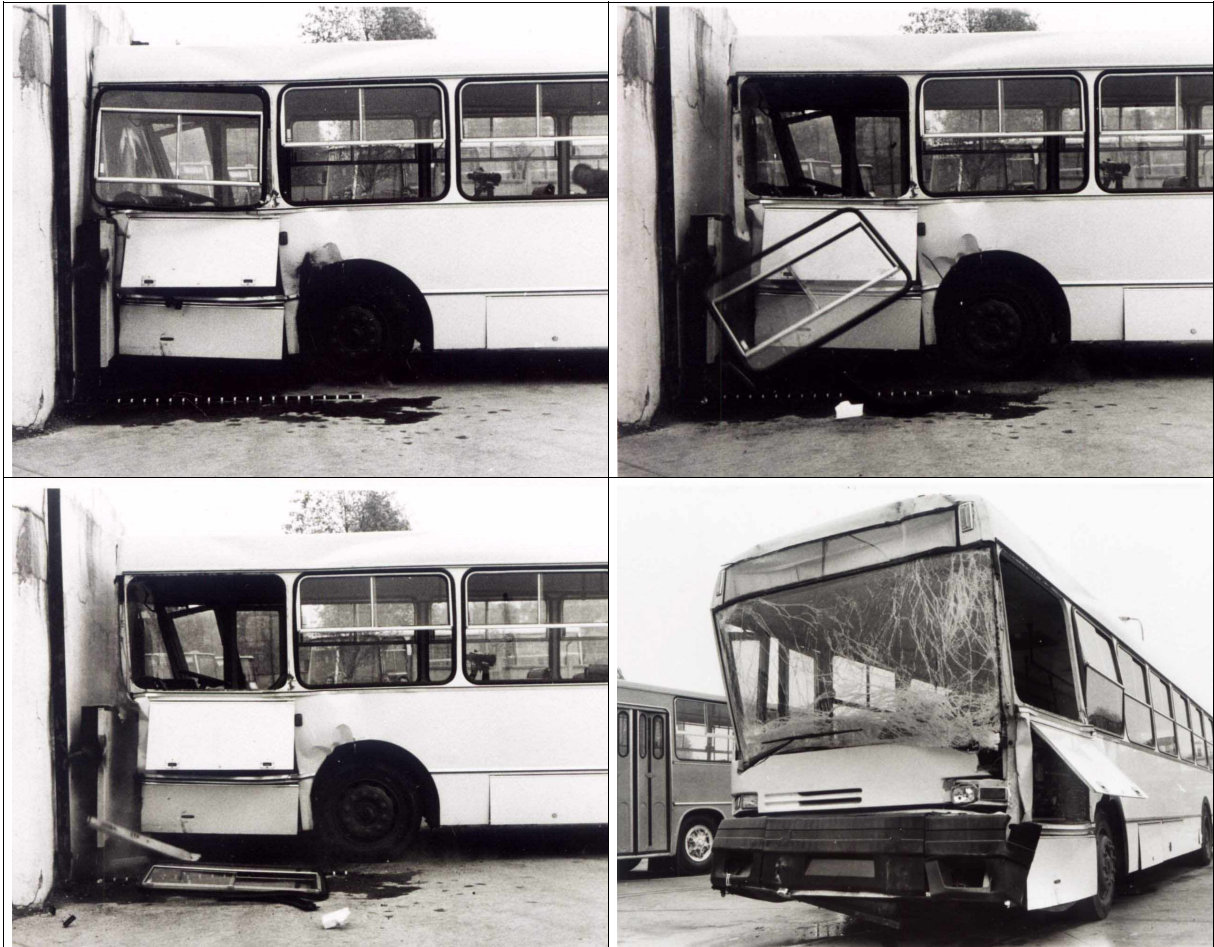


**Figure 2a-d.** Phases of frontal impact with 29,76 km/h speed; the front-wall wrinkled up onto the wooden impact surface which measured distance was 250 mm from the concrete block and the roof's edge reached the block too.

The left beam has suffered significant deformation after the 29,76 km/h speed impact; 130 mm was the measured specific compression. (**Fig. 3.a.**) On the right beam the measured compression was less, only 80 mm. (The left side is less rigid as the right one due to the left-side front door-frame.) The

driver seat has slid back thanks to the driver safety platform and the dashboard has cracked. The free distance between the steering wheel and the frontal surface of driver seatback was 330 mm, which ensures the survival due to the safety platform. (**Fig. 3.b-c.**)



**Figure 3a-c.** Consequences of the 29,76 km/h speed impact

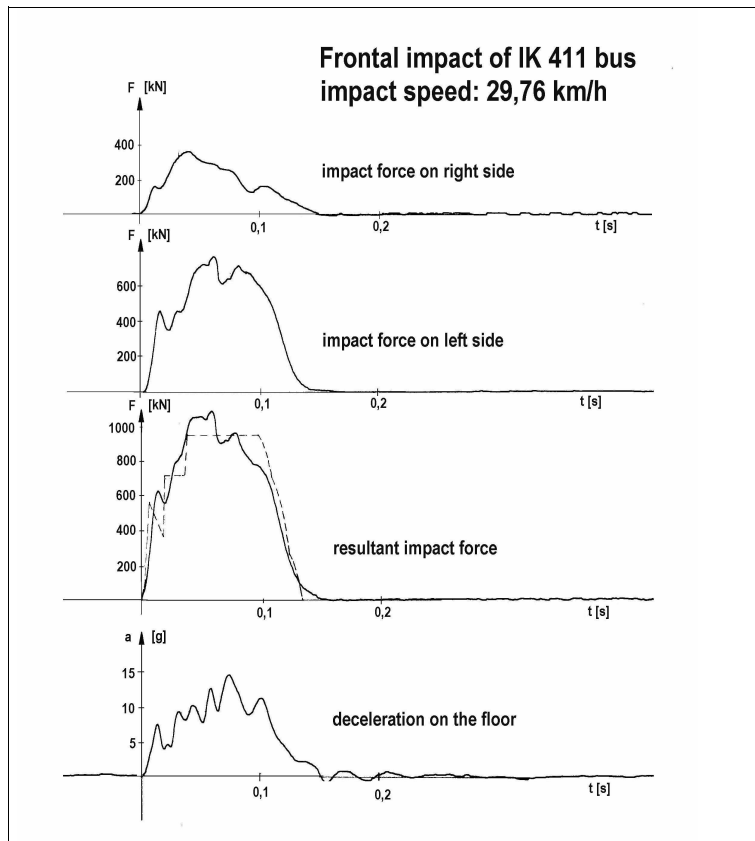


**Figure 4. Force and acceleration diagrams of 29,76 km/h speed frontal impact**

The rigidities of right and left side of bus are significantly different, the measured impact force is doubled on the right side as the left one. At 30 km/h speed impact the observed floor deceleration is little bit higher than the prescribed value of ECE R80. The standardized average value shall be between 8-12 g related to the regulation of ECE 80, which is determined for testing of bus seat-frame strength and fixing.

The next statements can be made if the result is evaluated according to the criteria of force, energy and metamorphosis:

The bumper elements shall have less rigidity than the chassis itself by the **critereon of force**. This became untrue at 7 km/h speed impact, the chassis would have been stiffened. (This reinforcing was performed during the serial modification of IK 415 buses.)

By the supposed **energy critereon** the kinetic energy of the vehicle must be absorbed by elastic deformation energy of other pre-determined elements of bus bumper and framework up to 3,5

km/h impact. Over this speed (up to 8 km/h impact speed in optimum) only the changeable elements of bumper can be destroyed.

This bus did not fulfill this presupposition due to the crumpling of understructure at 7 km/h impact.

By the **deformation critereon** during the energy absorbing process the (elastic and residual) displacement possibility of structural elements shall be limited and the deformation order of structural elements shall be in presupposed way. The damage-free conditions of elements can be allowed or ensured due to this. It was fulfilled.

#### **Bus front-wall (driver cabin) tests**

The so-called safety platform serves the ensuring suitable and adequate survival space (free space between the dashboard, steering wheel and driver seat) for the bus driver during and after crash process. It was experimented on development of IK 200 buses and applied in final serial models.

Different types of static and pendulum impact tests were carried out to clarify the mechanism of safety platform. (Figures 5, 6.)

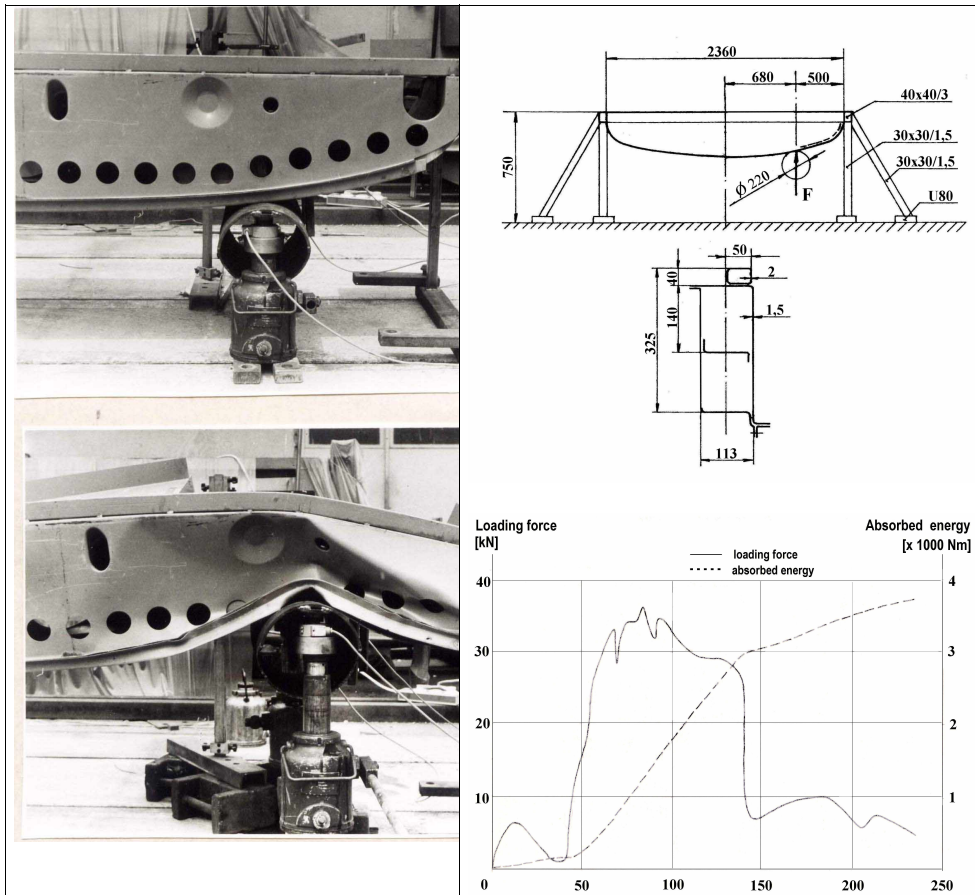


Figure 5. Static energy absorbing test of front-wall rail (in case of impact with a tree)

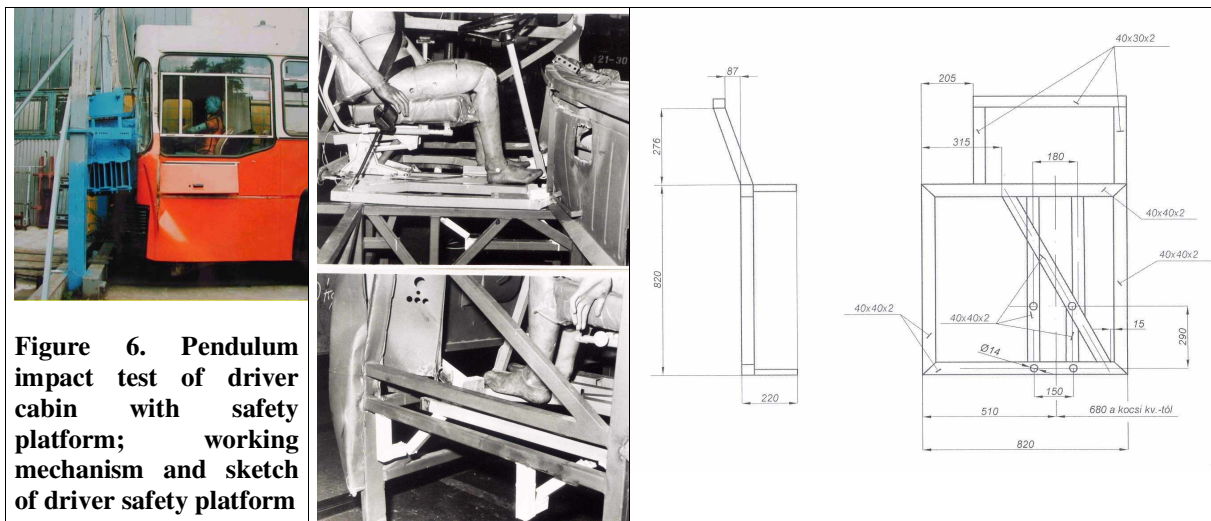


Figure 6. Pendulum impact test of driver cabin with safety platform; working mechanism and sketch of driver safety platform

### Static and dynamic test of IK 411 understructure [3]

Quasi-static laboratory compression test was carried out on the IK 411 K1 understructure and the force demand for the first plastic joint was measured in value of 305 kN. Newly tested after modification, reinforcement, the measured maximum compression force was 400 kN.

Two pendulum tests happened on this understructure with a 4.1 ton-pendulum from two different heights. By an impact with  $E_1=16$  kJ energy only slight deformations occurred, then four plastic joints were detected after impact with  $E_2=18,5$  kJ energy, the understructure crumpled. (Figure 7.)

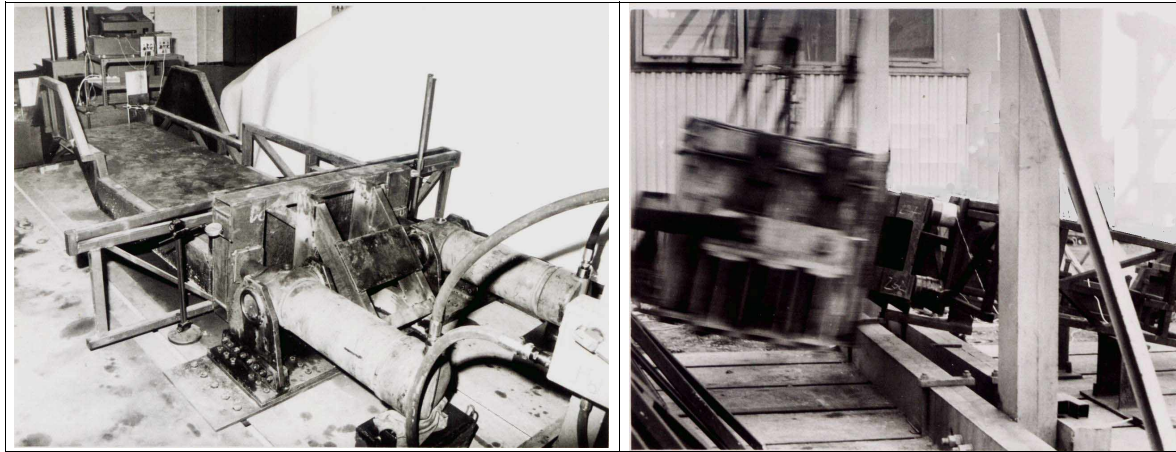


Figure 7. Static and dynamic tests of bus understructure

### Static test of inner elements of IK 411 bus

Energy absorbing elements of IK 411 bus bumper were designed from 4 pieces of 60/40x2 mm cross-section rectangular tubes with length of 175 mm. The maximum force due to stability limit of four inner elements was 580 kN, which force was decreased to 380 kN after 100 mm displacement. The crushed tubes were deformed not only in

longitudinal direction, but buckled too due to the oblique connection. Maximum resultant compression of inner elements was 115 mm. (The yield stress of mild steel bumper elements was 240 MPa.) The bumper is able to suffer 240 mm of accumulated compression. (Figure 8.)

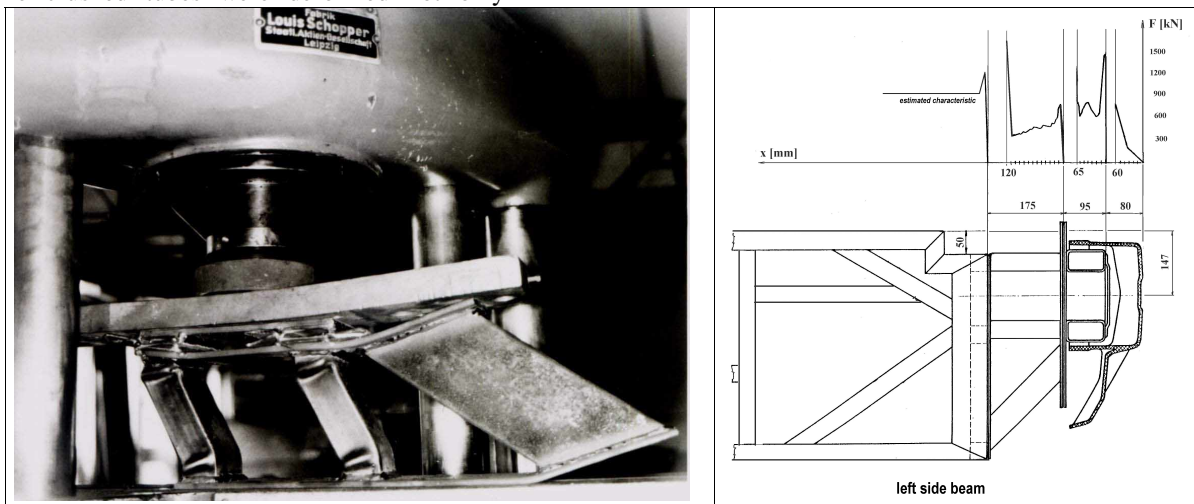


Figure 8. Static compression test of bumper energy absorbing elements of IK 411 bus

## FEM SIMULATIONS

### Simulation model [5]

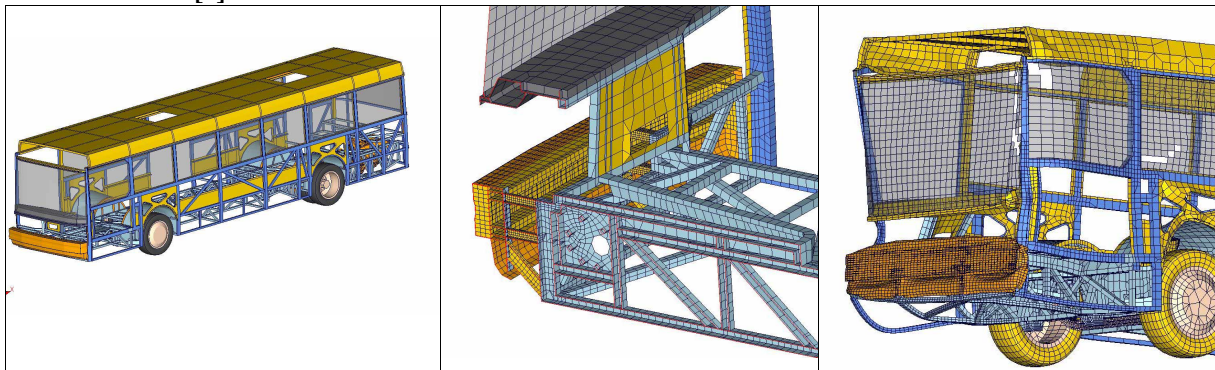


Figure 9. Elastic material properties for glazing with rupturing are defined by max. plastic strain

The bus model in the used PAMCRASH program is structured by sheet elements. The layout of front and rear axles, engine-gearbox connections to the frame-structure happened with joint-balled bar elements.

Dynamic Crash analysis has been performed on the FEA model detailed below:

*Analysis type:* Front Crash, impacting into rigid wall under three load cases as initial velocity (3,6km/h, 6,98 and 29,76 km/h)

*FEA model:* Number of Element: 79091 (SHELL) - Number of Nodes: 71432 – Number of properties: 98

Total model mass: 10007 kg

*Bumper:* The Bumper structure as energy absorbing part was composed of three major components.

- a) Covering plastic shell
- b) Foam (polyurethane) (*applied stress-strain curve in Fig. 11*)
- c) Steel tubes (*applied stress-strain curve in Fig. 10*)

*Material type:* Elastic-plastic material properties with strain rate dependent hardening for steel parts. Elastic material properties for glazing with rupturing is defined by max. plastic strain. (*Fig. 9*)

*FEA Solver:* PamCrash v.2001

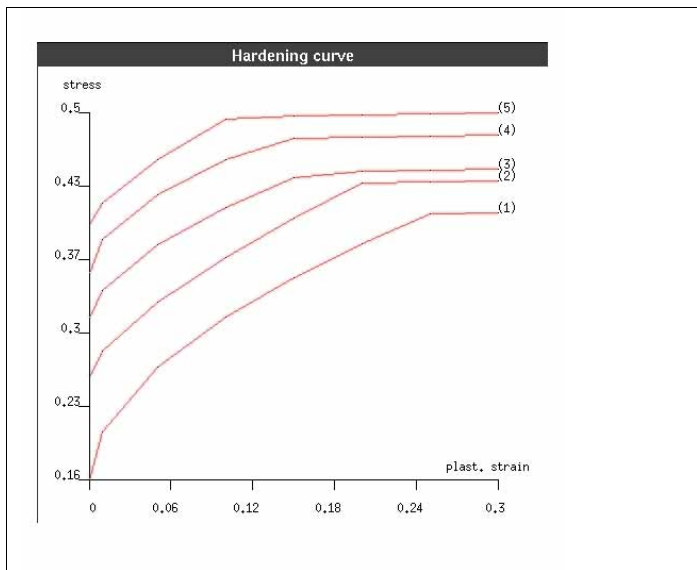


Figure 10. Applied stress-strain curve of steel tubes

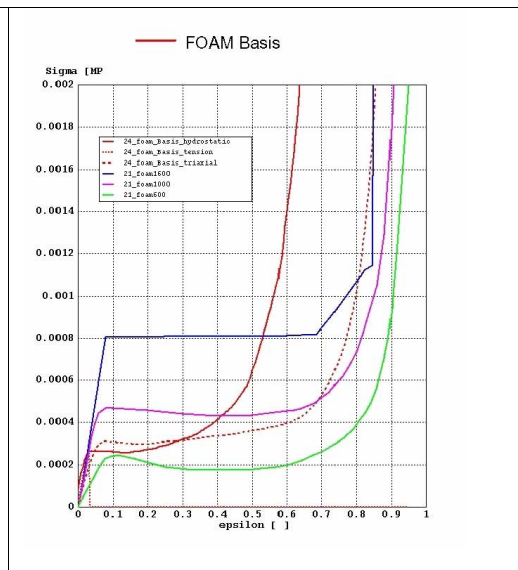
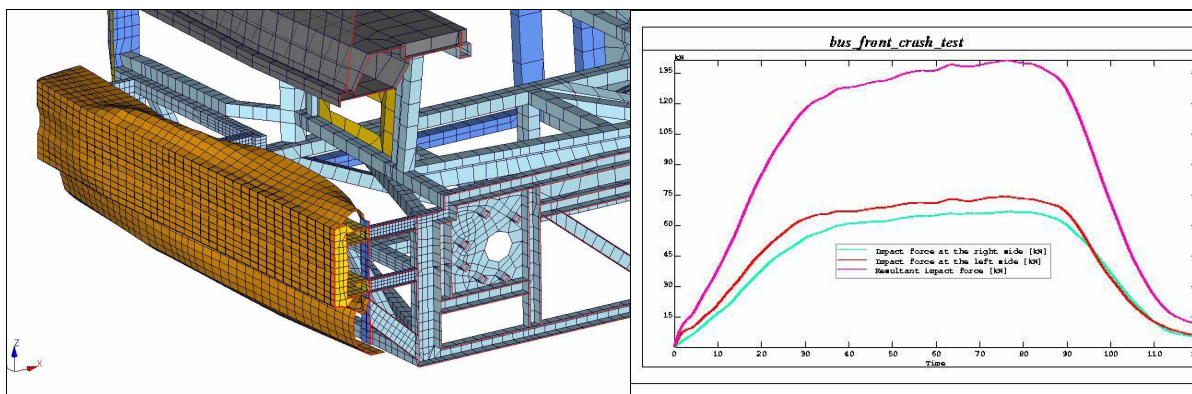


Figure 11. Polyurethane applied stress-strain curve

### Impact simulation test with 3,6 km/h speed



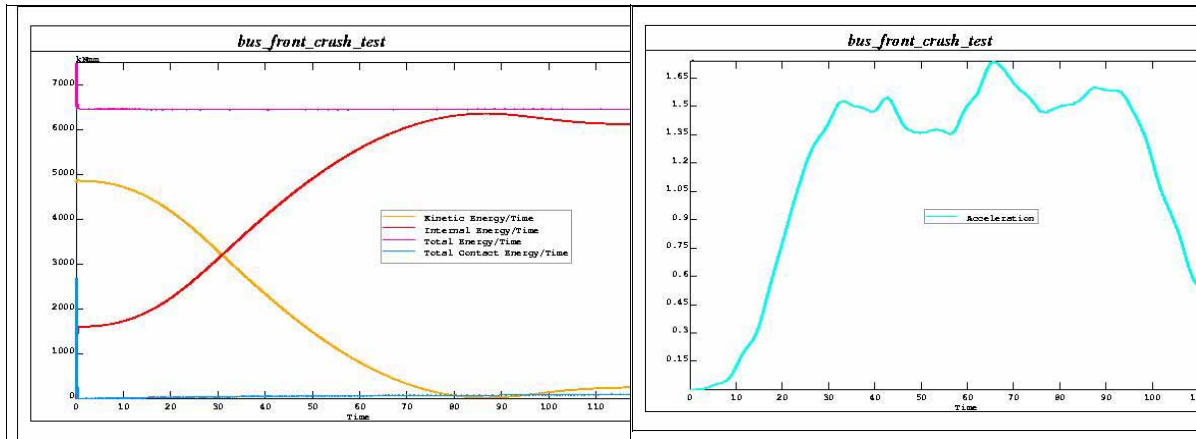


Figure 12. Elastically deformed bumper at the 3,6 km test [maximum deformation](a); the [left, right and resultant] force curves (b); energy diagrams (c); deceleration on the floor at CG in [g] (d)

Impact simulation test with 6,98 km/h speed

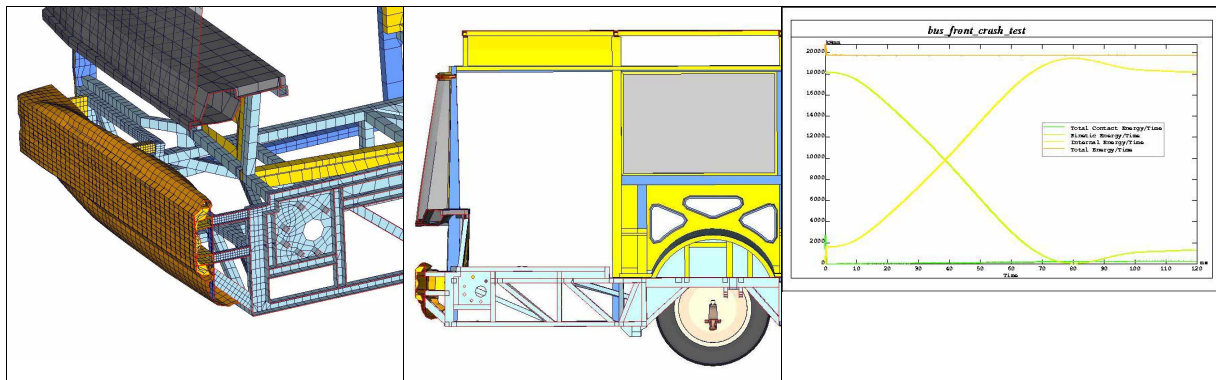


Figure 13. Deformed energy absorbing elements of bumper at the 6,98 km test (a,b); energy diagrams (c)

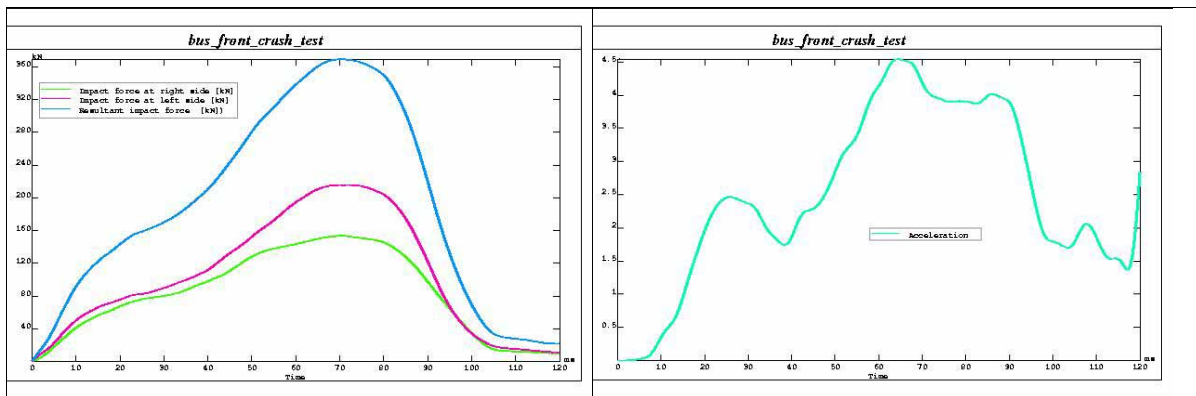


Figure 14. The [left, right and resultant] force curves at the 6,98 km test (a); deceleration on the floor at CG in [g] (b)

## Impact simulation test with 29,76 km/h speed

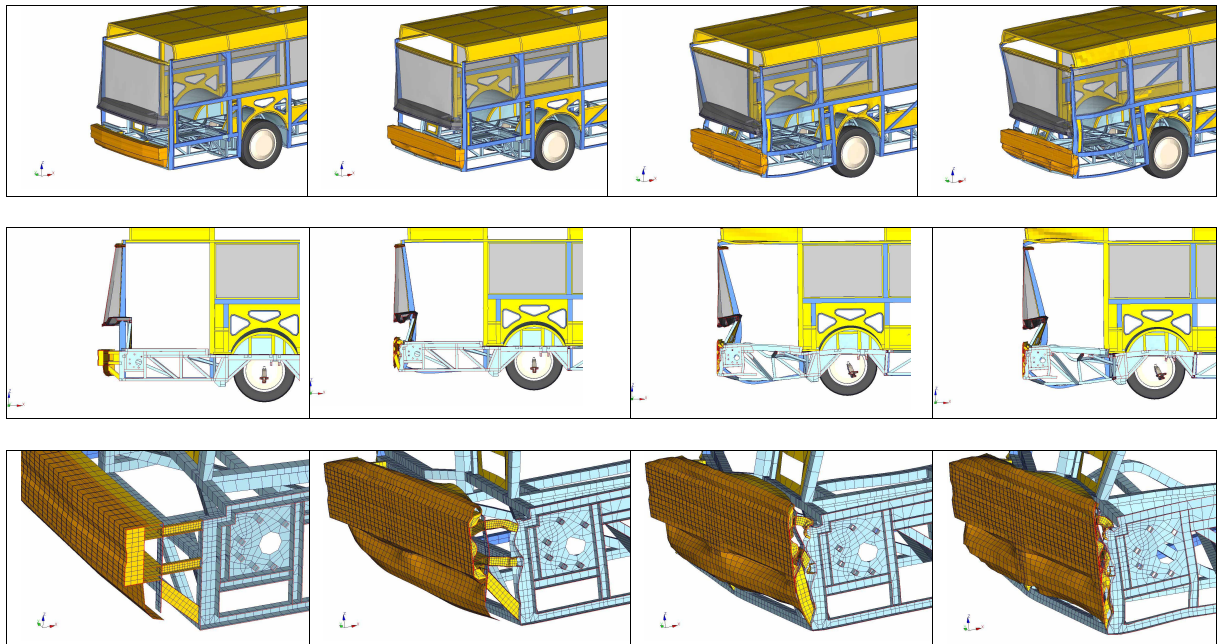


Figure 15. Some pictures on deformation process at 29.76 km/h speed impact

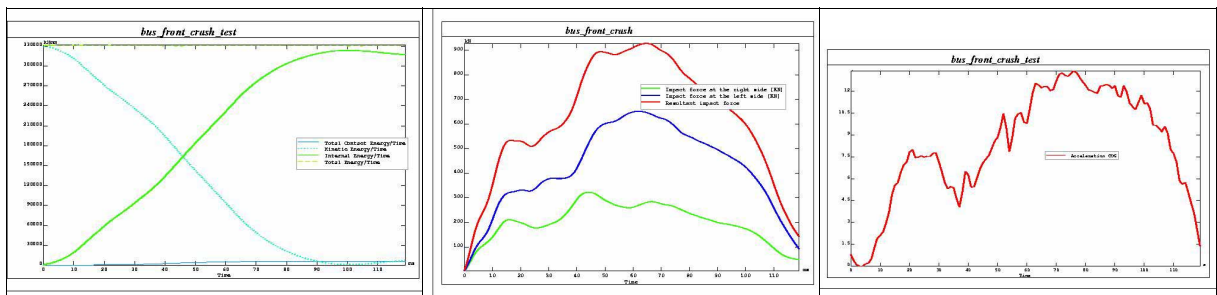


Figure 16. Energy diagram curves at the 29,76 km test (a); the [left, right and resultant] force (b); deceleration on the floor at CG in [g] (c)

## CONCLUSIONS

At full test with 29,76 km/h speed the measured floor deceleration is a bit higher than with prescribed trolley deceleration by ECE R80. (ECE R80 prescribes 8-12 g deceleration for trolley at 30 km/h speed standardized impact. The measured values are rather congruent with the force (rooted from 11-13 g deceleration) required by ECE R14 related to M3 bus category seat-belt anchorages. [4]

The front-wall, understructure, bumper energy-absorbing capability shall be examined together and

shall be linked them due to the force, energy and kinematical deformation criteria.

The detailed and accurate FEM model simulation has lead to analogous result as real impact test. (Fig. 17.)

This developed model set-up and simulation version is very effective tool for checking the bus impact behavior in the design process.

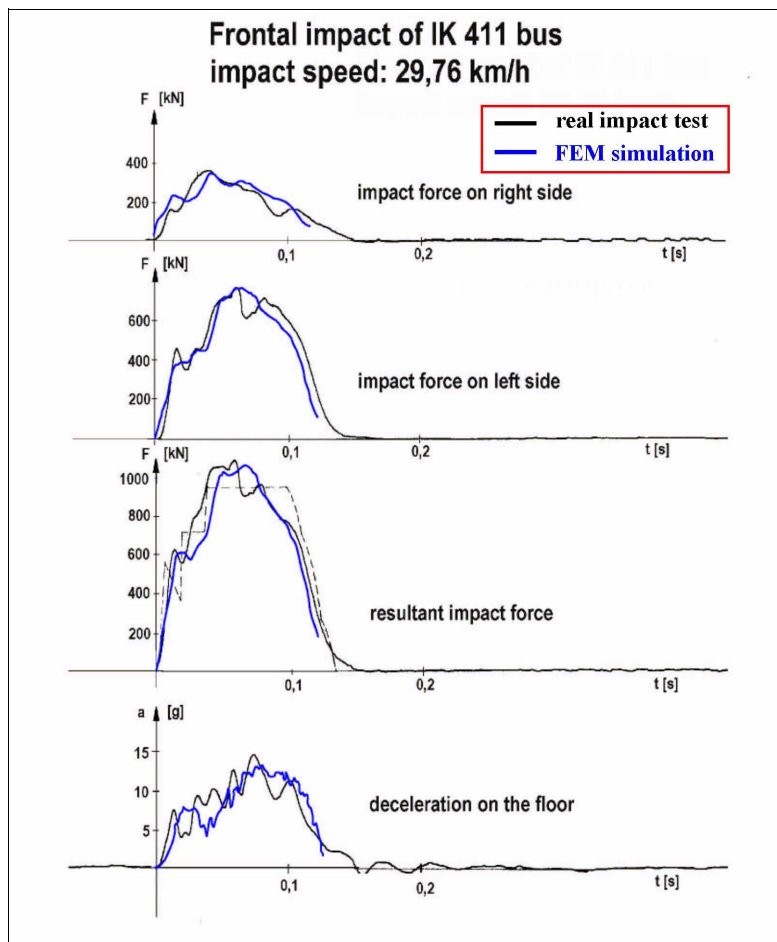


Figure 17.  
Interlocking the real and simulation  
impact test results. The measured  
and calculated curves are well  
congruent.

## REFERENCES

- [1] *S. Vincze-Pap*: Tests evaluation on passive safety requirements for bus driver cabin (AUTÓKUT Test Report, JÁ-244/80/14–1980)
- [2] *L. Albrecht*: Front-wall test of IK 411 K1 bus (AUTÓKUT Test Report, AU-53/85 –1985)
- [3] *S. Vincze-Pap*: Stability tests on understructure of IK 400 bus (AUTÓKUT Test Report, JÁ-244/80/21–1980)
- [4] ECE Regulation 80: Uniform provisions concerning the approval of seats of large passenger vehicles and of these vehicles with regard to the strength of the seats and their anchorages, 07/2001
- [5] *S. Vincze-Pap, N. Horváth, A. Csiszár, A. Szász*: Autóbuszok passzív biztonsági vizsgálata számítógéppel (*Bus passive safety tests with computer*), Paper No.: 308 on the CD, ISBN 963 9058 17 3, 33<sup>rd</sup> Meeting of bus and coach experts, 2-4 September, 2002, Keszthely, Hungary

# **FRENCH STUDY PROGRAM TO IMPROVE ACTIVE AND PASSIVE SAFETY ON MILITARY VEHICLES**

**Vincent Schmitt  
Christian Renou  
Norbert Guiguen**

DGA/ETAS (Etablissement Technique d'Angers)  
France  
Paper number 05-0308

## **ABSTRACT**

As far as military vehicles are concerned, in particular heavy logistics trucks, French land forces must face various constraints, often unknown to classical safety requirements.

In fact, the main requirements for these vehicles are :

- 1) long life, which implies, after years' service, the risk of old-fashioned vehicles lagging behind, when it comes to new technologies ;
- 2) cross-country capacities, which are often possible using off-road tyres and big-stroke suspensions, with sound behaviour on muddy or sandy soils, but only fair or even poor behaviour on asphalt roads ;
- 3) important payload with a high centre of gravity, which is detrimental to sound behaviour, increasing the risk of rollover in cornering conditions.

To improve safety on these vehicles, a study program is in progress within the French MOD. In this paper, we are describing the genesis of this program, and the means we have chosen, summarised as follows :

- 1) an analysis of all accidents involving French military vehicles will be carried out, as a result of which a complete accident database will be set up ;
- 2) an exhaustive list of active or passive safety systems will be established ;
- 3) a global matrix between all real accidents and all these safety systems will be created, using such methods as simulation : for each accident and, with the vehicle equipped independently with each safety system, this matrix is aimed at estimating if :
  - the accident would ever have occurred (with a level of likelihood) ;
  - the seriousness could have been reduced ;
  - no real changes would have occurred at all.

At the end of the study due 2007, a list of the top 10 safety systems, in terms of a cost/efficiency ratio, will eventually be drawn to equip new or refurbished military vehicles, and a specific safety demonstrator made and tested.

## **INTRODUCTION**

A study program is in progress within the French MoD, aiming at reducing human and material losses due to traffic accidents involving military vehicles. Accidents concerned are of all kinds, from single open road accidents to accidents happening during military operations, for example in cross-country conditions.

Likewise, all kinds of military vehicles could be integrated within this study ; different categories such as light vehicles (4x4), heavy trucks, and armoured tanks are defined to distinguish them.

This program is made up of different parts detailed below ; it is meant to be exhaustive towards all potential sources of loss reduction. The main goal is to obtain a global quantification of the potential contribution of actual, new or future civilian safety systems, issued from automobile industry, in relation to real accidents pertaining to military vehicles.

## **GENERAL SURVEY**

On military vehicles, there are four essential elements likely to constitute a risk factor :

- . The vehicle,
- . The load of the vehicle,
- . The driver,
- . The environment.

The vehicle can be a risk factor if its conception is inadequate or obsolete, if the maintenance is not sufficient, or in case of a sudden breakdown, such as for example a brake system failure ;

The load of the vehicle can be a risk factor if it is inappropriate in relation to the vehicle (too heavy, or with a centre of gravity too high), or in case of the vehicle bad coupling securing;

The driver can be responsible if he makes a driving mistake, if he is under the influence of drugs or alcohol, if he is inattentive because of

smoking, phoning, or if he does not respect road regulations, etc ;

The environment constitutes the last factor ; external environment includes other vehicles, meteorological conditions (rainy, foggy, snowy and all slippery conditions), roads and their adhesion or flatness characteristics, and off-road specific tracks (sandy, muddy or underwater) ; internal environment includes noises and typical cold or warm conditions in armoured vehicles with enclosed cell, and big stress due to the military operations.

Accident causes obviously vary ; one generally speaks of lack of attention, excessive speed or skidding, as the primary elements bearing a direct influence on the accident ; and as secondary or complementary causes, those which only contribute to the realization of the accident, the last case being considered as an aggravating factor.

### **SHORT RETROSPECTIVE**

In France, the accident toll on the roads has decreased from about 17 000 to 5 200 (i.e. year 2004) in the last thirty years ; during the same period, the number of kilometres travelled has been multiplied by about 3. It means that the risk of having a fatal road accident is at present the same for a 1000 km trip as it was three decades earlier for a 100 km trip.

Risk reduction is due to multiple factors apparently difficult to quantify precisely; one can however safely pinpoint among those and for the last thirty years : the compulsory seatbelt, the reduction of legal alcohol intake, the MOT technical check-up of old vehicles, the vehicle on-board active and passive safety systems growing in importance, the improvement of road infrastructures and road markings, etc.

Concerning active and passive safety systems, we wish to note that light vehicles have been equipped before heavy trucks (e.g. ESP program, airbags, etc...).

### **MILITARY VEHICLES IN FRANCE**

1. Military vehicles constitute a specific category ; they often have a very long service-life, of up to 40 years, contrary to civilian vehicles, which can only boast of a life ranging from 8 to 15 years. Refurbishment is always possible, but it will only be after a long time (often half-way through a life span), hence the other problem of having similar safety equipments on both types of vehicles.

2. A lot of technical points could also cause problems, when it comes to integrating new safety systems to military vehicles. Here are some examples regarding active safety :

- armour causes the kerb mass to be heavier on military vehicles than on civilian vehicles ;
- the load often has a high level of centre of gravity ;
- road mobility and behaviour can be limited by off-road capacities, not always compatible among themselves ;
- small windcreens and armours are detrimental to external visibility.

And other examples of passive safety are :

- the capacities for structural deformations to occur during a crash are very poor for an armoured vehicle ;
- a lot of metallic and hard elements in the driver's cab or passenger cell could easily become blunt. Very often, doors, roof or pillars do not have any padding at all.

3. The actual state of safety equipments on military vehicles point out a lot of potential improvements ; some examples of which are :

- ABS systems only appeared about five years ago on military vehicles ; and only for new or refurbished ones ;
- ESP systems (and other similar systems) do not exist at present ;
- safety belts, when they are present, are old-fashioned models, often with only two points of anchorage ;
- head restraints rarely exist ;
- no vehicle is equipped with airbags.

### **POSSIBLE ANSWERS**

#### **Statistical survey**

Before dealing with the reduction of accident losses properly speaking, one should first acquire a sound knowledge of the accident typology involving military vehicles. In fact, we must establish the nature of accidents occurring most frequently, and the type of vehicles to which they apply. This question needs a statistical survey of French military road accidents in the last decade, based on the practices of specialised civilian laboratories.

We shall thus constitute a database of all military accidents, with a lot of details, making it possible to acquire a good knowledge of real-life accidents.

In this database, we shall have for example the following standard data :

- a description of the circumstances (date of accident, estimated speed, meteorological and traffic conditions, type of road...);
- the probable main cause ;
- the aggravating factors ;
- crash type : frontal, rear or side impact, rollover, location of first impact, eventual second impact ;
- number of vehicles or pedestrians involved ;
- toll of dead or injured ;
- cause of injuries (e.g. head impact on steering-wheel) ;
- etc

And specific data linked with the military field :

- the type of vehicle involved (light 4x4 vehicle, armoured vehicle, logistics truck, heavy tank...);
- the type of movement (within or outside France) ;
- the cancellation or not of the military mission because of the accident ;
- the global estimated cost of the accident (considering human losses, material costs, and other costs linked with the military mission) ;
- etc...

This statistical survey could last about six months ; it will be necessary to obtain all detailed accident reports from French land forces authorities, in different regiments.

Once this database is complete, the second phase of the study can start.

### Security improvement

In France, in Angers in particular (ETAS, MoD unit), specific skills required to assess road and off-road behaviour have been developed. This competence makes it possible to impose within an internal regulation frame (French MoD instruction, partially published in April 2004), specific behaviour tests, compulsory for all military vehicles, whether they be new or refurbished.

These tests include, for example, steady-state circular tests, braking in a 100m-radius turn, severe lane change manoeuvre, emergency braking, etc. On these grounds, ETAS has been granted ISO/CEI 17025 accreditation.

For each test, a minimum threshold is required to qualify a military vehicle. Specific test conditions are described in official documents.

Thanks to this regulation, only vehicles having at least a fair behaviour will be selected ; vehicles with bad or poor behaviour are eliminated. However important this can be for active safety, it is always possible to go beyond.

A lot of work has been carried out by the civilian vehicle industry in the last decade (e.g. : VDC or ESP with different functions such as cornering braking control), and research laboratories keep working on these safety elements (e.g. : CWAS –crash warning and avoidance system) ; the development of such safety systems could be of great interest to improve military vehicles.

Passive safety has, likewise, made great progress ; airbags have become standard ; new vehicle structures can now absorb an important kinetic energy, passenger protection is drastically different from those which still existed in the '80s.

For that matter, a complete study of existing or future safety systems is needed, to evaluate which ones could have a real interest to military vehicles.

### METHODOLOGY CHOSEN

Once the accident database has been established, a complete state of the art, concerning safety systems, must be carried out.

ETAS proposes a global organisation of this state of the art, by grouping existing and future systems into specific categories.

The table 1 defines the different categories and the corresponding systems ; it must be correctly completed :

Safety improvement by...	In detail	Examples
environment analysis	detection of other road users detection of obstacles vision improvement (night vision, fog vision, rain vision...) detection of slippery conditions detection of nearby road profile (curvatures, crossings, bumps...)	CWAS <sup>1</sup> , Infrared sensors, Grip estimator, GPS system with precise map,...
vehicle static state analysis	detection of overload detection of a bad position of the centre of gravity payload	No example (not yet!) for in-board sensor

<sup>1</sup> Collision warning avoidance system

Safety improvement by...	In detail	Examples
vehicle dynamic state analysis	detection of rollover threshold detection of inadequate speed in relation to road profile	Accelerometer and GPS, pre-crash systems, ABS, ESP,...
driver behaviour analysis	detection of inattentiveness detection of alcohol or drug detection of excessive duration of driving,...	Driver surveillance camera, specific sensor on steering-wheel, autopilot, ...
use of regulation constraint	limitation of regulation derogations (usually made for military needs)	Addition of a rear protective device (eventually retractable)
improvement of the road-holding ability	Improve behaviour by mechanical components	New chassis or suspension components, ...
analysis of the effects of crash on armoured vehicles	understand the problematic of military vehicle during a crash	Will be dealt with later
structure improvement	creation of capacities to absorb kinetic energy	specific bumpers,...
improvement concerning passenger protection	Shock absorbers for vehicle occupants	Airbags, padding systems, enhanced seatbelts...
Improvement concerning pedestrian or other road users' protection	Other road users crushing avoidance	Protective devices around vehicles,...

**Table 1**  
**Categories of safety systems**

At this point of the study, the important thing is to evaluate how each safety system could have an impact on the different accidents in the database.

So, for each system and each accident, experts must analyse, with different tools such as dynamic simulation, the probability of :

- the event suffering no real changes ;
- avoiding accidents ;
- reducing the seriousness of accidents ;
- or, on the contrary, increasing the seriousness of accidents.

For a proper evaluation of each system, this analysis must be carried out in terms of global costs.

For example, if the cost of one accident is estimated at 70 000 € (10 000 € for injuries, 25 000 € for the vehicle and 35 000 € for the military system), the best safety system will be the one which makes it possible to reduce the cost of 70 000 € (probability of 100% for accident not happening) ; but often, a good system will be the one allowing a cost reduction of at least 50%.

At the end of this procedure, we shall obtain a table (table 2) summarising all the results :

Type	Accident case (#)	Global cost (€)	COST REDUCTIONS					etc
			System #1	System #2	System #3	System #4	etc	
Frontal	#1- F	15000	4500	7500	1500	0	...	
	#2- F	28000	12000	14000	7000	3000	...	
	#3- F	12000	0	3000	etc	...	...	
	#4- F	18000 0	15000	165000	...	...	...	
	etc	...	...	...	...	...	...	
Rollover	#1- Ro	66000	0	66000	21000	...	...	
	#2- Ro	94000	45000	45000	etc	...	...	
	#3- Ro	18500 0	0	0	40000	...	...	
	#4- Ro	12000	12000	12000	2500	...	...	
	etc	...	...	...	...	...	...	
Rear	#1- Re	14000	0	0	2000	3500	...	
	#2- Re	35000	0	0	1500	6000	...	
	#3- Re	67000	etc	...	...	...	...	
	#4- Re	11000 0	...	...	...	...	...	
	etc	...	...	...	...	...	...	
Side	#1- S	45000	0	4500	1500	15000	...	
	#2- S	72000	2000	18000	3000	...	...	
	#3- S	48000	etc	...	...	...	...	
	#4- S	12000	...	...	...	...	...	
	etc	...	...	...	...	...	...	

**Table 2**  
**Accident cost reduction vs safety systems**

This table records, for each type of accident, and eventually each category of vehicle, the best

<sup>2</sup> example : #1 = ABS , #2 = ESP, #3 = Frontal airbags, etc...

systems available in terms of accident cost reduction.

## **CONCLUSION**

So, it will be possible to extract a “top ten” marking of the best systems, in accordance with their respective costs. In fact, this last parameter will also have to be taken into account for the best possible choice.

A global refurbishment programme based on this “top ten” marking system will eventually be launched for the main land forces vehicles.

Prior to this refurbishment, we mean to carry out an experimentation on demonstrator vehicles, including different systems derived from our “top ten” marking system, testing vehicles in hard conditions, ranging from bad weather with slippery conditions, to off-road configurations with important vibrations.

In the near future, a lot of military vehicles will hopefully have a global safety performance at a high level, with a minimum factor two accident reduction cost.

# **A COMPUTER SIMULATION FOR MOTORCYCLE RIDER INJURY EVALUATION IN COLLISION**

**Hideo Namiki**

**Toyokazu Nakamura**

**Satoshi Iijima**

Honda R&D Co., Ltd. Asaka R&D Center

Japan

**Paper Number 05-0309**

## **ABSTRACT**

Honda is developing a computer simulation technology designed to predict injury levels from an impact to when an MATD dummy strikes the ground during testing. Correlation of results of full scale impact tests and computer simulation specified in ISO/CD 13232, were examined. As the result, it was validated that the computer simulation can predict injury levels from an impact to when a dummy strikes to the ground. The performance and effectiveness of an airbag system for a GL1800 in 200 impact configurations and 400 cases specified in ISO/CD 13232 was evaluated by using the computer simulation. As a result, the total average benefit was 0.048, risk was 0.004. The highest average net benefit appears at the range from 20 to 25 m/s in the relative impact speed.

## **INTRODUCTION**

Honda has been researching ways to increase the protection of motorcycle riders in accidents since the 1960s<sup>(1)</sup>. In recent years, research has been conducted on the possibility of motorcycles equipped with an airbag system as a means of enhancing rider protection. In the research, an airbag system including impact detection sensors was manufactured on an experimental basis and mounted on a GL1500, a large touring motorcycle of Honda. Impact tests were conducted using the motorcycle. The results obtained were reported at the ESV conferences in 1998<sup>(2)</sup>, and 2001<sup>(3)</sup>. One of the findings from the research was that the changes in measured values of injury to the dummy most often affected by the airbag occurred at impact with the ground. ISO/CD 13232<sup>(4)</sup> contains test and analysis procedures for research

evaluation of rider crash protective devices fitted to motorcycles. It specifies that the performance of rider crash protective devices should be evaluated by computer simulation in addition to impact tests using actual motorcycles (hereinafter referred to as full scale impact tests). The computer simulation is intended to cover a 0.5 second time period, from the start of impact through dummy impact to the opposing vehicle (hereinafter referred to as primary impact sequence). We determined, however, from consideration of the results of the tests described above that it would be necessary to evaluate the injury from the start of impact to when the dummy strikes the ground.

Therefore, we conducted tests to establish a computer simulation technology that allows for the prediction of injury levels from start of impact to when a dummy strikes the ground (hereinafter referred to as entire impact sequence). For this analysis, an explicit method FEM software, which is easily expresses shapes and reproduces deformations of vehicles, was selected. In the FEM software, mesh sizes, which largely affect the calculation time and the accuracy of the calculation, were studied and decided. Models of motorcycle, airbag, dummy and opposing vehicle were created and computer simulation calculations were performed. From these calculations, the compliance of dummy motions at the time of dummy strike to the ground was evaluated using the dummy head velocity and torso angles.

As a result, a computer simulation method reproducing testing results with high accuracy was developed. At the same time, a very effective method of shortening the calculation time was contrived. These results were reported to 2003SETC<sup>(5)</sup>. Using the aforementioned computer

simulation method, the research was carried out to evaluating the injury index from the start of impact to the point in time when the dummy struck the ground. Correlation of the results of full scale impact tests and computer simulation, as specified in ISO/CD 13232, covering seven impact configurations and twelve cases, were examined. As a result, it was confirmed that the computer simulation can predict injury index from the start of impact to when the dummy strikes the ground.

## EVALUATION OF INJURY INDEX TO WHEN DUMMY STRIKES GROUND

Developing the computer simulation method reproducing dummy motions with high accuracy, and one which predicts injury levels in the entire impact sequence was carried out. The seven impact configurations specified in ISO/CD 13232 were employed to verify the accuracy of the computer simulation research. The impact configurations are shown in Fig.1. Basically, simulations were conducted both with an airbag and without an airbag. However, incase of with-airbag in No.1 and No.4 of the impact configurations shown in Fig.1 were omitted from the correlation simulation results and full scale test results because the airbag did not deploy in the full scale tests in these configurations. Computer simulations for examination of the correlation were conducted with twelve cases in seven impact configurations. The impact speed of the full scale tests was set at a higher level than that defined in ISO/CD 13232, to evaluate under more sever conditions. The impact speed in the computer simulation was also set at the same speed as the full scale tests.

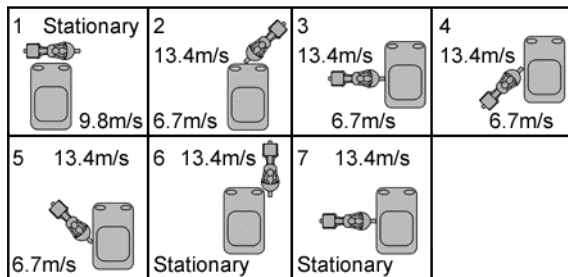


Figure 1. Full scale impact test configurations

## Model Creation Methods

### Motorcycle Model

In the previous study reported in 2003SETC, the motorcycle model used to validate dummy motion was the GL1500, a large touring motorcycle. The motorcycle, however, was changed from the GL1500 to the GL1800 in the subsequent research. In the computer simulation, therefore, a model of the GL1800 motorcycle was created. The motorcycle model was created using the procedure reported in 2003SETC. The whole of the motorcycle model was created as a deformable body for enhancing the calculation accuracy. The motorcycle model is shown in Fig.2.

### Opposing Vehicle Models

Models of opposing vehicles were also created in accordance with the diversification of impact configurations. Because the rigid parts of opposing vehicle model are highly effective for shortening the calculation time, parts with no contact with the motorcycle and dummy and with no deformation employed the rigid model. Four kinds of opposing vehicle models were created, changing rigid parts. The models were used properly in accordance with the impact configurations. Figure 3, 4, 5, and 6 show the opposing models created. Opposing vehicle, HONDA ACCORD 4-door, 1998 to 2001 model, of Japanese specification is shown in Table 1.

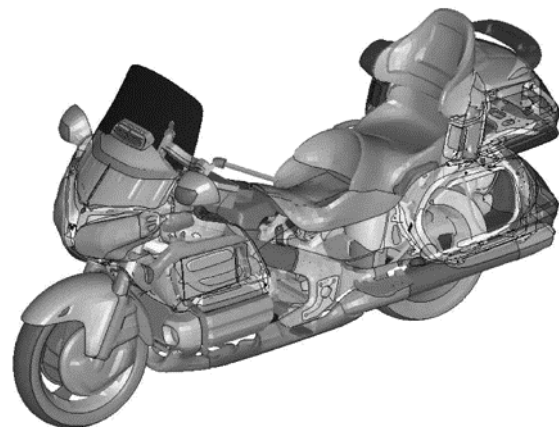
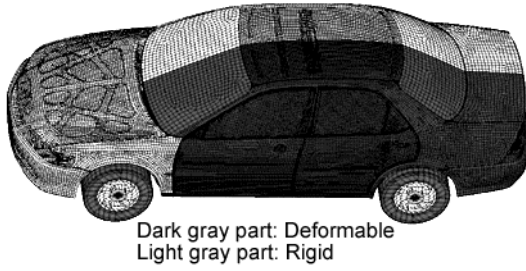
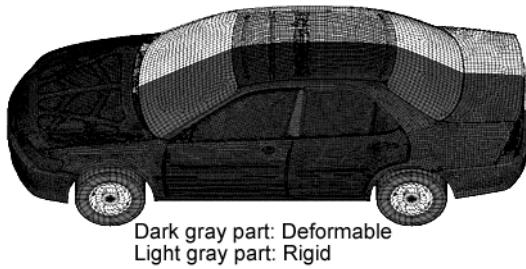


Figure 2. Motorcycle model



**Figure 3. Oposing vehicle model for side impact**



**Figure 4. Oposing vehicle model for front-side impact**

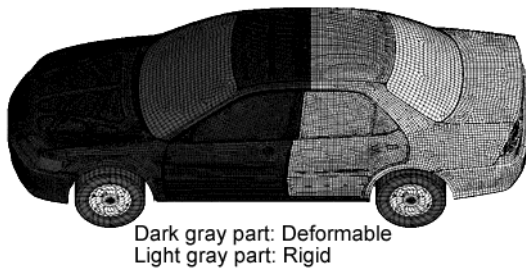


**Figure 5. Oposing vehicle model for front impact**

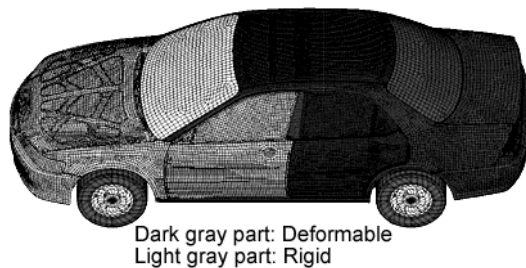


**Figure 6. Oposing vehicle model for rear impact**

**Table 1 Specifications of opposing vehicle**

Manufacturer	Honda
Model	Accord, Japan
Year	1998 -2001
Mass	1300 kg (average)
Overall length	4635 mm
Overall width	1695 mm
Overall height	1420 mm
Wheelbase	2665 mm
Engine displacement	1997 cm <sup>3</sup>

**Dummy Model**

Dummy models were based on the hybrid III 50 percentile model for LS-DYNA<sup>(6)</sup>. They were adjusted to MATD dummy specifications as defined in ISO 13232. Since the evaluation method of injury index of the neck, undefined in ISO 13232, was defined in ISO/CD 13232, a neck model was created faithfully based on ISO/CD 13232. Created models of the neck are shown in Fig.7. The bending characteristics of the neck model were adjusted to conform with the static and dynamic characteristics defined in ISO/CD 13232. The results of static correlation are shown in Table 2. Dynamic characteristics of the neck model such as extension, flexion, lateral and torsion are shown in Fig.8 to Fig.18.

As a result of this research, we determined that the model was usable as the neck model for simulation.

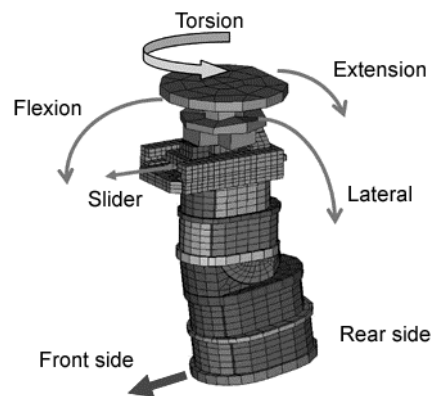


**Figure 7. Neck model of MATD (ISO/CD 13232)**

**Table 2 Neck static characteristics of MATD model**

Characteristics	Load	Required value	CAE model
Flexion angle	20 kgf	17.6±2.6 deg	15.9 deg
Slider displacement	20 kgf	14.0±3.0 mm	13.8 deg
Extension angle	20 kgf	30.9±4.6 deg	27.7 deg
Lateral angle	20 kgf	28.7±4.3 deg	25.8 deg
Torsion angle	3.2 kgf	41.5±6.2 deg	43.6 deg

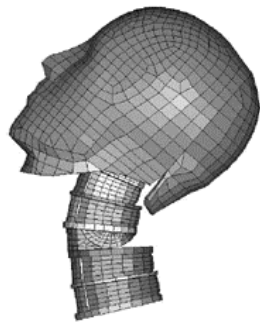


**Figure 8. Dynamic extension position**

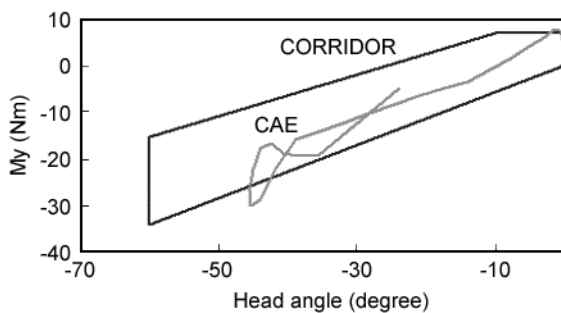


**Figure 9. Dynamic extension moment vs. head angle**

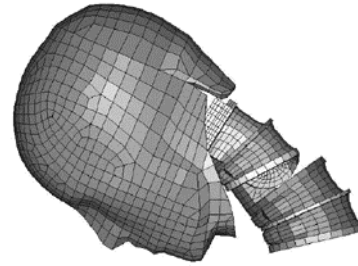


**Figure 10. Dynamic flexion position**

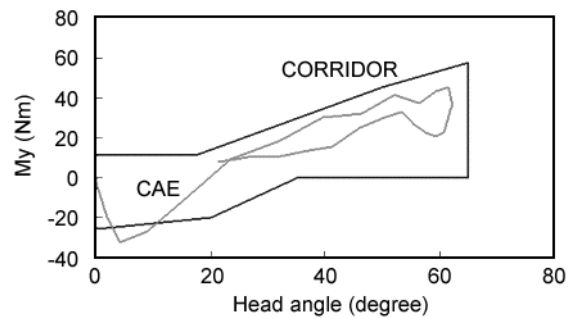


**Figure 11. Dynamic flexion bending moment vs. head angle**

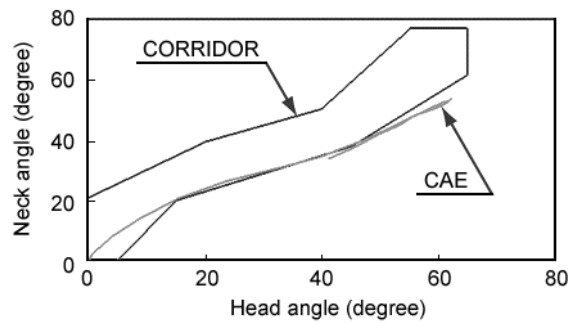


**Figure 12. Dynamic flexion neck angle vs. head angle**

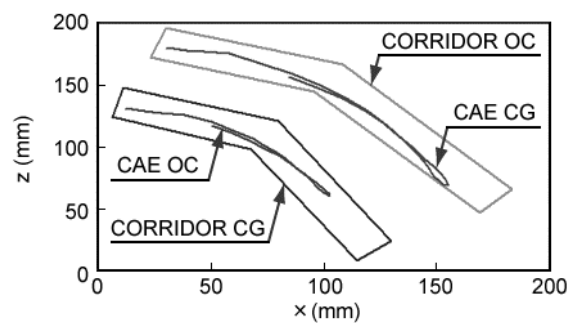


**Figure 13. Dynamic flexion occipital condyle and head center of gravity position**

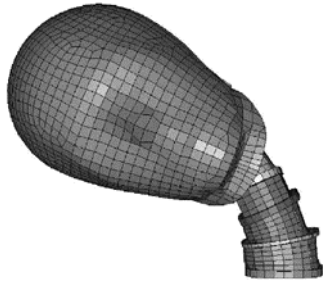


Figure 14. Dynamic lateral position

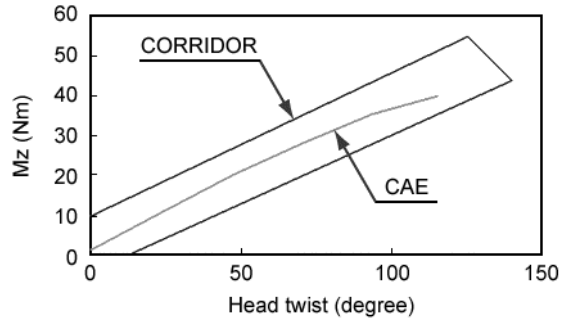


Figure 18. Dynamic torsion stiffness

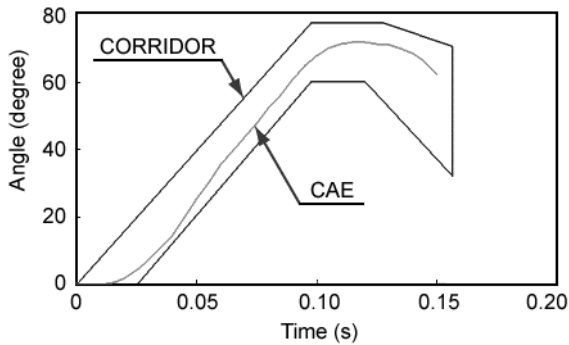


Figure 15. Dynamic lateral head angle vs. time

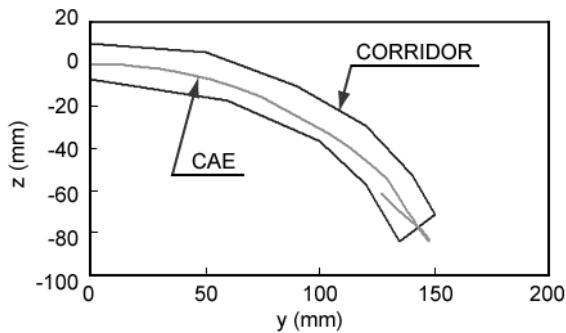


Figure 16. Dynamic lateral head center of gravity position



Figure 17. Dynamic torsion position

### Airbag Model

An airbag model was created based on the airbag redesigned for GL1800. The V-shape of back of the airbag to hold the rider and the connecting and supporting belts from the back of airbag to the motorcycle frame were faithfully modeled. The computer simulation model of the airbag mounted on the model of GL1800 is shown in Fig.19.

### Methods of Improving Accuracy of Models

Each model created requires high accuracy to enable the evaluation of injury index in entire impact sequence.

As the first step for that, parts predictable of deformation in impact were faithfully modeled to simulate the actual test vehicles and motorcycle.

As second step, tests under simple conditions such as the unit test defined in ISO/CD 13232 and the rigid barrier impact tests using motorcycles and opposing vehicles were conducted. Simulation models and some calculation factors were adjusted to conform to the actual tests with high accuracy.

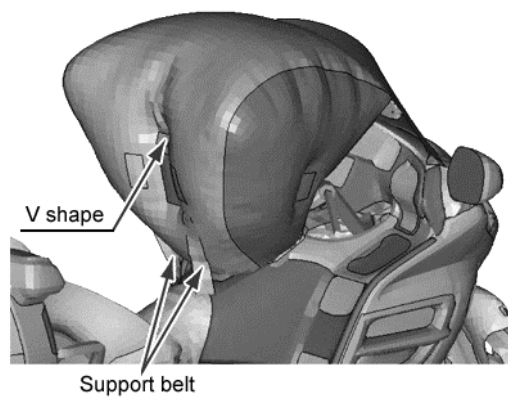


Figure 19. Airbag model

As the final step of validation, model accuracy and some calculation factors were improved by correlation with the test results of 12 test cases using seven impact configurations defined in ISO/CD 13232. Some factors that are not in the simple unit tests or the rigid barrier tests are in the full scale tests, which includes complex phenomenon. Factors such as friction properties as well as detail structural parts of the motorcycle and the opposing vehicle that had been eliminated in prior simulation were added to models of the motorcycle and the opposing vehicle. With respect to these models, the accuracy of the reproducing motion and deceleration of motorcycle and dummy with the seven impact configurations was enhanced. Simulation results of impact configurations of No.3, No.5 and No.7, shown in Fig.1, in which the motorcycle collides with the side of the opposing vehicle, were examined, and the accuracy of models of the side of opposing vehicle and frontal part of motorcycle were enhanced. Next, using impact configuration No.2, shown in Fig.1, in which the motorcycle collides against the front of the opposing vehicle, the accuracy of model of the front part of the opposing vehicle was enhanced. In impact configurations No.4 and No.6, shown in Fig.1, the accuracy of models of the front side of the motorcycle and the opposing vehicle were enhanced, while in the impact configuration No.1, the accuracy of the model of the side of motorcycle was also enhanced.

### Correlation of Evaluated Injury Index

The correlation was verified using the injury index of the dummy with 12 test cases using seven impact configurations. The head injury index, values of HIC in the primary impact sequence are shown in Fig.20; values of HIC after the primary impact sequence to the point in time when the dummy strikes the ground (hereinafter referred to as secondary impact sequence) are shown in Fig.21. The  $r^2$  correlation coefficient in the primary impact sequence and in the secondary impact sequence is 0.94 and 0.77, respectively.

Figure 22 shows the maximum compression ratio on the chest in the primary impact sequence. Because the airbag receives the primary impact,

this is an important factor. The  $r^2$  correlation coefficient was 0.62.

Table 3 shows a comparison between the full scale test results and the simulation results for the fracture of leg bones and knee dislocation. The conforming rate of the test results and the simulation results was 96% in femur and 100% in knee and tibia.

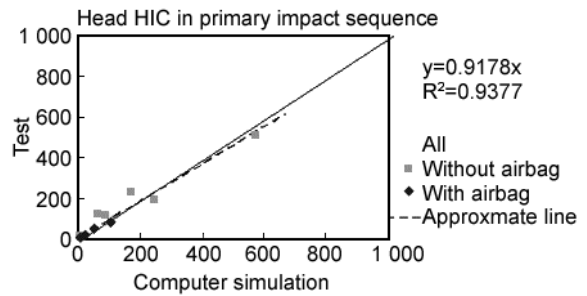


**Figure 20. Correlation of HIC at primary impact sequence**

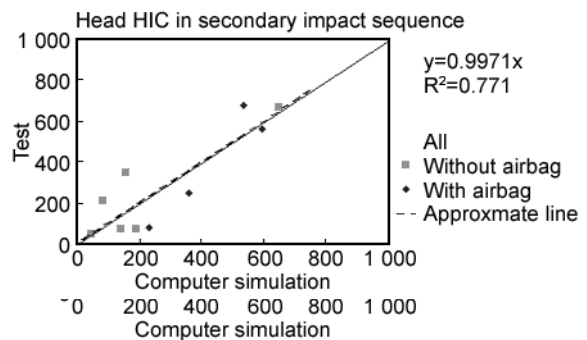


**Figure 21. Correlation of HIC at secondary impact sequence**

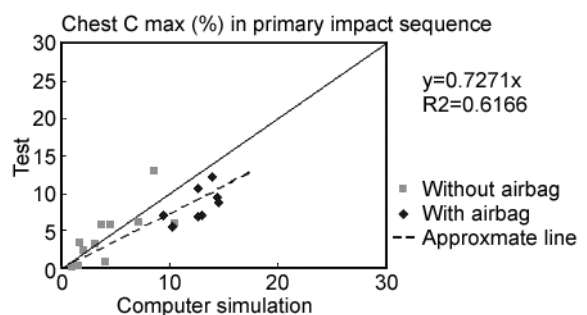


**Figure 22. Correlation of chest sternum compression at primary impact sequence**

**Table 3 Correlation of leg injury for entire impact sequence**

<u>Femurs</u>		Full scale tests		Present collect
		Fracture	No fracture	
Simulations	Fracture	0	1	96%
	No fracture	0	23	

<u>Knees</u>		Full scale tests		Present collect
		Fracture	No fracture	
Simulations	Fracture	0	0	100%
	No fracture	0	24	

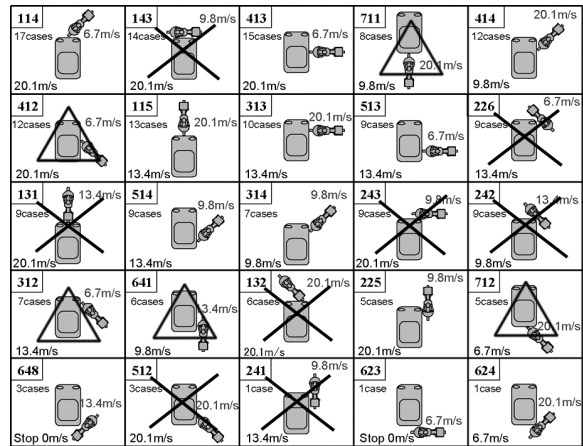
  

<u>Tibias</u>		Full scale tests		Present collect
		Fracture	No fracture	
Simulations	Fracture	1	0	100%
	No fracture	0	23	

From the results above, we judged that this simulation method enables us to evaluate the injury index of the dummy from start of impact to the point in time when the dummy strikes the ground. We judged that this computer simulation enables us to evaluate the risks and benefits of the airbag system using the 200 impact configurations defined in ISO/CD 13232.

**EVALUATION OF INJURY REDUCTION PERFORMANCE OF AIRBAG FOR GL1800**

ISO/CD 13232 defines the methodology for conducting the computer simulation of 400 impact cases, which are 200 impact configurations and with and without the proposed rider crash protective device. The combination of relative heading angles and contact points of 25 impact configurations are shown in Fig.23, and the differences in impact speeds are also defined. In combination, the impact configurations become 200. In these 25 configurations, those configurations marked with X were omitted from simulation because the airbag did not deploy, or deployed but did not influence to the motion of riders or its injury index. Those configurations marked with a triangle were omitted from simulation because the airbag did not deploy from influences of impact speed. The injury index in the omitted configurations was defined, with and without airbag, as no differences of injury index. The final calculation of the computer simulation was made using 121 impact configurations and 242 simulation cases.



**Figure 23. Impact configurations for computer simulation**

**Evaluation Results of Airbag System by Computer Simulation**

121 impact configurations and 242 simulation cases were calculated. Injury reduction performance by the airbag was evaluated based on the methodology of ISO/CD 13232, including omitted simulation cases. As a result, the injury reduction performance of the airbag system, and its characteristics against various impact configurations were determined.

**Rider's Injury Reduction Effectiveness**

Figure 24 shows the results of the influence of airbags to injury during the primary impact sequence and secondary impact sequence in the area of the opposing vehicle where the dummy strikes. The vertical axis represents NIC values, (0 in NIC indicates the level without injury and 1 in NIC indicates level of equivalent of the fatal). Figure 24 shows the total average benefit and total average risk in the primary impact sequence. The total average benefit is 0.038 and total average risk is 0.001. The ratio of risk against benefit is 0.026. Also the average net benefit is 0.037. Figure 24 shows the total average benefit and total average risk in the secondary impact sequence. The total average benefit is 0.022 and total average risk is 0.011. The ratio of risk against benefit is 0.500. Also the average net benefit is 0.011. Consequently, the airbag system appears to provide a greater reduction of injury in primary impact sequence than in secondary impact sequence.

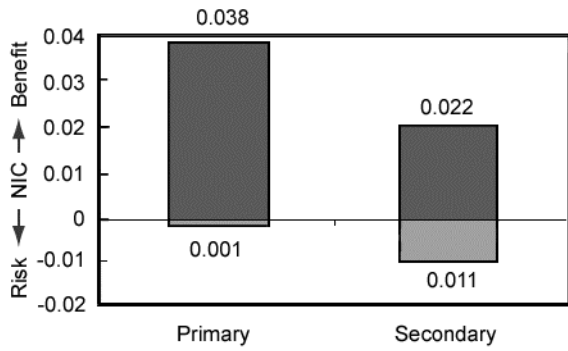


**Figure 24. Total average benefits and risks, all calculation, primary and secondary impact sequence**

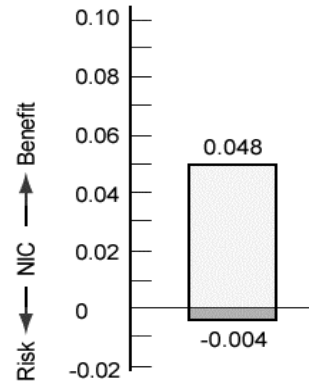


**Figure 25. Total average benefits and risks, 200 impact configurations**

Figure 25 shows the total average benefit and total average risk in the entire impact sequence. The total average benefit is 0.048 and total average risk is 0.004. The ratio of risk against benefit is 0.083. Also the average net benefit is 0.044. From these results, it was judged that the airbag system has appropriate injury index reduction performance.

**Influence of Impact Speed**

The average net benefit values were compared by impact speeds. Figure 26 shows their results. Impact speed in this case indicates relative speed. When colliding to the side of the opposing vehicle, the speed of motorcycles is used as the relative speed. When colliding to the front of the opposing vehicle, the combined speed of both vehicle speed is used as the relative speed. When colliding to the rear of the opposing vehicle, the speed of the opposing vehicle subtracted from motorcycle speed is used. When colliding to the front and rear of the opposing vehicle, and the impact configuration is angled, the impact speed of opposing vehicle is subtracted from the angled impact. For instance, in No.2 of configuration shown in Fig.1, the motorcycle collides into the front of opposing vehicle at an angle of 45 degrees. The relative impact speed in this case was calculated with "13.4m/s (motorcycle speed) plus 6.7m/s (opposing vehicle speed) times  $\cos 45^\circ$ ".

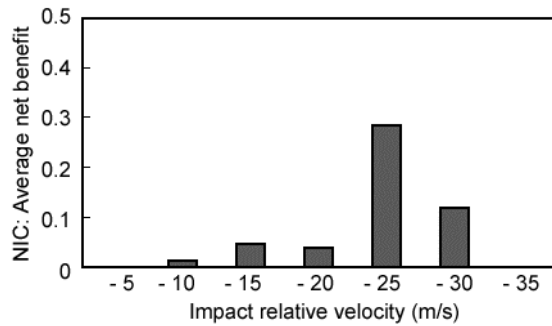


**Figure 26. Average net benefits by relative impact speed**

Referencing Fig.26, the benefit of the airbag for the GL1800 is verified from low to high speed ranges, and thus judged effective. The highest benefit appears at the range from 20 to 25 m/s in the relative impact speed. Therefore, the effect of injury reduction is significant at a high-speed range.

An example of an impact configuration where the effect of airbags in a high-speed range appears clear is shown in Fig.27. Dummy motion during collision of the base motorcycle, without an airbag is shown in Fig.28. Dummy motion during collision of an airbag-equipped motorcycle is shown in Fig.29. In the base motorcycle, without an airbag, the head of dummy strongly impacts the roof of the opposing vehicle. In contrast, in the airbag-equipped motorcycle, the head of dummy softly impacts the opposing vehicle. The injury index is shown in Table 4. The injury index on the

dummy is shown as AIS. AIS 1 is a minor injury level while AIS 6 is a fatal injury level. The injury indices are expressed in six steps. In the base motorcycle, without an airbag, AIS on the head was calculated as 6, i.e. fatal, whereas the calculated AIS on the head in the airbag-equipped motorcycle was representative of no injury. Similarly, the AIS on the neck in the base motorcycle without an airbag was AIS 4, whereas the AIS on the neck for the motorcycle equipped with the airbag was equivalent to no injury.

**Table 4 Comparison of AIS between baseline and with airbag**

	Base line	Airbag
Head	6	0
Neck	4	0
Chest	1	1
Abdomen	0	0
Leg	3	3

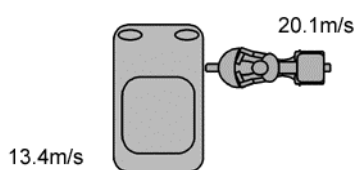


**Figure 27. Benefit impact configuration**

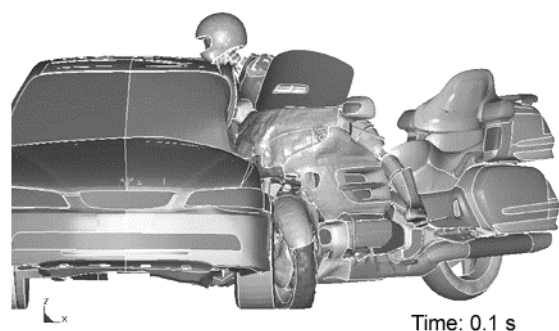


**Figure 28. Baseline impact case**

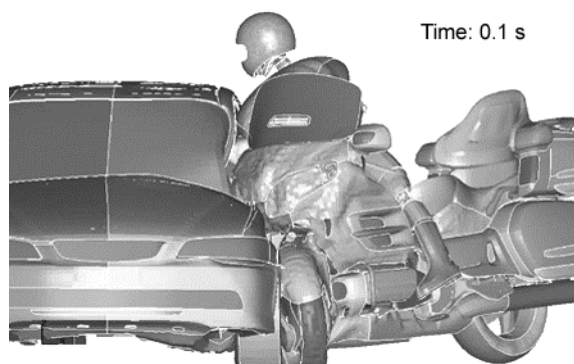


**Figure 29. With airbag impact case**

## CONCLUSION

Computer simulation using the explicit method FEM software permits the evaluation of injury index on the dummy in entire impact sequence in the impacts between motorcycles and opposing vehicles. Using this simulation method, the injury reduction performance of an airbag mounted on the GL1800 was evaluated based on ISO/CD 13232.

The following conclusions regarding injury reduction are drawn from this research:

- The total average benefit was 0.048, risk was 0.004. The performance of the injury reduction system is appropriate.
- The highest average net benefit appears at the range from 20 to 25 m/s in the relative impact speed.
- The injury reduction effect when striking against opposing vehicle is greater than on impact with ground.

## REFERENCES

- (1) Inoue, T., Miura, K., et al.: Experimental Collision Test on Motorcycles with Passenger Car, Paper No.15 of the Safety Research Tour in the USA from the Viewpoint of the Vehicle Dynamics, Society of Automotive Engineers of Japan, October 1969
- (2) Iijima, S., et al.: Exploratory Study of an Airbag Concept for a Large Touring Motorcycle, Paper No. 98-S10-O-14, Sixteenth International Technical Conference on the Enhanced Safety of Vehicles, Windsor, Canada, 1-4 June 1998

- (3) Yamazaki, T, et al.: Exploratory Study of an Airbag Concept for a Large Touring Motorcycle, further research, Paper No. 01-S9-O-240, Seventeenth International Technical Conference on the Enhanced Safety of Vehicles, Amsterdam, Netherlands, 4-7 June 2001
- (4) ISO 13232 Motorcycles Test and Analysis Procedures for Research Evaluation of Rider Crash Protective Devices Fitted to Motorcycles, 1996-12-15
- (5) Hideo, N, et al.: A Computer Simulation for Motorcycle Rider-Motion in Collision, Paper No.2003-32-0044, Small Engine Technology Conference & Exhibition, Madison, Wisconsin, USA, 15-18 Sep 2003
- (6) LS-DYNA User's Manual: Livermore Software Technology Corporation

# A NEW CONCEPT FOR A THREE-POINT SEAT BELT AND CHILD RESTRAINT SYSTEM FOR BUSES

**Ignasi Ferrer**

**Joaquim Huguet**

Applus<sup>+</sup>IDIADA

Santa Oliva, Spain

Paper Number 05-0310

## ABSTRACT

Buses are one of the safest modes of transport available and one of the options that governments in Europe are especially trying to promote, in order to meet congestion and emission targets. When a bus accident occurs it often becomes the focus of media and public attention, especially because the people involved had confidence in the transport and sometimes it is their sole transport reliance. In particular, school bus accidents cause great public anxiety and often make the relative safety of buses be overlooked. While the incidence of bus occupant trauma is relatively low, there is concern on how best to improve bus safety.

Three-point seat belts are a good way of improving the level of protection for occupants and it is likely that future legislation worldwide will move towards compulsory installation and use in buses. One of the problems with conventional three-point seat belts is that they need to be compatible with child restraint systems to be effective for children; otherwise the shoulder belt adds a significant risk of injury. There is an availability problem of sufficient numbers of universal child restraint systems for different mass categories (G0/G0+, G1, G2 and G3 according to ECE R-44) that ensure an adequate level of protection for occupants of all age groups. If child restraint systems are vehicle specific or integrated there is still a problem with adjustments and there is evident risk of misuse.

This paper describes the development of a new concept of three-point seat belt for buses that is compatible with adults and children over 3 years, and self-adjustable. Applus<sup>+</sup>IDIADA designed, developed, tested and patented the system under contract to FITSA (Spanish Foundation Institute of Technological and Automotive Safety). This concept intends to provide an effective, inexpensive solution to the safety of children in buses.

## INTRODUCTION

Various studies of accidents involving buses have proven that the main cause of severe and fatal injuries is partial or full ejection or projection from seats.[1] [2]. Any action taken in provision of restraint systems translates to improving the relative safety of buses by means of; in the first place, avoid full or partial body ejection, from seats and secondly, reduce the risk of the bodies contacting any rigid parts in the vehicles.

Restraining all occupants, in addition to the guarantee of a survival space in case of a rollover, prevents the majority of the injuries suffered in vehicles involved in accidents. The correct use of safety belts (the main restraint system in transport) prevents the ejection of occupants in collisions where the most important direction of deceleration is the longitudinal axis of the vehicle, and also in rollovers. This can substantially reduce the number of serious injuries in the event of an accident.

The inspiration of the project comes from a study based on the reconstruction of 8 severe accidents that occurred in Spain between 2000 and 2001 involving buses, which showed the reality of the protection offered to users. None of the passengers used a safety belt including the drivers. The majority of the serious injuries and fatalities were due to non-use of restraint systems, (resulting in impacts with rigid interior parts of the vehicle following occupant projection or partial/full ejection from seats). Ejection played a role in 86% of the fatalities, and 18% of the serious injury cases.

The most relevant conclusion of this study was a recommendation that adequate restraint systems for all occupants would reduce the severity of injuries, and the number of fatalities in accidents. Of course, this is true for adults and for children, as well. Therefore, a restraint system that is compatible with all users represents an increase of safety for all users. It is a big difficulty to approach the problem of child protection in buses and coaches with the same concept as for passenger cars. Most child restraint systems to be fitted in passenger cars have been designed for a particular group of age and need a complicated set of adjustments that are almost inapplicable to public transport.

Current safety belt design is meant for adult occupants and could cause injuries when applied to children. The design and homologation of a restraint system that is compatible for adults and children would mean a significant improvement in safety of public transport.

## BACKGROUND

### Standards and regulations

The standards and regulations that are currently applicable to buses and public transport fail to provide a sufficient guarantee of safety to all occupants. Applus<sup>+</sup>IDIADA recognises this project as a pre-legislative step; future trends in legislation are expected to move in the direction of making seat belts in buses and coaches compulsory.

The Spanish Royal Legislative Act 443/2001: Safety Conditions in School Transport. The retention of the occupants of buses is to be offered by the seat or structure immediately in front of each occupant, except in the case where there is no such structure, then a seat belt is required, and in the case that this position is to be occupied by children from 5 to 11 years then the seat belt shall be used in combination with a booster seat.

EC Directive 2003/20: In vehicles of categories M2 and M3, the use of seat belts is compulsory for all occupants over three years old, provided that their seats are equipped with safety belts.

EC Directives 2000/3, 96/37 (Seats and their anchorages) & 96/38 (Anchorage and safety belts): It is compulsory to install seat belts in vehicles of categories M2 and M3. Two-point seat belts are allowed. There is no exact date of this directive coming into force.

ECE Regulation 80 (Seats and their anchorages): There are static and dynamic requirements for the vehicle to restrain the occupants through the divisions in the vehicle (seats and structures).

ECE Regulation 44 (Child restraint devices): There are static and dynamic requirements for the child restraint systems to guarantee the protection of children in frontal and rear impacts.

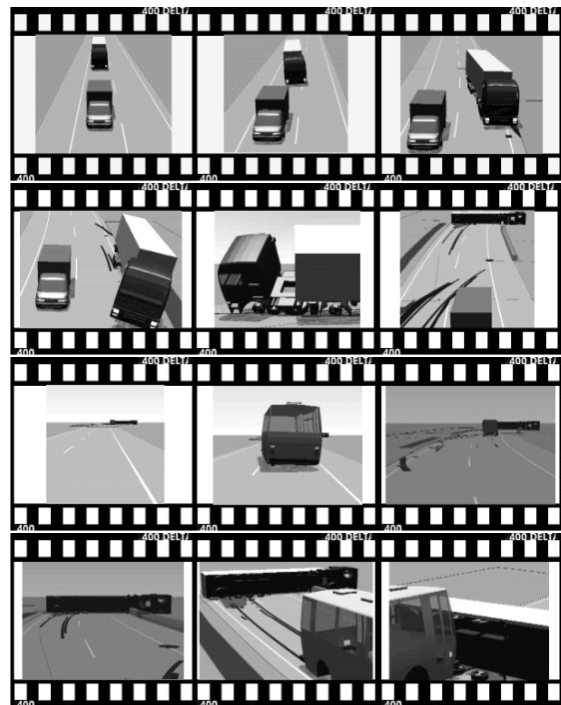
The current legislation needs to be revised. Future legislation is expected to be a comprehensive system that makes the installation and use of restraint systems compulsory in all seating positions for all occupants of all vehicle categories, including buses and coaches.

### Case studies

Applus+IDIADA carried out a study of 8 cases involving buses that occurred in Spain between 2000 and 2001. In order to relate the levels of injury to the kinematics of the occupants, a study was undertaken to analyse the case of the driver, the occupants of the first row on the right side, the occupants of the first row on the left side, the occupants of the seats in front of the stair case area, and the passengers of a central area on the right side and the left side of the vehicle.

Case 1 (2000-01): Frontal impact, Vehicles: Mercedes Benz / O 404, Touring; Truck Volvo / FH12 4X2; Trailer Lambert/ LVFS BAST. Following a an ill-fated overtaking manoeuvre by the truck, which ended in the total ejection of the driver, and the truck on lying across the road, broadside, the bus struck the rear half of the trailer at 105 km/h. The decelerations suffered are the most important consideration in frontal impacts. The lesser lateral component influenced the movements of the occupants in the bus, due to inertia; in this case, because the driver attempted to avoid the

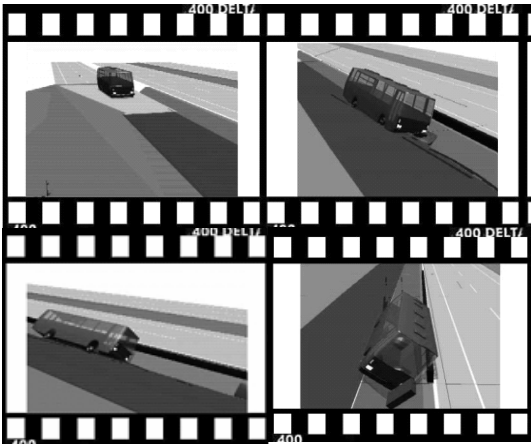
crash by steering left, the occupant inertia was to the right. There was no utilisation of seat belts by any of the occupants.



**Figure 1. Reconstruction of vehicle kinematics (Case 2000-01)**

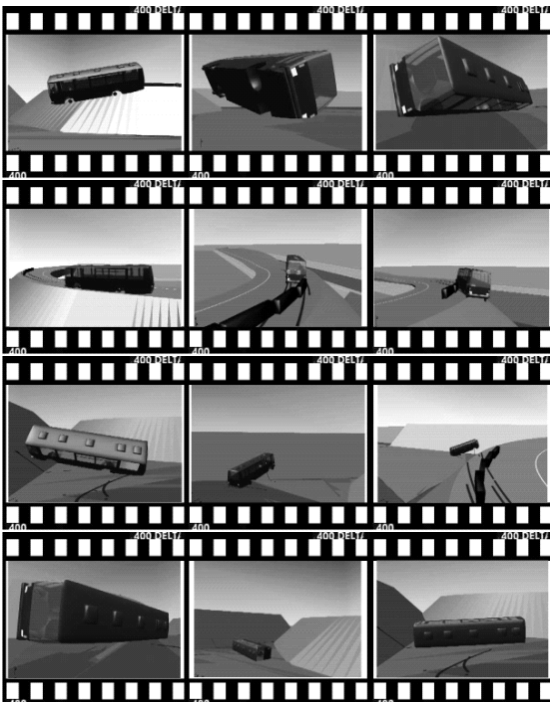
The impact speed of the bus was 70 km/h and its post-impact velocity was 47,74 km/h. The difference of 22,7 km/h translates to 36 km/h EES (*Equivalent Energy Speed*) which is a measure of the deceleration pulse that the bus experienced and the value used in the simulations. For simulations, the first phase of the crash was simplified to an angled full frontal crash with the rear half of the trailer. The duration of the crash is limited to equal the duration of the deformation. If the deformation of the coach and the trailer is simplified by a uniform model, the coach and trailer suffered deformations of 0,6 m and 0,15 m respectively. The estimated deceleration pulse through the coach structure in the initial phase of the crash was 13,7 g for 46 ms. There were 3 fatalities, 18 serious injury cases and 27 minor injury cases; 48 occupants all in all.

Case 2 (2000-02): Coach careers off-course; Mercedes Benz O-303. There was 1 fatality, 10 serious injuries and 29 minor injuries – 54 occupants all-in-all. The coach careered off the road at 86 km/h and into what the driver thought was a slip road. He realised and tried to correct the error, but the drainage gutter was too deep to cross. The left side made contact with the ground at 50 km/h. This velocity was down to 18 km/h after the impact with a boulder in the gutter ( $\Delta V = 9$  km/h and EES 5 km/h). Maximum inclination 45°, rest inclination 37°. There were lateral and frontal intrusions of 0,19 m and 0,45 m respectively.



**Figure 2. Reconstruction of vehicle kinematics (Case 2000-02)**

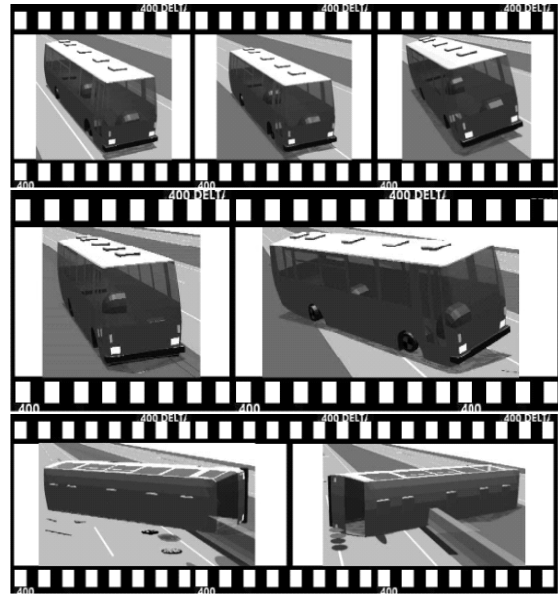
Case 3: Careered off-course on a curve followed by multiple impacts; Mercedes Benz O-404. There were 24 occupants, 15 had minor injuries, 6 were seriously injured and there were 3 fatalities.



**Figure 3. Reconstruction of vehicle kinematics (Case 2001-03)**

According to the curvature and the coefficient of friction for asphalt, the vehicle was over the critical velocity. The coach failed to negotiate the curve at 80 km/h, went into the hard shoulder, took out the safety barrier at 74 km/h and went down an embankment finally coming to rest on a dry riverbed after impact with a wall on the edge of the bed. All the seats had safety belts; three point seat belts for the driver and the guide, and two point seat belts for the rest of the seats, but none of them were utilised.

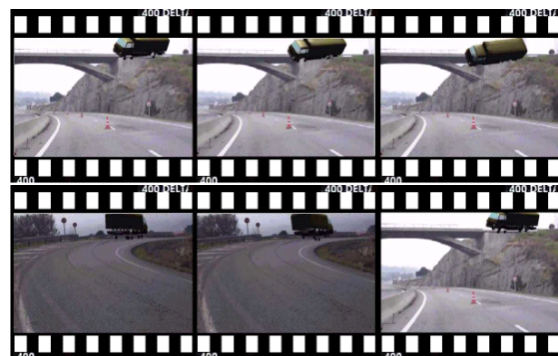
Case 4: Careered off-course and over steered back in; Iveco Eurorider.



**Figure 4. Reconstruction of vehicle kinematics (Case 2001-04)**

Because of the rolling, the shell of the coach rather than the chassis took the brunt of the impact force. There were 7 fatalities, 10 serious injury cases, 2 minor injury cases, all in all 19 occupants. The coach careered off-course at 100 km/h. The correction attempt over steered and the result was that the coach turned over and skidded broadside into a safety barrier (motorway division). The impact velocity with the barrier was 30,28 km/h translating to EES of 16,15 km/h.

Case 5: Frontal Impact, Volvo B7R. There was one fatality, 8 seriously injured occupants and thirty seven minor injury cases; 46 occupants. A speeding truck failed to negotiate a curve approaching a fly-over. The truck went off the fly-over bridge coming to rest on the carriageway below, lying across two lanes on the left side. The coach and a passenger car were unable to avoid the truck; frontal crash for both vehicles.



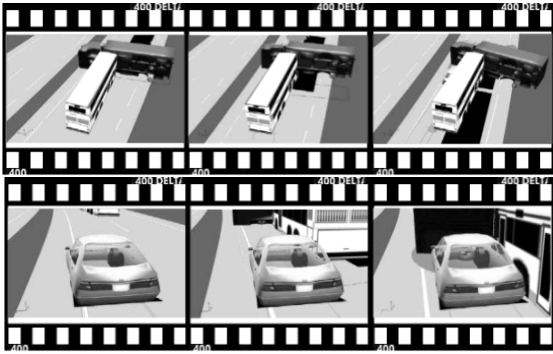


**Figure 5. Reconstruction of vehicle kinematics (Case 2001-05)**

The coach was travelling at 90 km/h and the calculated  $\Delta V$  of the coach was 53 km/h, about 46 km/h EES. The calculated deceleration pulse of 20,3 g for 74 ms was used in simulation. There were three-point seat belts in the coach, none of which was used.

Case 6: Frontal impact, Pegaso 5036; Skoda Felicia

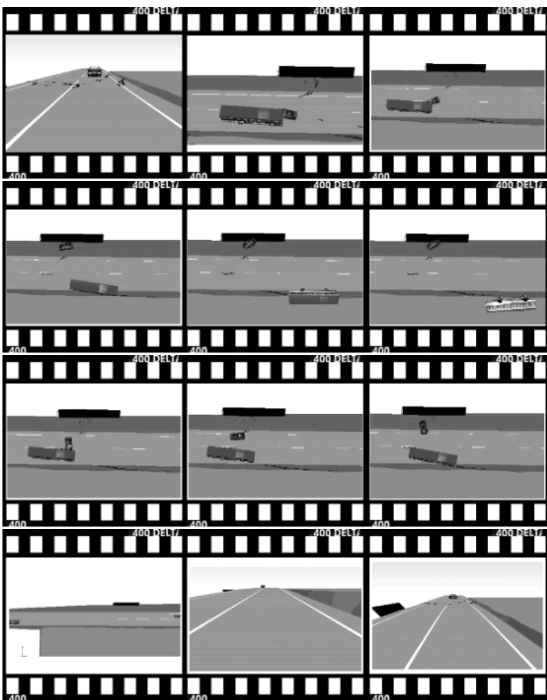


**Figure 6. Reconstruction of vehicle kinematics (Case 2001-06)**

There was a 30% overlap frontal crash when the Skoda failed to clear the lane during an overtaking manoeuvre. The coach left the road on the right, and went on to rollover. The impact velocity of the coach was 60 km/h and the post impact velocity was 54,5 km/h.  $\Delta V = 5,7$  km/h, EES 13,3 km/h. The calculated longitudinal average deceleration pulse was 1,7 g for 90 ms at the moment of the impact with the car. A more significant pulse of 6,5 g was produced by the impact in the gutter after the roll. Maximum intrusion: 1,80 m (front longitudinal).

There were 56 occupants in total. 16 of them suffered minor injuries and there were no other casualties.

Case 7: Career off-course and rollover; Mercedes Benz O-404. The coach careered off the road to the right, on an approach to a steep embankment (11,3 m below level road). The vehicle came to rest on its roof.

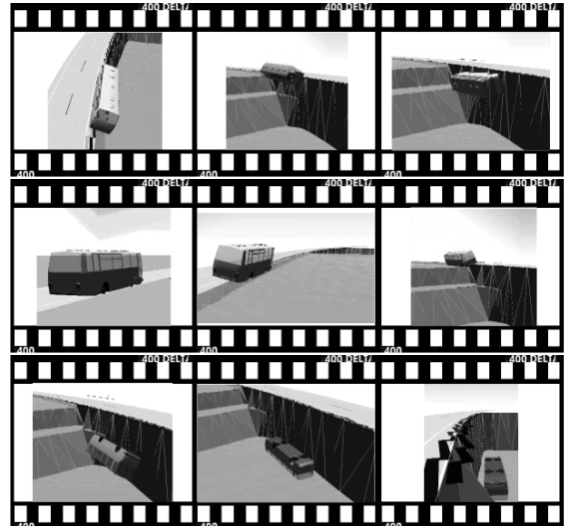


**Figure 7. Reconstruction of vehicle kinematics (Case 2001-07)**

There were 5 fatalities, 5 seriously injured occupants and 2 minor injury cases; 12 occupants all in all. The coach – Mercedes Benz O-404 – was travelling at 58 km/h at the moment of roll. The final resting position determined the pulse that the vehicle structure was put through, as it landed on the roof. The static deformation of the vehicle was 100 cm longitudinally in a simplified uniform model. The change of velocity  $\Delta V$  was 37 km/h horizontally and the vertical velocity was 6 km/h. The calculated pulse, used in simulation, was 8 g for 140 ms.

Case 8: Mercedes Benz O-404; there was a judgement error in clearing distance during an attempt to overtake.

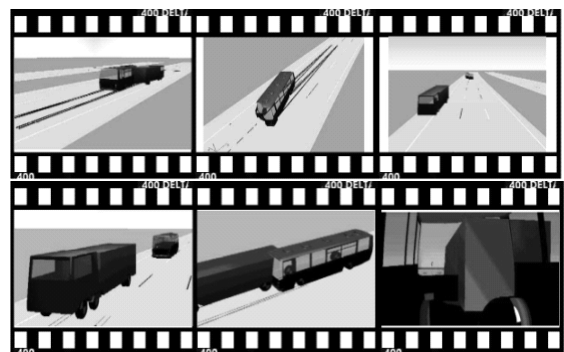


**Figure 8. Reconstruction of vehicle kinematics (Case 2001-08)**

There were 29 minor injury cases, 3 seriously injured people and one fatality, following an impact on the left side.

## Recommendations

The study showed that in frontal impacts, the survival space of the driver and the guide is substantially reduced. The existing screens of separation between the first row and the driver or the guide, as well as between the central access and the row located in front of it, collapsed because of the load exerted by the occupants of the mentioned rows and they did not retain the occupants in these compartments as proposed by the principle of the regulation that the structure in front of the occupant should provide restraint capacity.

The general area-by-area injury characteristics show that the driver suffered fatal injuries to the head, as a direct result of impact with part of the trailer chassis, and rib-cage, due to partial ejection and impact with the steering wheel.

Occupants in the first row left suffered serious injuries due to impact with the separation screen between them and the driver. In the first row right, occupants suffered fatal injuries after ejection and impact with the trailer chassis and the other suffered lethal internal injuries due to full ejection followed by violent impact with the driver's separation screen. In the stair case area, the injuries suffered were a result of impact with the separation screen; vertebrae injuries, and head impacts following full or partial ejection. In the central areas, the occupants suffered dislocations and concussions as a result of impacts with the backs of the seats in front of them. The actual injuries depended on the seating orientation of the passengers just before the crash.

The figure below illustrates the general casualty summary for the seating positions (frontal crash); serious and/or fatal injuries in black, and minor injuries in white/grey.

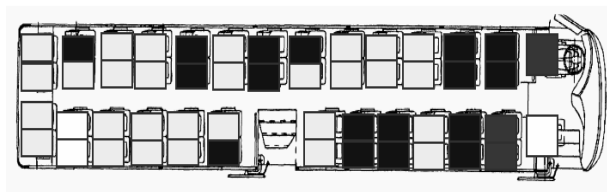


**Figure 9. Area by area injury summary**

In the cases of rollover there is a more even distribution of the risk of injury, due to the nature of the accident. This is due to the fact that the simplified model of a rollover can have multiple loading directions – a function of the number of turns and other cinematic properties of the vehicle. In these cases, such as the case 2001-4, the rollover that produced the most fatalities, the restraint of occupants could indeed have saved lives or at least prevented some of the severe and fatal injuries.

## INTEGRATION OF CHILD RESTRAINT SYSTEM IN SEATS

The full or partial ejection or projection of the occupants was found to be the main event preceding the impacts that resulted in serious or minor injuries in all the cases that were studied. Applus+IDIADA carried out accident reconstructions, and with simulation techniques, the mechanism of the injuries sustained was illustrated – the results of one simulation are shown below.

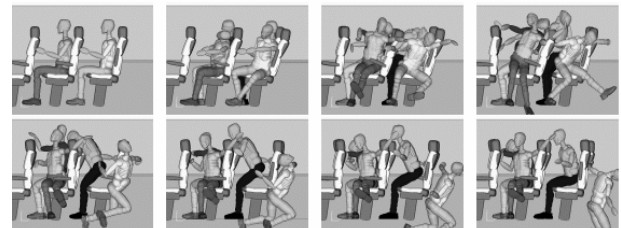


**Figure 10. Without seat belts**

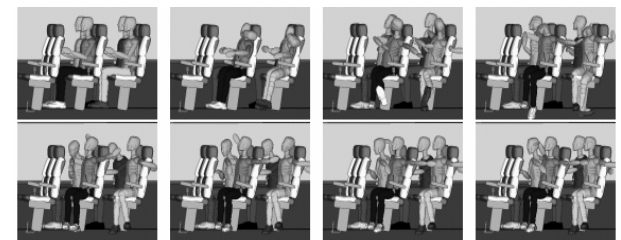


**Figure 11. With seat belts (animation in MADYMO® for occupants on the right-isle seats, case 2000-1)**

It is reasonable to conclude that the correct use of seat belts could have saved lives, as well as prevent some of the serious and minor injuries that occurred, simply through restraining the occupants which would have reduced the probability of impacts. In all of the cases studied, there were no restraint systems in use, either for the reason that there were not provided for all seating positions, or there were none at all. In the cases where restraint systems were provided, none of them was in use. This fact points to a fault in legislation and user awareness.

In tackling this problem it is necessary to make sure that any proposed design is compatible for use by adults as well as by children, without conceding to misuse problems, especially for children. The guarantee of restraint should cover all age-groups, and physical make-ups in order to sufficiently provide an increase in the overall safety for occupants.

In our consideration for school buses, the use of child restraint systems, integrated or accessories, is becoming a general practice. Nevertheless, technical solutions do not exist that make their incorporation in the vehicles viable.

In Spain the use of school buses is very widespread, especially for children over 3 years old – the age at which compulsory primary education starts. This raises the necessity to design a restraint system adapted to these users, but ensuring that its use is simple and foolproof.

### Analysis of failure and error modes

An analysis of the different failure modes that occur related to the current restraint system was done, and there were three main categories of failure found; use of the locking system by children in adult configuration, use of the locking system in infant configuration by adults, and restraint system misuse in any configuration. In school buses, misuse is a serious issue, and in some cases it means that there is a need for guardians to check the proper use of these systems. In the cases where adult seat belts are used in combination with child restraint accessories, the process of making sure that the correct systems are anchored properly has inherent error due to the long list of criteria that need to be met. This translates to an overall risk for children even in the cases where a guardian is available, as they are also prone to errors.

The ideal solution needs to provide restraint capacity that is foolproof, and needs no preparation for any types of users, and as little supervision as possible to limit the possibility of misuse or failure in any of the modes described above.

In school buses the role of the guardian will be conveniently limited to verifying the ‘use’ rather than the ‘proper use’ of the locking system by all the travellers. This function could in the end be incorporated into the vehicle safety functions such as seat belt reminders.

### Failure and related injury

Incorrect use of seat belts can result in injuries, and the risk is especially high for children. Different accident studies have found that in the cases of injuries caused by the belt, the majority of these are abdominal injuries. These injuries relate to the mechanism known as submarining, consisting of the sliding of the occupant below the lap belt. This is known to be the biggest threat posed by the lap belt when incorrectly installed or used.

Submarining takes place when the lap belt section does not retain the occupant by means of the pelvic crests, but rather by leaning into the soft weave of the abdomen, causing internal injuries in organs such as the liver or even spinal injuries. [3]

### Child dummy tests

Applus+IDIADA carried out tests aimed at assessing the performance of the three-point seat belt, and the relative modes of failure; in the application of a restraint for children using a P3 dummy.

Following successful modification of the initial designs, the results of the fourth test were the following. Resulting acceleration of thorax during 3 ms: 48,61 g (below the limit of ECE R-44; 55 g), time with negative acceleration Z at thorax over 30 g: 0 ms (below the limit of ECE R-44; 3ms). No abdominal penetration was observed (in agreement with ECE R-44). The head of the dummy was contained (it did not cross planes BA and DA, in agreement with ECE R-44 vertical and horizontal displacement limits). In this test it was possible to find a configuration of a seat belt meeting the requirements described in ECE R-44.

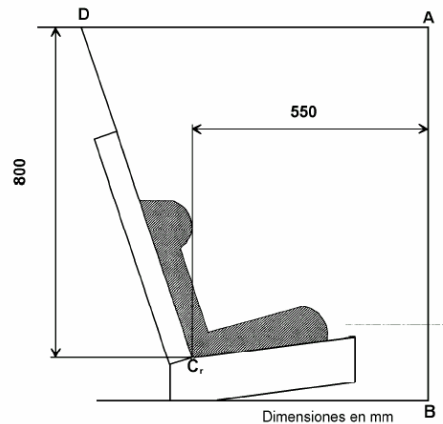


Figure 12. ECE Regulation 44 procedure

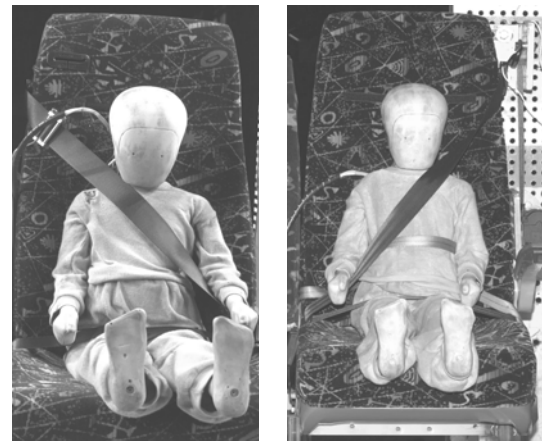


Figure 13. Dummy tests

Although there are other smaller size dummies, it is considered that this restraint system design is inappropriate for the categories they represent.

### DESIGN AND DEVELOPMENT

The design by Applus+IDIADA was developed with the purpose of developing a locking system that guarantees the protection of the occupants, adults just as well as children, maintaining convenience for all type of statures, with no need of adjustments or preparation.

Applus+IDIADA raised a solution for the integration of child restraint systems in bus seats which consists of placing an extra guide of the belt at one side of the seat back.

Figure 14 shows (clockwise from left) the simulated model of the proposed system in child and adult configurations.

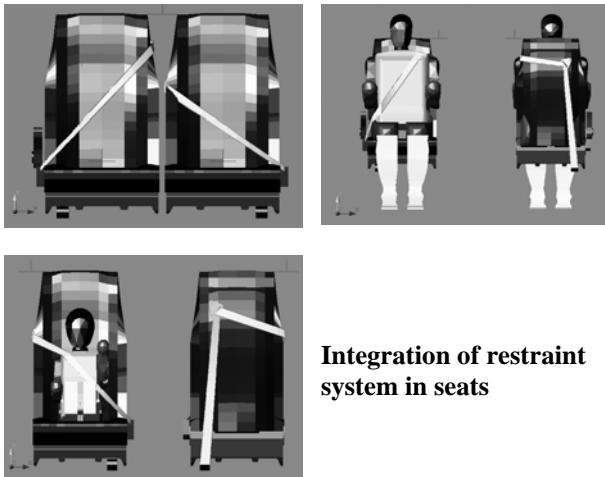


**Figure 14.**

By means of a fixed guide the belts' tendency to fall off the shoulder can be controlled to adapt to different heights according to the stature of the occupant. In the cases of adult passengers, the shoulder belt would be located at the height stipulated by ECE Regulation 14, whereas in the case of children, it would be located at the lower end. In either of the cases, the setting would not affect passing homologation since the consideration of child restraints as well as adult restraint system regulations would be addressed.

The pelvic points of anchorage will have to be placed within the vertical angle ( $30^\circ$ ) of the P3 dummy by default. The belt will have to be equipped with a load limiter in the event that the rigidity of the seat is such that the tension produces too high decelerations of the thorax.



**Figure 15. 3D model**

## CALCULATION OF ADULT OCCUPANT KINEMATICS WITH SIMULATION TECHNIQUES

### Occupant Simulation

Prior to performing experimental tests using dummies, simulations in MADYMO® were carried out. These allowed the behaviour and performance of the system and the set-up to be evaluated through the virtual reproduction of the dummies and by simulating the true decelerations from live tests. Later, the correlation between the results of the simulation and the experimental tests was carried out in order to validate the simulation model.

Since the system developed is to be used by children as well as adults, simulation of the behaviour of an ample margin of users was reasonable. The following family of dummies was used: P3, P6, P10, Hybrid III 5th percentile female, Hybrid III 50th percentile male and Hybrid III 95th percentile male. This assures the analysis for a complete array of possible users, from a three-year-old child weighting 15 kg to an adult of over 98 kg.

### Deceleration pulse

For the purposes of simulations, average pulses were used, meeting the limits of the regulations. The average pulse is shown in the graph.

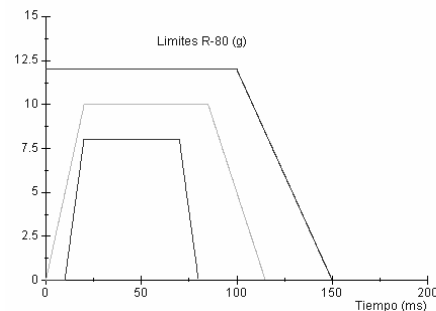


**Figure 16. Limits of pulse in ECE Regulation 80 and average pulse used**

The values associated with this graph are shown below.

**Table 1  
ECE R-80 Average pulse**

Time	Acceleration
0 ms	0 g
20 ms	10g
85 ms	10g
115 ms	0 g

For the case of the child dummies (P3, P6 and P10) the same pulse was used – average within ECE Regulation 44 limits.

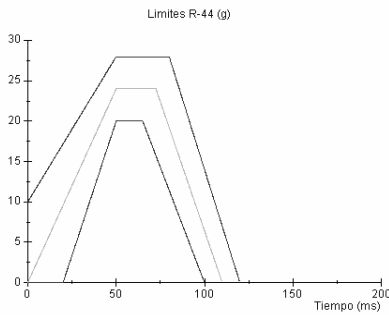


**Figure 17. Average pulse used in Simulation – within limits of ECE Regulation 44**

The values associated to this graph are in the table below:

**Table 2  
ECE R- 44 Average pulse**

Time	Acceleration
0 ms	0 g
50 ms	24g
72,5 ms	24g
110 ms	0 g

### Description of the simulation model

One of the objectives of the project was the development of the technology of computer numerical simulation of the behaviour of the seat belt system for trials in the laboratories of Applus<sup>+</sup>IDIADA.

A by-result of this project is that it created the possibility of making predictions on the behaviour of the restraint system for different dummies. For the accomplishment of this objective, the method of calculation by finite-element analysis techniques was used - through commercial software which is commonly used in the automotive industry.

MADYMO® was used for the preparation of virtual models and calculations, Easy Crash® for the processes, Hyper View® for the post processing. The hardware used for all the simulation works was SGI Octane R12K/300 computers.

Laboratory data was obtained using Wincarat®, and the processing of data in the laboratory was made with Diadem®.

The model used the following characteristics, in the calculations by simulation: Row of two seats with anchored belt in each seat; dummy placed in the H-point, so that their position is natural.

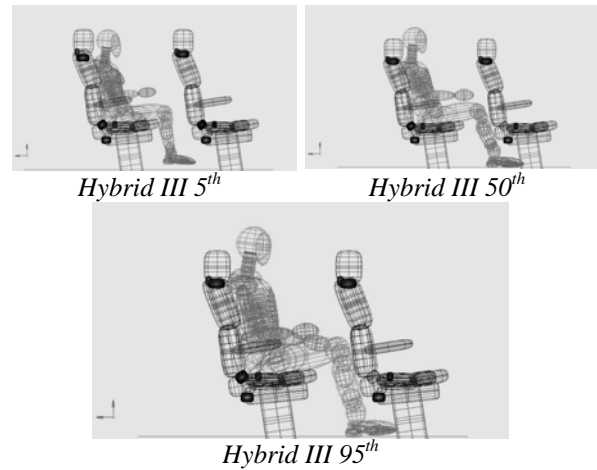


**Figure 18. Simulation Model**

The seat belt was modelled as consisting of nine bar sections: 1<sup>st</sup> bar; from the reel placed and fixed in the rigid part of the seat (down left) and going up to a first guide slot fixed in the back. 2<sup>nd</sup> bar; from the first to the second guide slot (right part of the seat). 3<sup>rd</sup> bar; right to the way out guide slot (excluding the thickness of the back) to the dummy's shoulder. 4<sup>th</sup> bar: right to the shoulder (up to here it is considered that there is no pretension or looseness. 5<sup>th</sup> and 6<sup>th</sup> bars: cross the thorax of the dummy 7<sup>th</sup> bar: reach the buckle, rigidly fixed to the immobile part of the seat. 8<sup>th</sup> bar: from the buckle to dummy's pelvis 9<sup>th</sup> bar: finally reaches the anchorage placed between both seats which is considered fixed to the immobile part of the seat).

In the 5<sup>th</sup> and 9<sup>th</sup> bars part, a looseness of 20 mm was considered. In each step of guide slot and on the buckle a friction coefficient of 0,1 is considered. The rest of friction coefficients are considered as 0,02.

The position of guides 2 and 3 varies based on the height of the dummy but their position is considered fixed during the impact for each dummy. The material of the belt allows an elongation of 10% for a 10 kN tension.

The contacts of the seat foam with the dummy are set according to the characteristic functions of the seat model. The ground support of the feet has been placed to a natural distance of the seat. In figure 19, the modelled system is illustrated with a Hybrid III 5th percentile female, a Hybrid III 50th percentile male, and a Hybrid III 95th percentile male.

### **Simulation of Hybrid III 5<sup>th</sup> percentile female**

This dummy has a weight of 46,3 kg and an equivalent height of 150 cm. The dummy is placed, belted-up in a natural seating position. The spacing of rows is 0,8 m and the interaction between the dummy and the back of the seats in front is monitored.

The model is put under a signal of deceleration generated from the limits in ECE R-80 (homologation of seats) as discussed in occupant simulation. The

results of the biomechanics values (those of greater importance for the evaluation according to ECE R-80) are shown in the table below.

**Table 3**  
**Results of H III 5<sup>th</sup> percentile female**

Parameter	Simulation Result	R-80 limits
HIC <sub>36</sub>	65,5	500
Thorax Acc <sub>3</sub> .	13,5 g	30 g
Femur Force	0,65 kN	10 kN
Femur Force <sub>20</sub>	0,4 kN	8 kN

The graphs below show the main biomechanical results of the simulation.

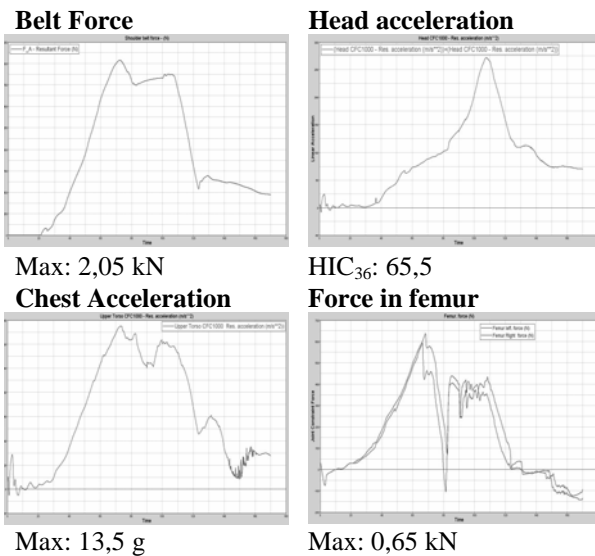


**Figure 19. Simulation biomechanical results**

**Simulation of Hybrid III 50<sup>th</sup> percentile male**

This dummy weight 74,4 kg and its stature is 180 cm. The dummy is placed, belted-up in a natural seating position. The spacing of rows is 0,8 m and the interaction between the dummy and the back of the seats in front is monitored.

**Table 4**  
**Results of H III 50<sup>th</sup> percentile male**

Parameter	Simulation Result	R-80 limits
HIC <sub>36</sub>	106,4	500
Thorax Acc <sub>3</sub> .	13,9 g	30 g
Femur Force	1,4 kN	10 kN
Femur Force <sub>20</sub>	0,68 kN	8 kN

The model is put under a signal of deceleration generated from the limits in ECE R-80 (homologation of seats) as in the 5<sup>th</sup> percentile female simulation. The results of the biomechanics values (those of greater

importance for the evaluation according to ECE R-80) are shown in the table above.

The graphs below show the main biomechanical results of the simulation.

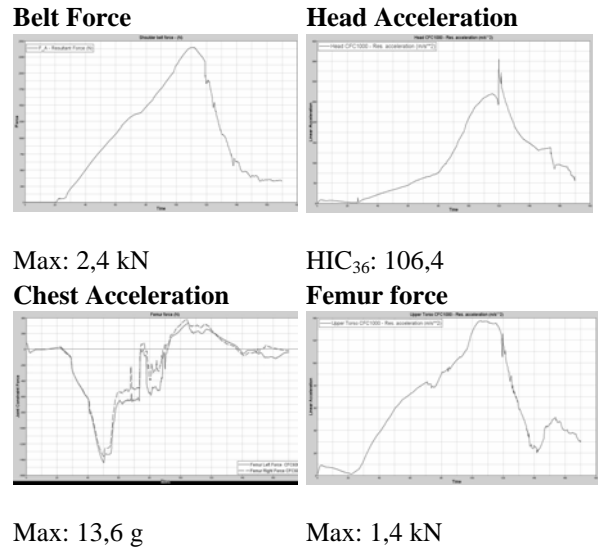


**Figure 20 Simulation biomechanical results**

**Simulation Hybrid III 95<sup>th</sup> percentile male**

This dummy has a stature of 185 cm and a weight of 97,5 kg.

The dummy is placed, belted-up in a natural seating position. The spacing of rows is 0,8 m and the interaction between the dummy and the back of the seats in front is monitored.

The model is put under a signal of deceleration generated from the limits in ECE R-80 (homologation of seats) as in the previous simulations.

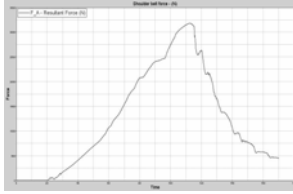
The results of the biomechanics values (those of greater importance for the evaluation according to ECE R-80) are shown in the table below.

**Table 4**  
**Results of H III 95<sup>th</sup> percentile male**

Parameter	Simulation Results	R-80 Limits
HIC <sub>36</sub>	115,0	500
Thorax Acc <sub>3</sub> .	14,5 g	30 g
Femur Force	1,5 kN	10 kN
Femur Force <sub>20</sub>	0,82 kN	8 kN

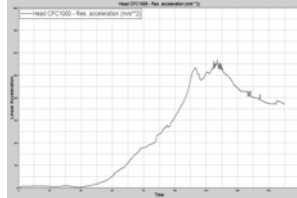
The graphs below show the main biomechanics results of the simulation.

### Belt force



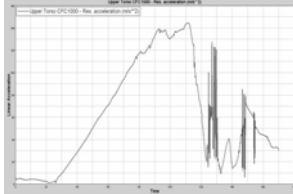
Max: 3,3 kN

### Head Acceleration



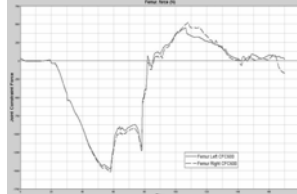
HIC<sub>36</sub>: 115,0

### Chest Acceleration



Max: 14,5 g

### Femur force



Max: 1,5 kN

**Figure 21. Simulation biomechanical results**

The phase of simulation was validated by experimental tests in Applus<sup>+</sup>IDIADA facilities; technical centre in L'Albornar (Tarragona - Spain). These tests, known as sled tests, are carried out by means of a movable platform, on which the seats and the dummies are placed, simulating the deceleration caused by the impact.

The sled is stopped by means of calibrated deformable bars, and a deceleration curve is obtained under the requirements demanded in the regulations that relate to the respective tests. In the set of tests of the system as adult restraint, the settings of ECE R-80 were used, and for the tests with child dummies the settings of ECE R-44 were adopted. The series of experimental tests correspond to the simulated cases.

Therefore, a series of dynamic tests with the family of adult Hybrid III dummies discussed below was done. These tests represent head-on collisions and the human models used were that from the US standard regulations of NHTSA, Part 572. Its use is standard world-wide for frontal impact testing. Hybrid III 5th percentile female; dummy that simulates an adult of small stature, Hybrid III 50th percentile male; dummy that simulates an adult of average stature, and Hybrid III 95th percentile male; dummy that simulates an adult of big stature. The test procedure is defined in the regulation ECE R-80.

The measured biomechanics values of the adult dummy family do not have to surpass the limits defined in the regulation: 500 in the case of HIC (Head Injury Criterion), 10 kN for the load in the femur, 8 kN with a duration greater than 20 ms for the load in femur and 30 g of acceleration in the chest with a minimum duration of 3 ms.

On the other hand, for the tests of the new design with child dummy family corresponding to ECE Regulation 44, there was clear intention of attempting to obtain

results that ensure performance well below the regulatory limits.

The tests were performed with dummies belonging to the P family, defined in the regulation ECE R-44. Its use is standard in Europe for frontal impacts with child restraint systems. The following dummies are the ones with which the test was done: P3 - dummy that simulates a 50<sup>th</sup> percentile three year old child, P6 - dummy simulating a 50<sup>th</sup> percentile six year old child, P10 - dummy representing the average ten year old child.

Although there are dummies representing younger children, the concept is not designed for children under 3 years.

During the test the dummy tends to move forwards due to inertia. To ensure the seat makes an adequate retention, it must withstand 55 g acceleration for the chest for longer than 3 ms in impacts for the head occurring over 24 km/h, with a vertical acceleration in the lower abdomen below 30 g for no longer than 3 ms and without abdominal penetration of any kind. Finally, it must be verified by means of high-speed camera shooting that the centre of gravity of the head of the dummy does not have an excursion exceeding a certain displacement point predefined with respect to the seat.

### First prototypes

After the completion of the first test series on a bench to test design concepts, the first prototype seats were manufactured. The following figures show these first constructed prototypes.



**Figure 22. First prototypes**

## HOMOLOGATION TESTS ON PROTOTYPES

Following necessary modifications on the first prototypes, a series of seats with the proposed new design for the purposes of homologation testing was built.



Figure 23 P3 dummy



Figure 24 P6 dummy

The different dummies were positioned in the seats to determine the compatibility of the device for the different users.



Figure 25 P10 dummy



Figure 26 H III 5<sup>th</sup>

The dummies used were P3, P6, P10, Hybrid III 5<sup>th</sup> percentile female, Hybrid III 50<sup>th</sup> percentile male and Hybrid III 95<sup>th</sup> percentile male. All of them displayed a suitable retention in the tests that were carried out, under the respective regulation requirements.



Figure 27 H III 50<sup>th</sup>



Figure 28 H III 95<sup>th</sup>

With the purpose of improving the retention of the dummy P3 (the one of smaller stature) and 95<sup>th</sup> percentile male Hybrid III (the one of large build), it was proposed to increase the dimension of the guide by 1 cm above and 2-3 cm below the initial design length. These modifications were carried out on the prototypes used for the homologation tests.

## Homologation tests

The homologation testing of the device was made following the procedures described in the following regulations. ECE Regulation 80: Seats and their anchorages (M2 and M3). EC Directive 96/37: Seats and their anchorages. EC Directive 96/38: Anchorages of lap belts EC Directive 2000/3: Lap belts and locking system. ECE Regulation 44: Child restraint systems.

After fulfilling all the acceptance criteria, it was verified that the integrated child restraint system developed for school bus transport seats in this project meets the requirements to be approved as a functional safety system. The following slides show the film of the homologation tests carried out with P dummies.



Figure 29. P3 and P6 Dummy homologation tests

## PATENT

Applus+IDIADA successfully patented the following system;

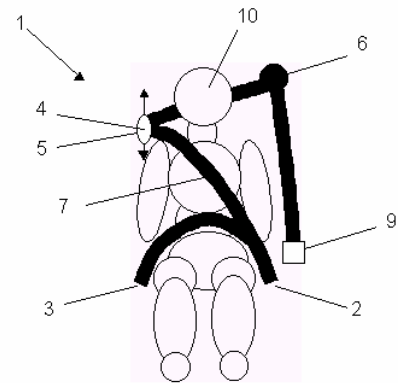


Figure 30. Patent

1.- System of guidance for lap belts (1), consisting of two lower points of anchorage (2, 3), located on both sides of the passenger, and a point of the guide (4) located at the height of the shoulder of the passenger, being the D-ring point (4) provided with a height adjuster (5), adapted to redirect the lap belt from one of the lower points of anchorage (2, 3) up to the locking system, adapted to fix the belt at the moment of the impact, positioning the strap (7) of the lap belt diagonally on the torso of the passenger, characterized because this height adjuster (5) of the D-ring (4) is automatic and consists of an element it guides fixed to the body or the seat of the vehicle, that it allows to freely move the D-ring (4) of the belt and to redirect the belt until a second fixed point of return (6), located at a height above that of the element it guides and arranged behind it, with which the height of the point of return (4) is regulated automatically, adapting to the height of the passenger. 2.- System of guidance for lap belts (1) according to vindication 1, characterized because the second fixed point of return (6) is shared in common with the seat and is located in the opposite side of the D-ring (4). 3.- System of guidance for lap belts (1) according to vindication 1, characterized because the second fixed point of return (6) is shared with the vehicle.

## CONCLUSIONS

Buses and coaches are convenient modes of transport, and their safety is important especially in the cases of school buses which not only transport large groups of people, but large groups of young passengers, whose retention has specific requirements.

The standards and regulations that are currently applicable to buses and public transport fail to provide a sufficient guarantee of safety to all occupants. The current legislation needs to be revised. Future legislation is expected to be a comprehensive system that makes the installation and use of restraint systems compulsory in all seating positions for all occupants of all vehicle categories, including buses and coaches.

Studies of bus and coach accidents, including the cases covered in this project, have proven that the correct use of safety belts in these vehicles represents an increase in safety by preventing total or partial ejection and projection of occupants, which is the cause of most serious and fatal injuries.

The innovative design by Applus<sup>+</sup>IDIADA is a contribution aimed at improving child safety in school buses. Applus<sup>+</sup>IDIADA designed, developed, tested and patented the system of a self adjustable safety belt, integrated into bus seats, for use by adults as well as children. It has been verified that the integrated child restraint system developed for school bus transport seats meets the requirements to be approved as a functional safety system.

## ACKNOWLEDGEMENTS

This project was undertaken on behalf of FITSA (Spanish Foundation of the Technological Institute for Automotive Safety), who owns the rights of the patent.

The authors want to acknowledge that the collaboration of the Traffic Accident Research Unit and Passive Safety Departments of Applus<sup>+</sup>IDIADA has also been essential to completing it.

## REFERENCES

- [1] Application of accident reconstruction in the assessment of the use of seat belts in buses; Dr.-Ing. Carles Grasas, Ing. Ignasi Ferrer; IDIADA Automotive Technology SA; EAEC 2001.
- [2] Assessment of the use of seat belts in buses based on recent road traffic accidents in Spain; Ignasi Ferrer (Applus<sup>+</sup>IDIADA), Juan L. de Miguel (Centro Zaragoza); ESV 2002.
- [3] Submarining Injuries of Belted Occupants in Frontal Collisions - Description, Mechanisms and Protection; and C. Leung.

# METHODOLOGIES FOR MOTORCYCLIST INJURY PREDICTION BY MEANS OF COMPUTER SIMULATION

**Nicholas M. Rogers**

International Motorcycle Manufacturers Association

**John W. Zellner**

Dynamic Research, Inc.

**Anoop Chawla**

Indian Institute of Technology

**Tamotsu Nakatani**

Japan Automobile Research Institute

Paper No. 05-0311

## ABSTRACT

Methods for predicting motorcyclist injuries by means of computer simulation have evolved since the 1970's and are critically reviewed in the context of International Standard ISO 13232. The latter was approved in 1996 in order to establish minimum scientific requirements for motorcyclist protective device research, including calibration of simulations against laboratory and full-scale test data. Data from an example ISO-compliant simulation are presented which indicate substantial agreement between the distribution of predicted and real injuries in n=501 accidents in Los Angeles and Hannover. Other data indicate that multi-body and finite element models can produce similar buckling responses when they incorporate similar levels of detail. Key emerging technologies and issues are identified.

## INTRODUCTION

COMPUTER SIMULATION METHODS for predicting motorcyclist injuries due to impacts have evolved since the early 1970's, from single mass models, to multi-rigid-body (MB) models, to finite element (FE) models, and to hybrid FE/MB models. This paper begins with an historical review of the development of these simulation methodologies, their standardisation under ISO 13232 [1], their capabilities to predict the distributions of rider injury severities observed in real accidents, and some comparisons between multi-body (MB) and finite element (FE) simulation methods and results. Conclusions and discussion are provided regarding the levels of agreement between simulations and real accidents, MB and FE models, and emerging technologies and issues that relate to future progress in this field.

## RESEARCH QUESTIONS

This paper addresses the following research questions:

- 1) What is the history and current status of motorcyclist injury prediction by means of computer simulation?
- 2) What standards exist for motorcyclist injury simulations, and what are their purpose and requirements?
- 3) How well can current simulations predict rider injuries distributions observed in real accidents?
- 4) Can either multi-rigid-body (MB) or finite element (FE) methods be used to predict structural phenomena such as buckling?
- 5) What are the key emerging technologies and issues in the motorcyclist injury simulation field?

## METHODS

### History and Status of Motorcyclist Injury Prediction by Computer Simulation

In order to address research questions 1 and 2, a global English language literature search and review was conducted of references that had key or title words including "motorcycle," "crash" or "impact," and "simulation." The resulting papers are reviewed herein.

### Prediction of Rider Injuries

In order to address research question 3, multi-body computer simulations of 501 LA/Hannover car/motorcycle accidents were run, as specified in ISO 13232[1]. The results in terms of distribution of predicted body region injury severities were compared to the corresponding injury distributions from the real accidents, as also described in ISO 13232-2, annex C [1]. The model is described subsequently.

### Model

As described by Kebschull et al. [16], an ISO Motorcyclist Anthropometric Test Dummy (MATD) was modeled using the US Air Force Articulated Total Body (ATB) code for multi-rigid body systems. The MATD includes 28 standardized modifications to a Hybrid III 50th percentile male dummy in accordance with ISO 13232-3, in order to make it compatible with motorcycle postures and multi-directional impacts. The motorcycle that was modeled was a Kawasaki GPZ 500, and for the current investigation this was examined in its

baseline, unmodified condition. The opposing vehicle that was modeled was a production Toyota Corolla 4 door sedan, as specified in ISO 13232-6. Mass properties, dimensions, joint locations, and suspension properties for the motorcycle and opposing vehicle were determined by laboratory measurements of exemplar vehicles.

### Model Calibration

ISO 13232-7 specifies that 20 dynamic and 11 static laboratory component tests be done and quantitatively compared with the corresponding computer simulations of these tests. In addition, a motorcycle barrier test is specified in order to provide a comparison between the modelled and measured response characteristics related to the front wheel, front suspension, and front fork bending properties and their effects on the motorcycle forces and motions resulting from frontal impact. As required by the Standard, Kebschull et al. [16] graphed the force vs. displacement for these 42 static and dynamic tests overlaid with the simulation results. As required, the simulation parameters used for the calibrations were used for all subsequent simulation runs.

The Standard also requires comparison and correlation of the simulation with full-scale impact test results. Data from 14 full-scale tests were used for correlation, and for the peak resultant head acceleration correlation the  $r^2$  correlation coefficient was found to be 0.91. The percentage of femur fractures, knee dislocations and tibia fractures correctly predicted by the simulation was reported to be 93%, 93%, and 100% respectively.

In addition, Kebschull et al. [16] presented the "overlaid" full-scale and simulation helmet displacement time histories. The authors reported that the limitation of this particular calibration method is that it compares only the end points of the time histories. An alternate, revised method to compare these time history variables, has been proposed as an amendment to the Standard. With this proposal, a correlation factor, analogous to an  $r^2$  correlation coefficient, is calculated over the time history as follows:

$$C = 1 - \frac{\sum_{i,k} (d_{i,k} - \bar{d}_i)^2}{\sum_{i,k} (r_{i,k} - \bar{r}_i)^2}$$

where:

- $C$  = correlation factor
- $i$  = subscript for each impact configuration
- $k$  = subscript for each time step

$$d_{i,k} = r_{i,k} - \hat{r}_{i,k}$$

$\bar{d}_i$  = average value (over time) of  $d_{i,k}$

$r_{i,k}$  = value for test i at time k

$\bar{r}_i$  = average value (over time) of  $r_{i,k}$

$\hat{r}_{i,k}$  = value for computer simulation i at time k

Using this method, the average correlation across all tests and all 13 variables was found to be 0.82.

### Model Validation

The injury (AIS) severities for each of six body regions that were calculated for the baseline motorcycle in the n=501 LA/Hannover impact configurations analyzed by Kebschull et al. [16] were compared to the actual injury severities from the real n=501 accidents. These new results are described subsequently.

### Comparison of MB and FE Simulations of a Simple Structure

In order to address research question 4, the aforementioned published references in this area were reviewed. Various references, discussed subsequently, have suggested that MB may be unsuitable for modeling buckling or energy absorption phenomena. In order to address this question, an MB model and an FE model of a deformable curved plate were developed, run and compared for various buckling-type impact conditions, in terms of their resulting deflections, velocities and buckling behavior. The two alternative models were constructed with the same 20 X 20 grid of elements, and such that they had the same overall static force-deflection characteristics for the type of calibration test defined in ISO 13232-7. This type of simple structure occasionally occurs in car structures such as the bonnet. The example plates were used to explore the buckling and energy absorption phenomena rather than the responses of specific motorcycle or car components. The two models are described subsequently.

### MB Model

A 20 X 20 grid of rigid hyper-ellipsoids comprising a curved plate was modeled with ATB, each hyper-ellipsoid with dimensions 63 mm long x 63 mm wide x 4 mm thick. The grid was modeled as 20 strips of 20 rigid hyper-ellipsoids. Three degrees-of-freedom joints were placed between each adjacent pair of hyper-ellipsoids along the length of each strip. Each hyper-ellipsoid in each strip was attached to each corresponding hyper-ellipsoid in the adjacent strips with one linear and one angular spring-damper. The mass, moments of inertia, and 3-axis torque-angle

characteristics were calculated based on aluminum alloy material characteristics. Linear damping with different compression and extension characteristics were used in order to model structural hysteresis (i.e., energy absorption), although other forms of energy absorption could have been used. The elements at one edge were constrained by a rigid joint to a wall. The plate was impacted at the opposite edge by a 150 kg rigid sphere 300 mm in diameter traveling toward the supporting wall at 6.7 m/s. The radius of curvature of the plate was 1.566 m.

**FE Model**

400, 4-node shell elements comprising the curved plate were modeled using MSC DYTRAN, each element having dimensions 63 mm long x 63 mm wide x 4 mm thick. Material properties of the same aluminum alloy as was used for the MB plate were used, as described in Table 1. The elements at one edge of the plate were rigidly constrained to a wall. The plate was impacted on the opposite edge in the same manner as was the MB plate.

**Table 1.**  
**Material Properties Used in MB and FE Model Formulation**

Property	Value
Material	ISO R209 AlMg1SiCu
Density	2700 kg/m <sup>3</sup>
Nu	0.33
E	69 GPa
Yield stress	0.275 GPa

**DATA SOURCES**

ISO 13232 (INCLUDING N=501 SUB-SAMPLES OF LA/HANNOVER DATABASES): As a basis of comparison for the predicted injury severity distributions, the real injury severity distributions from the n=501 LA/Hannover car/motorcycle accidents were generated, based on the data in ISO 13232-2, annex C. The latter comprise sub-samples of “car-motorcycle/seated-single-rider/upright-motorcycle” accidents which were provided for use in the ISO Standard, which were drawn from the n=900 census of accidents investigated by Hurt et al. [14], as well as a similarly sized sample of accidents investigated by Otte et al. [24], as reported by Pedder et al. [25].

**RESULTS**

**Literature Review**

The global review of literature revealed the papers listed in the references. These are critically reviewed subsequently. A key aspect that is noted is the extent to which each simulation was quantitatively “calibrated” against laboratory and full-scale test data.

**Early Research**

Perhaps the earliest published attempt to model rider/motorcycle/barrier impacts was that of Knight et al. [17] as summarized by Bothwell et al. [2] in their phase I research for the US/DOT/NHTSA. This involved a 2 dimensional multi-rigid-body Lagrange formulation of a 5 mass rider and a single mass motorcycle. Single-point non-linear contact forces acting on the masses were dependent on displacement and/or time. The rider model contacted the motorcycle at its hands, feet and pelvis, and the motorcycle front wheel contacted the ground and a rigid barrier. The rider was initially in contact with the motorcycle, and could separate from the motorcycle after it contacted the barrier. Time histories of the dummy cg displacement, front wheel force, pelvis/motorcycle force and torso pitching rate are presented, but these were not compared to the full-scale tests that were done. There was no discussion of parameter measurement or component calibration tests. Plans were described for adding an airbag model.

Bothwell et al. [3] report on the addition of an airbag model, and the further work of Knight et al. [18] to develop a 3 dimensional multi-rigid-body motorcycle, rider and barrier simulation. This involved an attempt to combine a new, 4 mass motorcycle model with the 15 mass CAL 3D human model simulation developed by Calspan Corporation for the US government. Some preliminary time histories are presented for the motorcycle portion of the model (with a simplified, rigid, point-mass rider) impacting a rigid barrier. Knight et al. [19] present further derivations of and example runs with this model, as well as with the integrated 19 mass model. These include time histories of forces and displacements, and stick figure animations of the rider model. As with the earlier work there was no discussion of parameter measurement, or component or full-scale calibration tests.

Spornor [27], as a doctoral dissertation, developed a 2 dimensional 10 degrees-of-freedom multi-body simulation of a seated rider that collides with a

stationary obstacle representing a passenger car. This was accomplished by converting a multi-body model of a car occupant. The motorcycle handlebars and car were rigid bodies against which the rider interacted. Danner et al. [10] describe how this simulation was used to assess the change in rider trajectory (but not the forces or injuries) resulting from fitment of knee-baffle pads on the motorcycle, without calibration against full-scale test data.

Happian-Smith et al. [12] describe a 2 dimensional, 3 mass model of a motorcycle mainframe, front wheel and rider torso, with single-point contact forces. This was used for analyzing motorcycle cg acceleration as the front wheel and headlamp assembly impacted a rigid barrier. The effects of cast wheels versus wire-spoked wheels were described, as well as the effects of a 120 l airbag (data for or details of which are not shown in this paper). Happian-Smith and Chinn [13] describe a similar simulation that was developed to include a gas-volume model of an airbag, and the effects of this on the angular and linear displacement and velocities of a single-mass rider. Some limited calibrations against laboratory test data are included.

Chinn et al. [7] and Chinn et al. [8] describe a 2 dimensional single mass model of a motorcycle impacting an angled rigid barrier. The model “assumed that the rider was either immediately flung clear or was rigidly attached to the motorcycle.” The effects of motorcycle and prototype leg protector geometry on the yaw rotation of the motorcycle (i.e., tail toward or away from the barrier) was studied, with both a purely rigid-body model, and with spring-dampers placed at the contact points. Rider motion, forces or injuries were not modelled. One example is presented which compares the simulation to full-scale test in terms of motorcycle linear and angular displacement. Happian-Smith et al. [13] describe further details and results with this model.

#### **Models Leading up to the ISO Standard**

Zellner et al. [32] describe a 3 dimensional multi-rigid-body model based on the ATB code. This comprised a 4 mass motorcycle, 25 mass Motorcycle Anthropometric Test Device (MATD) dummy, 7 mass car and 62 elliptical and planar contact surfaces. The model was applied to 163 impact configurations based on groupings of accidents in LA and Hannover. The simulation results were input to an injury cost model developed by Biokinetics, Ltd. No time histories comparing the simulation with either laboratory or full-scale test were presented. Comparisons between the simulation and n=14 full-scale tests are shown in terms of peak resultant head accelerations and simulated leg fractures. The

correlation coefficient for head accelerations was 0.80, and the percentage agreement for upper and lower leg fractures and knee dislocations was greater than 90%. A comparison between one frame of an animation and a test film was shown.

Nieboer et al. [23] describe a hybrid MADYMO 2830 element FE airbag model and MB model of a motorcycle sled and modified Hybrid II dummy, along with some comparisons of measured and simulated dummy acceleration time histories. Nieboer et al. [23] describe an extension of this to a 6 mass motorcycle model including comparisons of some component tests and some test data of dummy and motorcycle time histories. It is noted that for “the motorcycle model as it is presented...the energy absorption is underestimated for large structural deformations,” and that the [then] current v 5.0 of MADYMO “offers adequate [MB] features to improve” this.

Yamaguchi et al. [30] describe an FE model of a motorcycle frame for barrier impact analysis. The FE frame model was connected to ground and barrier via spring and dampers. Time history comparisons of material strain are presented.

Rogers [26] describes simulations of rider injuries with a baseline and a modified sports motorcycle. The model was similar to that reported by Zellner et al. [32]. Time histories of laboratory and full-scale tests are not shown, however correlations of peak resultant head acceleration and leg fractures are reported. These indicate correlation coefficients of 0.84 for the head, and between 82 and 88% for the upper and lower legs and knees. The model was applied to 163 LA and Hannover impact configurations.

Yettram et al. [31] describe a 3 dimensional multi-rigid body model of a rider, motorcycle and rigid barrier. The rider comprises 16 masses, the motorcycle 4 masses, and the barrier an infinite mass. Contact surfaces in general consist of “cylinders” (consisting of a series of overlapping spheres) and planes. The models are calibrated against 14 dummy laboratory tests and 6 motorcycle laboratory tests. Time histories for the overall model are then compared to full-scale test data in terms of motorcycle and dummy head and pelvis forward linear displacement and velocity.

Zellner et al. [33] describe extensions of the Zellner et al. [32] simulation model, including a control volume airbag, an airbag mechanical sensor model, an igniter time delay, separate helmet mass,

deformable chest and abdomen models, and a refined injury cost model. Calibration data for a laboratory test of an airbag deployment with a prone dummy are included, comparing measured and simulated head and neck forces.

Chinn et al. [9] describe a multi-rigid-body MADYMO simulation with FE airbag model. Descriptions of the models are not provided, except that the dummy was a Hybrid III rather than a motorcyclist dummy. Although the model is reported to be based on and compared to laboratory and full-scale tests, no data or calibrations are shown.

### **The ISO Standard for Motorcyclist Injury Research**

Van Driessche [28] describes development of ISO/CD 13232, which specifies “Test and analysis methods for research evaluation of rider crash protective devices fitted to motorcycles. The paper summarizes the ISO committee process involving experts from 10 nations, at the request of United Nations ECE/TRANS Working Party 29. The Standard was subsequently approved at a worldwide level as ISO 13232 [1].

The ISO Standard provides a set of common requirements and assumptions for *minimum levels* of modelling detail, parameter measurement, output variables, post-processing (in terms of three dimensional animations and injury indices), quantitative (rather than qualitative) calibrations, correlations and comparisons against recorded test data.

Specifically, the calibration procedures in the Standard are intended to enable physics-based simulations to be used to *interpolate* between conditions that have been tested in full-scale or in laboratory. For example, simulations are to be done only up to the component force levels that have been measured in laboratory tests, and not extrapolated beyond these. The purpose of the simulation tool, and the ISO Standard itself, is to assess the relative injury benefits and risks of protective devices across large (e.g., n=200) representative samples of conditions reported in real accidents, a task which is too costly to do exclusively by means of full-scale impact tests.

Efforts were made during development of the Standard to ensure that it was “technology-independent” and not “technology-restrictive.” Measures were taken to ensure that, for example, either MB or FE techniques could be used, and that the minimum level of modelling detail for each was consistent with what was achievable at the time,

consistent with the large number of simulations needed to support the purpose of the Standard. The Standard is not intended to be either a workbook or user manual for “how to” implement a motorcycle crash simulation, but rather a standard which ensures that minimum levels of detail, performance and calibration are used, so that the results of the overall analysis may be relied upon.

### **Models Since the ISO Standard was Approved**

Kebschull et al. [16] describe the only published work to date that reports all laboratory and full-scale test calibrations and conventions required by the ISO Standard. The simulation comprised a 7 mass motorcycle, a 30 mass MATD dummy and a 7 mass car. Seventy-two time histories are shown comparing simulation to laboratory tests for various dummy, motorcycle and car components. One series of time histories is shown comparing simulation to full-scale helmet displacement in one full-scale test. Simulation/full-scale correlation data are reported, and the correlation coefficient was 0.91 for peak resultant head accelerations, and the percentage of injuries correctly predicted was between 92 and 100% for the leg regions. The model was subsequently applied to the n = 200 LA/Hannover impact configurations.

Iijima et al. [15] describe a hybrid FE/multi-body simulation involving the LS-DYNA3D and ATB codes. This comprised a 7 mass motorcycle, a 614 element FE airbag, a 30 mass dummy and a 7 mass car. Time histories were not shown, but the correlation coefficient for peak resultant head accelerations was 0.88, and percentage injury agreement for the leg ranged from 94 to 97% across the n=14 required ISO full-scale impact configurations. One frame comparing a simulation animation to a test film is shown. The model was subsequently applied to the n = 200 LA/Hannover impact configurations.

Wang and Sakurai [29] describe a multi-rigid-body MADYMO model of a Hybrid III dummy, a motorcycle and ISO Toyota Corolla saloon car. The dummy comprises 21 masses, the motorcycle 8 masses, and the car 14 masses. The contact surfaces are ellipsoids, cylinders and planes. The model is described as being an initial model, which was not yet developed, calibrated or correlated in accordance with ISO 13232. The paper shows general comparisons of simulation animations against test films, but does not present any time histories. The paper notes that “shape inaccuracy” may occur and notes that “introducing finite element models for

some related parts may be an effective way to remove most of the influences of the limitations.”

Chawla et al. [5] describe a finite element model of a motorcycle and car using the PAMCRASH software, and a reverse-engineering approach to generate the model. This is based on digitizing exterior portions of the motorcycle and car, and adjusting the simulation data in order to match component test data. The standard PAM-CRASH Hybrid III dummy model is used. The objective was to simulate the side-of-car impacts of ISO 13232, however, this preliminary paper did not address the other requirements of ISO 13232, or present any quantitative data. A comparison of an animation with a test film of a motorcycle-to-rigid barrier test, without dummy, is shown. The paper also mentions the need for a finer mesh size in high deformation zones in FE simulations. Mukherjee et al. [20] describe this model in more detail, and state that the goal at this stage was to examine the overall kinematics of the motorcycle and car in side-of-car impacts, and that in the future an MATD dummy model should be used to examine the finer details of the response. The motorcycle model involved 1K elements, and the car model involved 15K elements. Only animation/film comparisons and subjective summaries are provided. They also point out the effect of some of the differences between the MATD model and the H-III model and specifically discuss the importance of the MATD hand grip in affecting the car-MC kinematics. Nakatani et al. [21] describe this same finite element model of a motorcycle (without rider) that impacts a rigid wall. The paper describes calibration of the simulation against various component tests, as well as the barrier force, displacement and acceleration time histories. Comparison of a simulation animation with a full-scale test film is presented.

Canaple et al. [4] describe a multi-rigid body MADYMO model of a motorcycle, dummy and car, used to generate head acceleration time histories for input to a finite element model of a human head and brain. The motorcycle model consists of 6 masses, and the dummy is the standard MADYMO Hybrid III (rather than the ISO MATD) apparently with the head modified in order to represent a helmet. The car is a rather unique multi-body model involving 25 or more rigid-body masses, modeled by a combination of physically cutting up and measuring various structural elements and by calculating force-deflection characteristics based on sub-structure FE modelling. Component calibrations are mentioned but not presented in the paper. Comparisons with an ISO-like full-scale test with an MATD dummy include time histories of motorcycle and dummy

accelerations (although with different dummies), and an animation/film comparison.

Chawla et al. [6] subjectively compare FE simulation animations with films of ISO 13232 car front impact tests. The simulation is a FE model of a Hybrid III frontal car occupant dummy (rather than the ISO MATD dummy used in the tests), a GPZ 500 motorcycle and the Toyota Corolla saloon car specified in ISO 13232. The paper provides only animation / film comparisons and subjective summaries. Certain statements made in the paper appear to be misleading. While the ISO Standard evaluates safety quantitatively, this paper only provides a qualitative comparison of the kinematics. This paper gives a preliminary, subjective and general comparison of animations against full-scale test films, and should not be misinterpreted as a direct comparison, as different dummies were used in the simulation and in the full-scale tests. The paper also reports using "nominal values" (rather than measured values) of impact conditions. The authors of the paper suggest that a quantitative comparison should be taken up only after a qualitative match is obtained. The paper also seems to imply that the Standard is only aimed at rigid body simulations. However, Part 7 of the Standard describes simulation requirements for both FE and rigid body models. The paper argues that "bonnet folding cannot be *effectively* modeled using rigid body models" probably because of the somewhat more predictive nature of FE models (based on material laws and detailed geometry) vis-à-vis rigid body models. However, both FE and rigid-body models require empirically determined input parameters, as well as empirical calibration against both component tests and whole vehicle tests, as discussed previously. The paper lists components which in the opinion of the authors were "critical" for simulating motorcycle impacts. However, the criticality of these components may vary from vehicle to vehicle and from impact to impact. Hence, it may be better to emphasize how well the simulation quantitatively agrees with the test data, rather than on mandating a "design" standard for simulation models. The ISO Standard uses this approach.

Deguchi [11] describes a hybrid FE/multi-body MADYMO model comprising a 21 mass motorcycle, 2200 membrane element airbag, a Hybrid III dummy (rather than a MATD dummy) and a rigid barrier. Force-displacement data comparing the simulation and laboratory tests are shown for the MC front structure, the MC cowl, the seat and the handlebars. The motorcycle and dummy models are then used in a "prescribed motion" simulation (using as inputs the

motorcycle motions recorded on a full-scale test film) in order to predict chest and head accelerations for two car side impacts, for which time history comparisons are shown. For a barrier test, simulation/full-scale comparisons are also shown for barrier force, MC cg and front fork accelerations, for a motorcycle-alone test.

Namiki et al. [22] describes a hybrid FE/multi-rigid body model using the LS-DYNA code, comprising a 35K element motorcycle, a 5K airbag, a 36K element dummy and a 169K element car. Time histories comparing simulation to full-scale are shown for various component tests and for full-scale car side impact tests. In order to reduce run time requirements, which were substantial, “contact search” and “non-involved rigid model” adaptive algorithms were used, which reduced the run time by 30%. Comparisons were made between animations and test films for 45 and 90 degrees car side impacts. A quantitative comparison between simulation and full-scale test was also made in terms of the torso angle and head velocity just before ground impact.

#### MB Simulations of 501 LA/Hannover Accidents

Figure 1 compares the predicted injury distributions from the ISO-compliant simulation of Kebschull et al. [16] to the injury distributions from the real LA/Hannover accidents, for the head, chest, abdomen, upper and lower legs and knees. There is substantial agreement for all body regions and all injury severities. Note that only certain severity levels exist for the lower extremities fractures and dislocations, as described in the AIS definitions and in ISO 13232, and the simulation is in reasonable agreement with those. Head AIS 1 injuries (i.e., headache, dizziness) are typically underreported in real motorcycle accidents, but the sum of “no head injuries” and “AIS 1 head injuries” closely match, between the actual and simulated accidents.

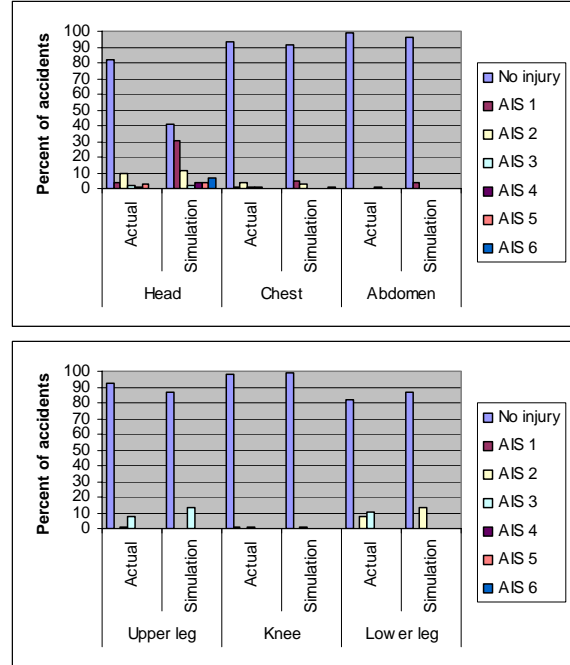


**Figure 1. Comparison of simulated and real injury severities for n=501 LA/Hannover accidents by body region**

#### Comparison of MB and FE Simulations of a Simple Structure

Figures 2 and 3 compare the MB and FE simulation results in terms of time histories for the sphere longitudinal deflection and velocity and mid-span transverse velocity, for the 150 kg 300 mm sphere impacting at 6.7 m/s. As can be observed, the MB and FE results are in generally close agreement in terms of longitudinal deflection and velocity. The transverse rigid-span velocity responses in Figure 3 are also similar in terms of peak velocity and decay time, with the MB model exhibiting a lightly damped mode. Each of these responses could be compared to actual test data for calibration purposes.

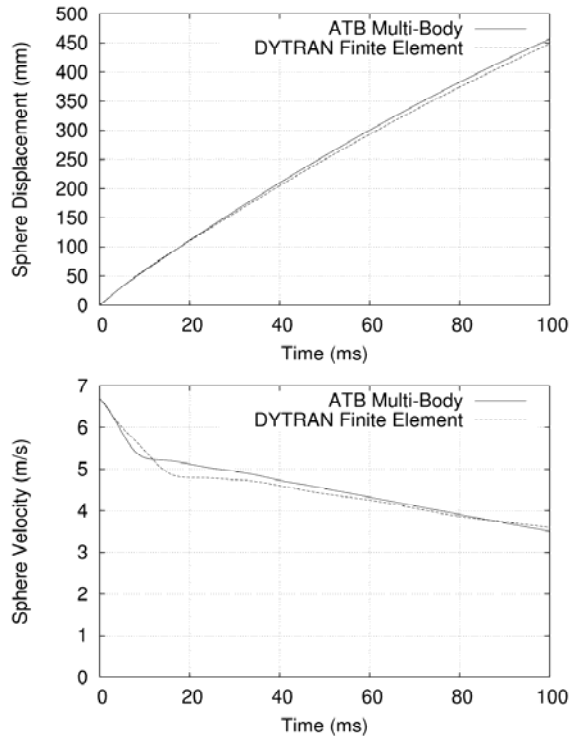


**Figure 2. Comparison of MB and FE time histories for sphere displacement and velocity for 6.7 m/s edge impact**

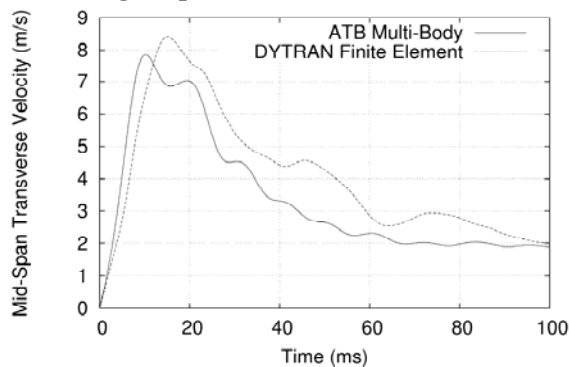


**Figure 3. Comparison of MB and FE time histories for plate mid-span transverse velocity for 6.7 m/s edge impact**

Figures 4a through 4c show the deflected plate shape at three points in time, for the FE model and the MB model. This indicates that both methods are capable of generating a very similar, non-linear buckling response. The notion that MB simulation methods cannot be used to predict buckling is not supported by these results.

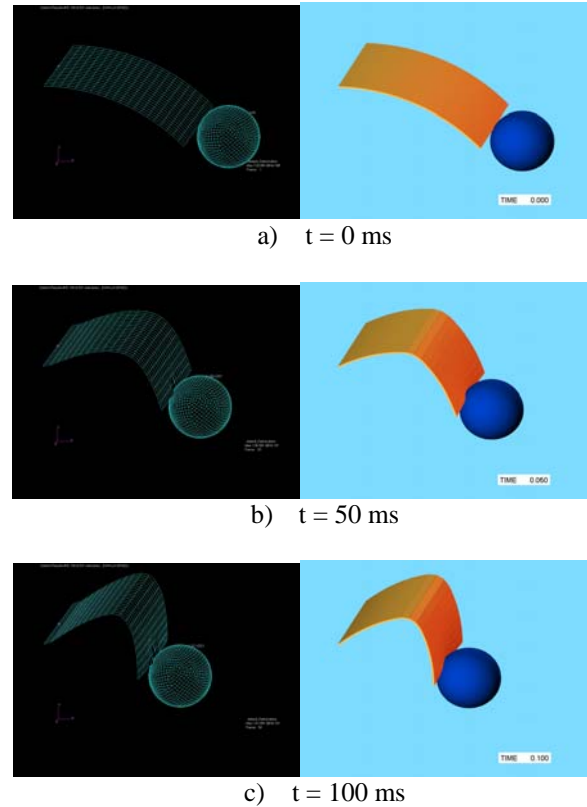


**Figure 4. Comparison of FE (left) and MB (right) plate shape at three time points**

## CONCLUSIONS

### Regarding Current Status of Motorcyclist Simulation Methods

The review of the substantial literature on the subject indicated that much progress has been made since the 1970's in the field of computer simulation of motorcyclist injuries. Early single and multi-mass models with single-point contacts indicated the usefulness of simulation as a crash analysis tool, and led to multi-rigid-body with multiple contact surfaces in the late 1980's, followed by finite element and hybrid MB/FE models. This evolution was made possible by the emergence of affordable high-capacity software and computational speeds. In the early 1990's, the question arose as to the purpose of such simulations in rider protection research, and the minimum requirements that they should meet, in order to be relied upon in providing accident sample-based analysis of the overall effects of various rider protective concepts. This led to standardisation of minimum requirements in ISO 13232 [1].

## **Regarding Standardizing Motorcyclist Injury Simulations**

The review of the technical literature indicated that there are strong reasons why “performance” (and not “design”) standardisation of simulation methods is of vital importance. Without *minimum* provisions for factors such as quantitative calibration, level of modelling detail, outputs and so on, there may be little or no connection to real experimental data, no means for comparing alternative simulations of the same protective device, and therefore little reliability for evaluating the complex phenomena of motorcycle crashes. Typically, a qualitative comparison (for example, as suggested by Chawla et al, [6]) will be done before a quantitative comparison is attempted, but finally the quantitative calibration of simulation “performance” as required in ISO13232 is of vital importance. Simulation “performance” standardisation as found in ISO 13232 provides minimum requirements that are aimed at those aspects which are most important, namely, rider motions and injury indices, regardless of whether multi-rigid body, finite element or other emerging methods are used. Specifically, the calibration procedures in the Standard are intended to enable simulation models to be used to *interpolate* between conditions for which the simulation has been calibrated against laboratory and full-scale tests, enabling a large, representative samples of real accidents to be simulated. At the same time, it is essential that such standardisation be in no way restrictive of new simulation technologies. A simulation standard must allow for evolution of emerging technologies, including for example, modal, continuum, voxel and hybrid methods. Finally, the currently continuing and open work of ISO/TC22/SC22/WG22 to improve and to revise ISO 13232 in order to reflect the experience of users is a process that benefits all researchers in the rider safety field.

## **Regarding Prediction of Rider Injury Distributions**

The example ISO-compliant multi-body simulation described by Keschull et al. [16], which was previously calibrated against data for 31 laboratory tests and 14 full-scale impact tests, was found herein to be capable of accurately predicting the general distributions of locations, types and severities of rider injuries across the head, chest, abdomen, upper and lower legs and knees in 501 real accidents.

There appears to be no fundamental reason why FE (or hybrid MB/FE) models, or other types of models

(e.g., continuum, modal, voxel, etcetera) could not also achieve this or a higher level of accuracy, although to date there has been no published research describing such calibration, validation and comparison for these types of models.

## **Regarding Comparison Between MB and FE Simulation Methods**

The comparison of MB and FE simulations of plate buckling-type impacts indicated that very similar deflections, velocities and deformed shapes were obtained when the models had the same number, size and shape of elements. This was the case for both longitudinal and transverse deflections and velocities and the buckling phenomenon itself. The notion that MB is unsuitable for simulating dynamic buckling is not supported by these results.

## **DISCUSSION**

Both multi-body (MB) and finite element (FE) simulations, when suitably calibrated against laboratory and full-scale impact tests in accordance with ISO 13232, have a strong potential to accurately predict rider injury severities outcome of motorcycle impacts. This of course relies on the existence of a suitably biofidelic motorcyclist dummy and corresponding injury probability curves which are used to generate the underlying laboratory and full-scale test. It is observed that committee ISO/TC22/SC22/WG22 continues to identify limitations of and areas for improvement in both the dummy and injury probability curves. Recently these have included upgrades for the motorcyclist dummy neck, to be in better agreement with the existing biomechanical and accident data, and as well as discussion of the potential improvements to other components of the MATD.

In general, the plate comparison herein provides one example where FE and MB can give similar results, when a similar level of detail is included. The FE model uses a somewhat more “predictive” approach based on material laws and empirically measured material properties, while the MB model is based on empirically determined relations and the laws of rigid-body mechanics. This illustrates the point that it may be the “number and size of elements”, and the “empirical relations used”, which may have stronger effects on the detailed accuracy, rather than whether the “calculation method” is FE, MB, continuum or some other method. This distinction is sometimes overlooked in the technical literature. With regarding to modelling alternatives, on the one hand, FE provides a somewhat more “predictive” method, as

the structure's material properties (e.g., elasticity and strength) can be specified *a priori*, but like MB, FE methods also require careful empirical verification of structural damping and energy absorption. In addition, in order to be predictive, FE requires close attention to sufficiently small mesh size in high deformation zones, internal surface geometry, bracing and stiffening bends, as well as co-ordinated mesh sizes on contacting surfaces, which has not always been the case in MC/car crash simulations to date. Typically, FE (or MB using similar numbers of elements) require extensive human and machine resources, and to date, no work has been published which uses FE model for simulation of the 200 impact configurations in ISO 13232, which is the main purpose of the simulation tool defined in the Standard. Further automation and optimization of FE and hybrid methodologies, as well as "contact search" and "non-involved rigid model" adaptive algorithms, and expected further increases in computational speeds, may improve this situation in the future and appear to be key emerging technologies. This needs to be done, however, with due attention to the calibration and correlation norms of ISO 13232. Needed updates, based on experience, to ISO 13232 and to the underlying methodologies include further allowances for new modelling techniques, and probably more rigorous calibration criteria, without the Standard becoming overly restrictive or difficult to conform to. At the same time, the Standard is not intended to be a workbook or users' manual for "how to" implement a given type of simulation, but rather a guideline for a simulation's reliability and performance in comparison to real test and accident data. The current Standard specifies calibration and correlation methods, but has minimal criteria for these, and it is clear that the quality and reliability of simulations would be further improved by implementing simulation performance criteria. In addition, a key issue continues to be the need for more detailed biomechanical and accident data, which have limited both the resolution and the domain-of-validity of the methodologies used to date.

### Limitations of this Study

In the 501 simulations of real accidents reported herein, the overall injury distributions rather than the "case-by-case" outcomes were compared between the simulated and real accidents. "Case-by-case" outcomes may not compare as closely, due to detailed differences between the modelled and the real motorcycle, opposing vehicle and rider types, and other extensive details of the real accidents. Further case-by-case validation work would be useful.

Nevertheless, as found herein, it is considered that at a macro level, the distributions of injury severities are highly reliable, and provide the "best available information" regarding the outcomes of representative samples of motorcycle accidents.

In addition, a key issue continues to be the need for more detailed biomechanical and accident data, which have limited both the resolution and the domain-of-validity of the methodologies used to date.

In the comparison between MB and FE models, the example used was a curved plate, which although it may be representative of some structures like car hoods, is less typical of motorcycle components such as wheels, which behave more as complex 3 dimensional structures. Analogous comparisons between MB and FE for these more complicated cases could reveal other results. All such models however, should be quantitatively calibrated against real dynamic test data in order to clarify the significance of such findings. In addition, this preliminary analysis did not examine in detail the contribution of individual finite element "shape" changes, or detailed differences in total damping and energy absorption, or their significance, which could be further quantified in the future.

### REFERENCES

- [1] Anonymous, "Motorcycles - Test and Analysis Procedures for Research Evaluation of Rider Crash Protective Devices Fitted to Motorcycle," ISO 13232, Geneva, 1996
- [2] Bothwell, P.W. and H.C. Petersen, "Dynamics of Motorcycle Impact, Vol. I," DOT HS 800 586, 1971
- [3] Bothwell, P.W., R.E. Knight, and H.C. Petersen, "Dynamics of Motorcycle Impact, 1971-1973, Vol. I," DOT HS 800 906, 1973
- [4] Canaple, B., et al., "Impact Model Development for the Reconstruction of Current Motorcycle Accidents," IJCrash, 2002
- [5] Chawla, A., et al., "A Methodology for Car-Motorcycle Crash Simulation," JARI Research J, 2001
- [6] Chawla, A., et al., "FE Simulations of Motorcycle-Car Frontal Crashes, Validation and Observations," 18<sup>th</sup> ESV, 2003
- [7] Chinn, B.P. and P.D. Hope, "Protecting Motorcyclists' Legs," 11<sup>th</sup> ESV, 1987

- [8] Chinn, B.P., J. Happian-Smith and M.A. Macaulay, "The Effect of Leg Protecting Fairings on the Overall Motion of a Motorcycle in a Glancing Impact," International J of Impact Engineering, 1989
- [9] Chinn, B.P., et al., "Development and Testing of a Purpose Built Motorcycle Airbag Restraint System," 15<sup>th</sup> ESV, 1996
- [10] Danner, M., K. Langwieder, and A. Sporer, "Accidents of Motorcyclists – Increase of Safety by Technical Measures on the Basis of Knowledge Derived From Real-Life Accidents," 10<sup>th</sup> ESV, 1985
- [11] Deguchi, M., "Modelling of a Motorcycle for Collision Simulation," 18<sup>th</sup> ESV, 2003
- [12] Happian-Smith, J., M.A. Macaulay and B.P. Chinn, "Motorcycle Impact Simulation and Practical Verification," 11<sup>th</sup> ESV, 1987
- [13] Happian-Smith, J. and B.P. Chinn, "Simulation of Airbag Restraint Systems in Forward Impacts of Motorcycles," SAE 900752, 1990
- [14] Hurt, H.H., J.V. Ouellet, and D.R. Thom, "Motorcycle Accident Cause Factors and Identification of Countermeasures, Vol. I," DOT-HS-805 862, 1981
- [15] Iijima, S., et al., "Exploratory Study of an Airbag Concept for a Large Touring Motorcycle," 16<sup>th</sup> ESV, 1998
- [16] Kebschull, S.K., et al., "Injury Risk/Benefit Analysis of Motorcyclist Protective Devices Using Computer Simulation and ISO 13232," 16<sup>th</sup> ESV, 1998
- [17] Knight, R.E. and H.C. Petersen, "Dynamics of Motorcycle Impact, Vol III," DOT HS 800 588, 1971
- [18] Knight, R.E. and H.C. Petersen, "Dynamics of Motorcycle Impact, Vol III," DOT HS 800 908, 1973
- [19] Knight, R.E. and H.C. Peterson, "Dynamics of Motorcycle Impact III," Denver Research Inst., 1976
- [20] Mukherjee, S., et al., "Motorcycle-Car Side Impact Simulation," IRCOBI, 2001
- [21] Nakatani, T., et al., "A Methodology for Motorcycle-vehicle Crash Simulation – Development of Motorcycle Computer Simulation Model," JSAE 20015417, 2001
- [22] Namiki, H., T. Nakamura, and S. Iijima, "A Computer Simulation for Motorcycle Rider-Motion in Collision," SAE 2003-32-0044, 2003
- [23] Nieboer, J.J., et al., "Motorcycle Crash Test Modelling," 37<sup>th</sup> STAPP, 1993
- [24] Otte, D., P. Kalbe, and E.G. Suren, "Typical Injuries to the Soft Body Parts and Fractures of the Motorized Two-Wheelers," IRCOBI, 1981
- [25] Pedder, J.B., D. Otte, and H.H. Hurt, "Motorcycle Accident Impact Conditions as a Basis for Motorcycle Crash," 12<sup>th</sup> ESV, 1989
- [26] Rogers, N.M., "Evaluation of TRL Designed Leg Protectors for a Medium Sized Sport Motorcycle," 16<sup>th</sup> ESV, 1994
- [27] Sporer, A., "Experimentelle und Mathematische Simulation von Motor-radkollisionen im Vergleich zum realen Unfallgeschehen," PhD Dissertation, TU München, 1982
- [28] Van Driessche, H., "Development of an ISO Standard for Motorcycle Research Impact Test Procedures," 14<sup>th</sup> ESV, 1994
- [29] Wang, Y. and M. Sakurai, "Development and Verification of a Computer Simulation Model of Motorcycle-to-Vehicle Collisions," SAE 1999-01-0719, 1999
- [30] Yamaguchi, H., et al., "Simulation of Motorcycle Low Speed Frontal Collision," Small Engine Technology Conference and Exposition, 1993
- [31] Yettram, A.L., et al., "Computer Simulation of Motorcycle Crash Tests," 14<sup>th</sup> ESV, 1994
- [32] Zellner, J.W., S.A. Kebschull, and K.D. Wiley, "Motorcycle Leg Protectors: an Analysis of Overall Effectiveness Via Computer Simulation," Institut für Zweiradsicherheit, 1991
- [33] Zellner, J.W., J.A. Newman, and M. Nicholas, "Preliminary Research into the Feasibility of Motorcycle Airbag Systems," 14<sup>th</sup> ESV, 1994

## **CHILD SAFETY RESEARCH IN SCHOOL BUSES**

**Linda B. McCray**

National Highway Traffic Safety Administration  
United States

**John Brewer**

Volpe National Transportation Systems Center United States  
Paper Number 05-325

### **ABSTRACT**

School bus transportation is one of the safest forms of transportation in the United States. Every day, our nation's 440,000 public school buses transport more than 23.5 million children to and from school and school-related activities.

The safety record is impressive: American students are nearly eight times safer riding in a school bus than with their own parents and guardians in cars. The fatality rate for school buses is only 0.2 fatalities per 100 million vehicle miles traveled (VMT) compared to 1.5 fatalities per 100 million VMT for cars.[1]

School buses have annually averaged about 26,000 crashes resulting in 10 deaths – 25 percent were drivers; 75 percent were passengers. Frontal crashes account for about two passenger deaths each year.

This paper describes past, present and near-term school bus research efforts.

### **INTRODUCTION**

The safety record for school bus transportation exceeds that of all other modes of travel. Students are nearly eight times safer riding in a school bus than in cars. Each school day, 440,000 public school buses transport 23.5 million children. The fatality and injury rates associated with school buses are consistent from year to year. On average, about seven passengers die in school bus crashes each year. In 2003, five passengers and six drivers died in school transportation vehicles (this includes school buses and other vehicles used as school buses), and 21 pedestrians were killed when struck by a school bus. NHTSA has several standards relating to school bus safety. NHTSA's requirements for compartmentalization on large and small school buses, plus safety belts on small buses contribute to the safe environment.

As a result of the passage of the National Traffic and Motor Vehicle Safety Act of 1966 and the School Bus Safety Amendments of 1974, NHTSA currently has 35 Federal Motor Vehicle Safety Standards (FMVSS) that apply to school buses. The 1974 amendments directed NHTSA to establish or upgrade school bus safety standards in eight areas: emergency exits, interior occupant protection, floor strength, seating systems, crashworthiness of the body and frame, vehicle operating systems, windshields and windows, and fuel systems.

### **BACKGROUND**

During the rulemaking process in the early 1970's, when the school bus safety standards were being established, NHTSA looked carefully at available injury and fatality data, existing research, and public comments submitted to the agency to determine what system of occupant protection should be required in school buses. Research conducted at UCLA in 1967 and 1972 evaluated existing seats on school buses. That research showed that school bus seating systems at that time did not provide adequate protection for the school bus passengers. Those findings led NHTSA to issue a contract to AMF Corporation to design new, protective school bus seating systems that provided uniform levels of protection to seated occupants ranging in size from a six-year old (21 kg (46 pounds) and 1,219 mm (48 inches) in height) to a 50th percentile male (75 kg (165 pounds) and 1,778 mm (70 inches) in height).[2]

Recognizing that school bus vehicles i) are generally heavier than their impacting partners, ii) impart lower crash forces on their occupants, and iii) distribute crash forces differently than do passenger cars and light trucks in crashes, it was determined that the best way to provide crash protection to children on large school buses was to use a concept called "compartmentalization." This concept provides a protective envelope consisting of strong, closely spaced seats that have energy-absorbing seat backs. These requirements are found in FMVSS No.

222, School bus passenger seating and crash protection, which became effective for newly manufactured school buses on or after April 1, 1977. This standard has not changed significantly since its inception.

### **Current School Bus Passenger Crash Protection**

Even though compartmentalization has proven to be an excellent concept for injury mitigation, NHTSA initiated an extensive research program to develop the next generation occupant protection system(s). The protective abilities of today's school buses have been reaffirmed by two years of research. No matter how safe our children are on school buses, it is vitally important to constantly reassess existing safety measures.[3] During this timeframe the National Transportation Safety Board (NTSB) had begun special investigations on school bus crashes.

### **National Transportation Safety Board Recommendations**

The National Transportation Safety Board (NTSB) initiated a special investigation to determine whether additional measures should be taken to better protect bus occupants. It examined school bus and motorcoach crashworthiness issues through the analysis of 6 school bus and 40 bus crashes and through information gathered at the Safety Board's August 12, 1998 public hearing. The special investigations addressed, in part, the crucial safety issues regarding the effectiveness of current school bus occupant protection systems. As a result of the investigations, the NTSB issued three safety recommendations pertaining to passenger crash protection in school buses.[4]

Recommendation H-94-010 was initiated to require NHTSA to evaluate occupant restraint systems, including those presently required for small school buses. The recommendation was made as a result of a crash between a small school bus and a tractor-trailer dump truck. The crash resulted in four passenger fatalities, all of whom were ejected from the school bus. In the investigation the Safety Board noted that the children were not instructed to wear the required lap belts due to the potential risk of injuries from use of lap belts in frontal impacts.

Safety Recommendations H-99-45 & H-99-46 were initiated to encourage NHTSA to develop and implement performance standards for school bus occupant protection systems that take into account frontal impact collisions, side impact collisions, rear impact collisions, and rollovers. These

recommendations resulted from the 1999 study on bus crashworthiness issues. NTSB evaluated six selected school bus crashes for this study. Based on that analysis, the Safety Board came to the conclusion that the current "compartmentalization" is incomplete in that it does not adequately provide protection in all crash scenarios.[5]

Safety Recommendation H-00-28 was initiated to encourage NHTSA to modify the Federal Motor Vehicle Safety Standards to prohibit protruding door handles or latching mechanisms on emergency doors. This recommendation resulted from a crash in October 1999 with a school bus/dump truck/utility trailer near Central Bridge, NY. NTSB concluded that, although the side emergency exit door met safety regulations, it presented a hazard for passengers because portions of door release mechanism protruded into the passenger compartment potentially injuring a person on the latch assembly. This seems to imply that it is unsafe to sit next to a side emergency exit door.

Thus far, the agency's school bus research efforts have focused on addressing these and other Safety Board recommendations.

### **NHTSA's School Bus Research**

As previously noted, no matter how safe our children are on school buses, it is vitally important to regularly reassess existing safety measures. Therefore, Congress requested that the Department of Transportation investigate potential approaches that could further enhance safety protection offered on our nation's school buses. An April 2002 report to Congress documents the program findings.[6]

The agency began a research program to investigate potential approaches that could further enhance safety on school buses. Phase I of the research program was to identify safety problems. The NHTSA reviewed several sources of information in an effort to define the effectiveness of the existing FMVSS requirements applicable to school buses. Data from the agency's FARS (Fatality Analysis Reporting System), NASS (National Automotive Sampling System)-GES (General Estimates System), and SCI (Special Crash Investigations), along with state and local officials' crash information and data from the NTSB were analyzed.

The problem determination showed that (1) most fatalities occurred for occupants of large school buses, and (2) the most significant factors in fatal, two-vehicle crashes are that they occur on roadways where the posted speed limit is 88-97 kph (55-60

mph) and involve heavy trucks (83% frontal impacts and 15% side impacts). Based on the analytical results from Phase I, two full-scale crash tests were defined to be representative of the real-world environment of large school bus crashes.[7]

### **Frontal Impact Research**

The agency conducted a frontal crash test of a large conventional style school bus (Class C) into a rigid barrier at 48 kph (30 mph) to evaluate the protection afforded by compartmentalization. Instrumented dummies of various sizes were used ranging from the 50th percentile male representing an adult or a large size teenager to the 6-year-old child. A small frame 5th percentile female adult (representing a large 12-year-old child) was also used in that test. In addition to measuring the dummy injury measures in the crash test, one other objective was to determine the crash pulse experienced in such school bus crashes so that similar tests could be carried out in a simulated sled environment.

The full-scale crash tests showed that the head and chest injury measures for all dummies were far below the accepted injury threshold values in frontal crashes. However, the FMVSS No. 208 neck injury criteria could not be met by neither the 6-year-old child dummies nor the 5<sup>th</sup> percentile female dummies in the frontal crash test.

Phase II of the program was the development of the frontal sled test pulse and evaluation of various restraint configurations in frontal crashes. A series of 25 sled tests was conducted using two sled bucks with various size dummies for evaluation of seats designed to comply with existing compartmentalization requirements as well as to evaluate the protection offered by lap belts and lap/shoulder belt systems in frontal crashes. Full details of these efforts are provided in ESV Papers No. 345[8] and Paper No. 313[9].

In response to the NHTSA research effort, the agency has pinpointed other improvements that could be made to improve the safety of school buses. The agency is considering the following changes to existing federal safety regulations: 1) increased seat back height to reduce the potential for passenger override in the event of a crash; 2) require lap/shoulder belt restraints in buses under 4536 kg (10,000 pounds); and 3) require standardized test procedures for voluntarily installed lap/shoulder belts .[10]

### **Side Impact Research**

A full-scale side impact test was conducted by towing an 11,406 kg (25,265 lb) cab-over heavy

truck, at 72 kph (45 mph) and 90°, into the side of a transit style school bus (Class D).



**Figure 1 Pre-Test Photograph of Side Impact School Bus Crash Configuration**

Pre- and post-test configurations are shown in Figures 1 and 2, respectively. Two 50th percentile male side impact dummies (SIDs), along with the Hybrid III 5th percentile female and 6-year-old frontal dummies, were positioned in selected seating locations in the side impact test. One Hybrid II 50<sup>th</sup> percentile male dummy was located at the direct point of impact to determine “survivability” within the impact zone.



**Figure 2 Post-Test Photograph of Side Impact Crash Test**

In the side impact test the dummy injury measures for the head, and the chest g's for the frontal dummies and the thoracic trauma index for the side impact dummy were far below the established threshold levels for those dummies not directly in the impact zone. The crash pulse varied depending on the relative location with respect to the point of impact. Accelerometers were positioned along the length of the school bus. The acceleration time histories are shown in Figure 3. No single pulse is fully representative of the range of vehicle responses observed in the side impact crash test. Acceleration levels dropped significantly away from the point of impact. [11]

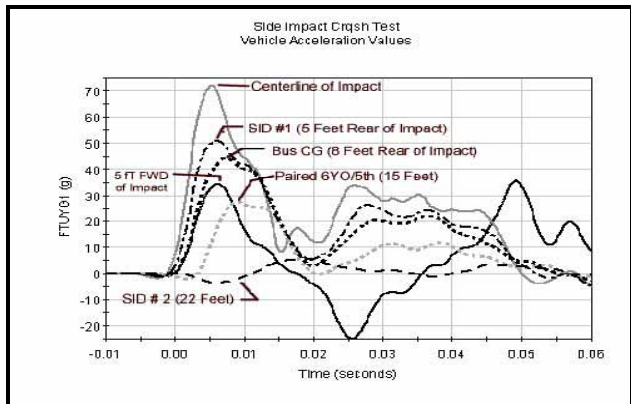


**Figure 3. Side Impact School Bus Acceleration at Various Locations in the Bus**

### Exploratory Side Impact Research

As previously noted, no single pulse is fully representative of the range of vehicle responses observed in the side impact crash test. The agency's Vehicle Research and Test Center (VRTC) conducted a small number of free-motion head-form impactor tests to determine the feasibility of reducing head injury and also to determine the feasibility of test methodology to assess side impact protection.

The exploratory research effort focused on impacting hard, interior contact surfaces. The areas of impact included: the top of the window frame, wheelchair belt attachment/mount, center of roof header, upper seam on roof header, window cross bar, side of window frame, upper roof rib, upper window frame, emergency exit hinge and above the emergency exit hinge. These surfaces were impacted at a speed ranging from 22 to 28 kph (15 – 17 mph). The 24 kph (15 mph) impactor target speed is the current test speed used in the FMVSS No. 201, *Occupant Protection in Interior Impact*, for occupant interior protection. It was believed that impactor test speeds similar to those used in FMVSS No. 201 was a reasonable starting point until further side impact research could be conducted. The head injury criterion (HIC) values were evaluated and some exceeded the injury assessment reference values. It was observed that the impact areas that were covered with raised sheet metal yielded lower HIC values. Raised sheet metal was applied to some locations in which high HIC values occurred. This effort demonstrated that high HIC responses can be reduced with the proper countermeasure application. The effect this would have on reducing real-world injuries cannot be quantified until the data analysis described in the next section of this paper is completed.

## **RESEARCH APPROACH**

Most of the earlier school bus research efforts focused on frontal crash protection. The current focus of the school bus research program is on side impact protection.

A 9-step approach has been undertaken for this school bus side impact research program. The approach includes the following steps:

1. Select and define a crash problem
2. Set countermeasure functionality
3. Survey technology for functions
4. Create countermeasure concepts
5. Estimate preliminary costs and benefits
6. Select the most promising concept(s)
7. Develop and conduct objective tests
8. Refine costs and benefits
9. Agency decision on next steps

Step 1 of the approach focuses on defining the safety problem. Earlier efforts that were undertaken identified that multi-vehicle impacts with trucks were the most injurious types of side impact school bus crashes. These crashes typically occurred on roadways with posted speed limits of greater than 72 kph (45 mph). In order to best focus agency resources, a preliminary estimation of costs and benefits must be determined (step 5). Steps 2 through 4 must be conducted at minimum costs to help identify the most feasible approach to be taken. These engineering evaluations are based on sparse data to direct a greater investment in countermeasure test development and benefits analyses. Once the preliminary estimation of benefits is determined, steps 6 and 7 are conducted. Based on these results, the costs and benefits are refined in step 8. Step 9 is an agency decision-making step. In this phase of the process, the research results, along with cost and benefits, are then assessed by the agency to determine the next action to be undertaken. While research efforts are conducted within the framework of steps 1 – 8, Agency involvement occurs throughout the entire process.

### **Problem Definition Underway**

#### **Database Interrogation and Synthesis**

A database interrogation and synthesis is being conducted to provide the status of injury and sources of injuries to children in side impact school bus

crashes. The framework of this effort encompasses Steps 1, 5 and 8 of the research approach.

The intent of this phase is to expand and update earlier approaches that attempt to define total frequency of injuries to children.[12] The analysis includes side impact crashes of full-size school buses. To the extent possible, segmentation of the data will include occupant age, occupant location (near or far side relative to impact), occupant restraint system used (e.g. compartmentalization vs. other restraint systems), crash orientation (right side vs. left side), injury location (head, thorax, etc.), and injury severity (AIS). Data on both absolute occurrences (total frequency) and rates relative to exposure (i.e., normalized by relevant vehicle miles traveled) will be pursued. An attempt will also be made to assess whether multiple impacts (including rollover) can be correlated with more severe injuries.

Fortunately, school bus crashes that result in fatalities are rare. For this reason, 101 school bus crashes since 1980 with associated fatalities can be studied on a case-by-case basis. Of these, 40 are side impact crashes. The cases have been extracted from FARS. Further information on each case should be available through the police accident report. Although the statistical significance of relative trends may be limited, the ability to ascertain details of these rare events should be valuable.

### **Next Steps**

Once the police reports have been reviewed, a more reasonable assessment of potential countermeasures can be made. This will serve as a foundation on which steps 1 – 8 of the process can be pursued.

### **CONCLUSIONS**

This paper sought to describe the status of child safety research related to school buses. It has shown that school buses are an especially safe mode of transportation. Nonetheless, given their importance to posterity, further research is warranted. The authors will continue their work to identify and exploit opportunities for increased safety.

### **ACKNOWLEDGEMENT**

The authors express their sincere appreciation to Jeffrey Elias, Charles Hott, Kenneth Paciulan, Susan Partyka, James Simons, Lisa Sullivan and a host of other staff for their technical support, guidance, endless input, and recommendations for this project. Your support has been instrumental in directing the school bus research efforts.

### **REFERENCES**

- [1] Report to Congress, School Bus Safety: Crashworthiness Research, April 2002, <http://www-nrd.nhtsa.dot.gov/departments/nrd-11/SchoolBus.html>
- [2] McCray and Barsan-Anelli, Simulations of Large School Bus Safety Restraints – NHTSA, 17<sup>th</sup> ESV, 1998, Paper No. 313
- [3] Report to Congress, School Bus Safety: Crashworthiness Research, April 2002, <http://www-nrd.nhtsa.dot.gov/departments/nrd-11/SchoolBus.html>
- [4] Highway Special Investigation Report: Bus Crashworthiness, NTSB Report Number: SIR-99-04, adopted on 9/21/1999, <http://www.nts.gov/publicctn/1999/SIR9904.pdf>
- [5] Highway Special Investigation Report: Bus Crashworthiness, NTSB Report Number: SIR-99-04, adopted on 9/21/1999, <http://www.nts.gov/publicctn/1999/SIR9904.pdf>
- [6] NHTSA 37-02, Press Release, NHTSA Sends School Bus Report to Congress, May 7, 2002
- [7] Elias, Sullivan, and McCray, Large School Bus Safety Restraint Evaluation, 17<sup>th</sup> ESV, 1998, Paper No. 345
- [8] Elias, Sullivan, and McCray, Large School Bus Safety Restraint Evaluation, 17<sup>th</sup> ESV, 1998, Paper No. 345
- [9] Elias, Sullivan, and McCray, Large School Bus Safety Restraint Evaluation-Phase II, 18<sup>th</sup> ESV, 2001, Paper No. 313
- [10] NHTSA 37-02, Press Release, NHTSA Sends School Bus Report to Congress, May 7, 2002
- [11] Report to Congress, School Bus Safety: Crashworthiness Research, April 2002, <http://www-nrd.nhtsa.dot.gov/departments/nrd-11/SchoolBus.html>

# COACH PASSENGER INJURY RISK DURING ROLLOVER: INFLUENCE OF THE SEAT AND THE RESTRAINT SYSTEM

**Giovanni Belingardi**

**Paolo Martella**

**Lorenzo Peroni**

Dipartimento di Meccanica

Politecnico di Torino

C.so Duca degli Abruzzi 24

10129 Torino

Italy

E-mail: paolo.martella@polito.it

Paper Number 05-0439

## ABSTRACT

In the last years the European Community funded several projects, whose general aim was to improve the safety of road users. Among them, the “Enhanced Coach and Bus Occupant Safety” (ECBOS) Project was set up in order to study improvements in current regulations and propose new standards for the development of safer buses and coaches.

For what concerns the rollover protection (ECE66 Regulation), one of the main suggestions, proposed by the partners of the ECBOS project [1], is to take into account the presence of the passengers on board both in the numerical and in the experimental homologation tests. An additional mass in the vehicle increases the energy assumed to be absorbed by the structure in order to pass the test. That could lead the bus manufacturers to increase the strength of the vehicle super-structure in order to obtain a deformation level below the limits stated in the ECE66 regulation.

A numerical study was performed to evaluate how an increment of the super-structure strength, that ensures the vehicle to pass the homologation test with the passengers onboard (i.e. to avoid intrusions into the residual space defined by the regulation), affects the injury risk for the passengers themselves. To perform such a kind of study, it is essential to model the interactions of the passengers with the coach inside environment accurately. One of the most important components that greatly influence the movement of the passengers inside the vehicle is the seat. For that reason, a detailed hybrid model (Mulibody – FE) of a seat was developed based of a real coach seat, whose data were provided by a seat manufacturer. Two configurations were analysed, changing the restraint system (two-point and three point belt). The injury risk for passengers was evaluated calculating the most significant injury parameters and criteria (HIC, TTI, VI, etc.).

## INTRODUCTION

Passenger transport in terms of buses and coaches is very safe nowadays. Statistical comparisons with other means of transport show evidence for the high safety level of buses and coaches, which is much higher than that of cars, being comparable with that of trains or even airplanes. Despite the high safety rating, particular serious bus and coach accidents still occur and arouse public attention casting doubt on the positive safety image of these vehicles. In the European Community approximately 20000 (4%) buses and coaches are currently involved in accidents with personal injuries each year [2]. More than 30000 persons are injured due to those accidents and about 200 occupants suffer fatal injuries. Among the bus and coach accidents, one of the most dangerous is surely the rollover of the vehicle.

The ECBOS project, started on January 2000 and ended on June 2003, was sponsored by the European Community to suggest improvements in current regulations and propose new regulations and standards for the development of safer buses and coaches. Seven partners from six European countries were involved in the project. As outcome of the project a list of suggestions for new regulations and written standards were jointly proposed by the partners in order to decrease the incidence and the severity of occupant injuries and social suffering which occur as a result of bus and coach accidents.

## ROLLOVER PROTECTION

Buses and coaches are transport means for which in Europe the regulation is not at the moment so strict as for cars. The high cost of the single vehicle makes the manufacturers unwilling to perform full vehicle tests like car crash-tests.

For what concerns the rollover of a bus or a coach, the point of reference is the UNECE regulation no. 66 (ECE66) [3]. The same requirements of this regulation are included in the European Directive 2001/85/EC [4]. The ECE66 applies to single decked vehicles constructed for the carriage of more than 16 passengers, whether seated or standing, in addition to the driver and crew. This regulation set the uniform provision concerning the approval of large passenger vehicles with regard to the strength of their super-structure. “Super-structure” means the parts of a vehicle structure which contribute to the strength of the vehicle in the event of a rollover accident.

In order to obtain the approval, the super-structure of the vehicle shall be of sufficient strength to

ensure that during and after it has been subjected to one of the test methods:

- no displaced part of the vehicle intrudes into the residual space
- no part of the residual space projects outside the deformed structure

“Residual space” means the volume within the passenger compartment which is swept when the transverse vertical plane shown in figure 1 is moved in along the vehicle longitudinal axis.

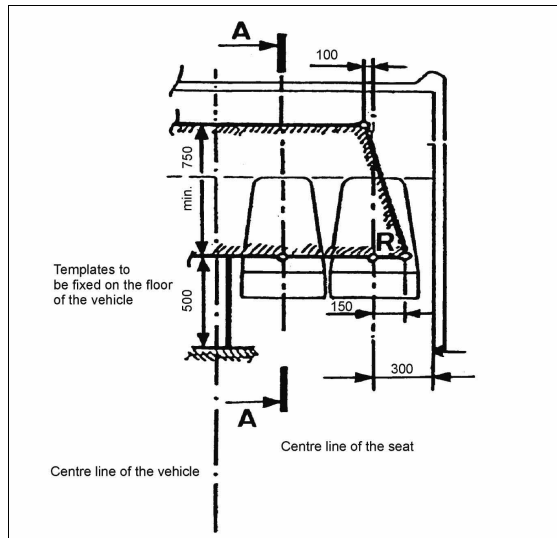


**Figure 1. Residual space as defined in the ECE 66 Regulation.**

Each type of vehicle can be verified according to one of the following methods at the discretion of the manufacturer or according to an alternative method approved by the competent authority:

- a rollover test on a complete vehicle
- a rollover test on a body section or sections representative of a complete vehicle
- a pendulum test on a body section or sections
- a verification of strength of super-structure by calculation

"Body section" means a section containing at least two identical vertical pillars on each side representative of a part or parts of the structure of the vehicle.

It is important to remark that in the homologation tests, proposed by the ECE66 regulation, the vehicle is verified without considering the presence of the passengers on board.

## NUMERICAL MODEL

A numerical model able to describe the behaviour of an M3 vehicle structure during a rollover was developed [5-8] through the multibody (MB) approach using MADYMO software.

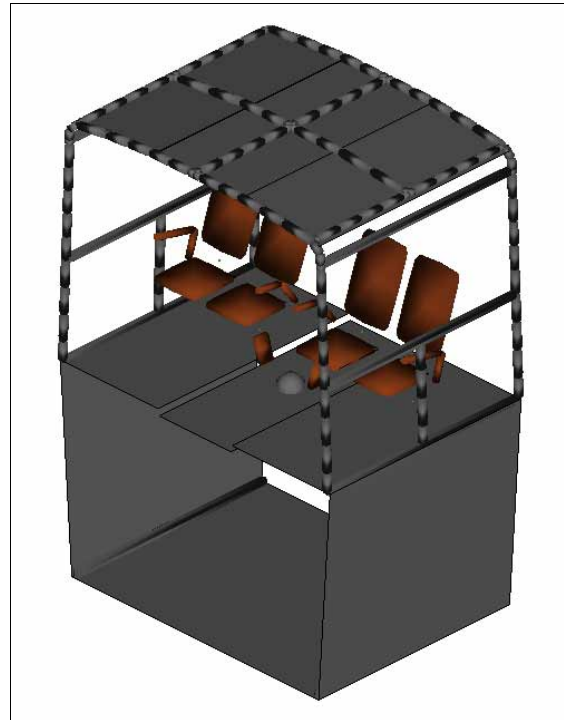


**Figure 2. Bay section MB model.**

The model (figure 2) was built according to a real bay section (figure 3) used by the Cranfield Impact Centre (CIC) to perform experimental tests within the ECBOS project [9].



**Figure 3. CIC bay section (courtesy of CIC).**

The general design of the bay section was taken from a typical existing ECE66 approved coach design. The bay section design used two complete body rings (i.e. one ring consists of two

window pillars, roof cross beam and floor cross beams). These two rings were connected via longitudinal beams at floor, waist and roof level. The bay section had one row of seats. The data about the bay section geometry and the materials characteristics were provided by CIC, together with the results of two experimental rollover tests. These results were used to check the behaviour of the model and to validate it [5,6].

The seats were modelled thought a simplified structure made up of three bodies (seat base, seat back and head rest) [5,6].

### MB SEAT MODEL

In order to study the consequences of a rollover on the passengers the movement of the occupants inside the vehicle must be described accurately. For this purpose it is necessary to set up a seat model able to represent the behaviour of a real seat during a rollover event properly. Therefore a detailed MB seat model was developed according to a real seat (figure 4) produced by Lazzerini, an Italian seat manufacturer of the Grammel group, one of the most important European seat producers. The information necessary to build the model was provided by the manufacturer itself.



Figure 4. Seat for M3 class coaches.

### Seat frame

The manufacturer provided the data about the frame of a double seat usually mounted on M3 class vehicles. This frame is made up of three components:

1. The linking element between the seat and the side wall of the coach (figures 5 and 6)
2. The seat leg on the aisle side (figures 7 and 8)
3. The transversal rods supporting the seats (figures 9 and 10)

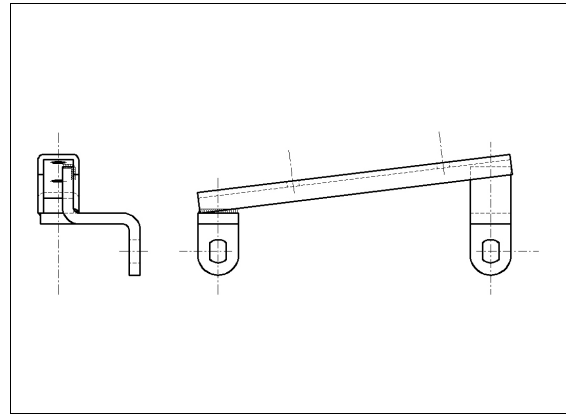


Figure 5. Linking element.



Figure 6. Linking element fitted.

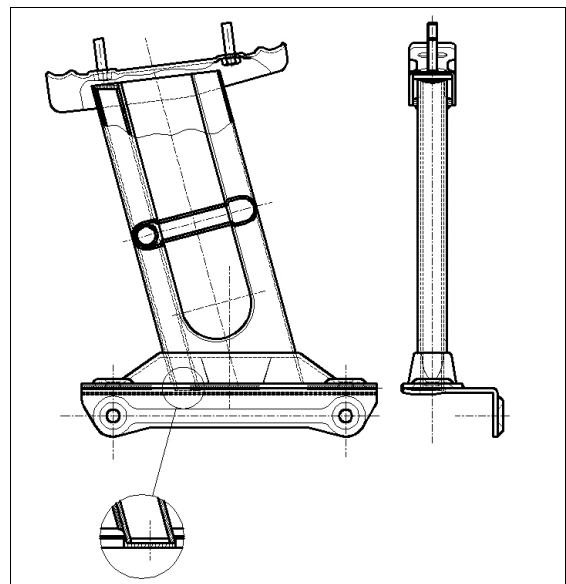
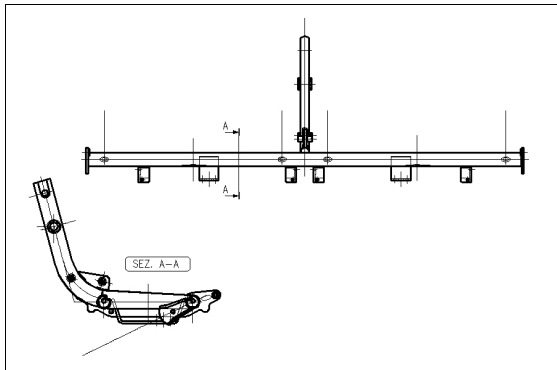


Figure 7. Seat leg.



**Figure 8. Seat leg fitted.**



**Figure 9. Transversal rods.**

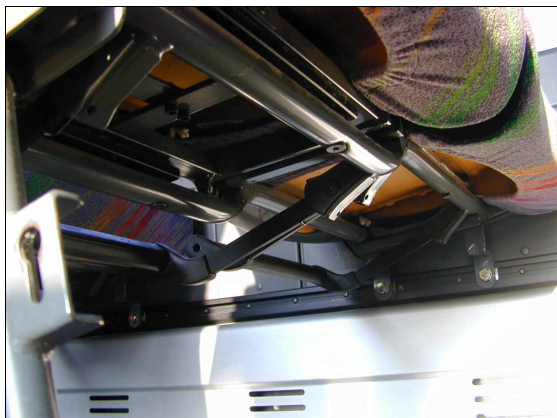


**Figure 10. Transversal rods fitted.**

The first component is made up of three parts welded together. The parts with holes connect the seat to the coach side wall through two bolts while

the horizontal plate bears the seat frame. In the seat leg two bolts in the lower side plate connect the seat to the coach deck. A second welded plate holds the housing for the vertical column. A beam is positioned inside the column to increase the bending stiffness of the structure. The upper part of the seat leg is shaped properly to house the transversal rods of the frame, which bear the seat.

The two transversal rods are connected at the aisle side to the seat leg and at the window side to the horizontal plate of the linking element. The connection is made by two blocking plates clamped by bolts.

### **FE model of the seat frame**

In a rollover the seat frame is usually deformed in the transversal direction beyond the elastic limit of the material.

In order to build the MB model of a structure submitted to an elastic-plastic collapse it is necessary to know in advance the deformed shape of the structure for the applied loads and its non linear stiffness characteristic. In this way it is possible to know the collapse points of the structure, in which the proper kinematic joints will be positioned, and the strength characteristic assigned to them [10]. Starting from the data provided by the manufacturer, the FE model of the seat frame was developed with the aim of studying how this structure collapses during the rollover of the vehicle. The three components of the seat were modelled with four nodes shell elements, while the welding was modelled with rigid beam elements connecting together the nodes of the components in the welded areas. For what concerns the connections between the three elements, due to the very high stiffness of the links, they were modelled as completely rigid.



**Figure 11. Deformed seat frame.**

## FE simulations of the seat under-frame collapse

In the FE simulations, carried out through MADYMO, a displacement field reproducing what happens during a rollover was applied to the seat frame. Looking at the deformed shape of a bay section after a rollover test (figure 11), it is possible to notice that the displacement of the seat frame is caused by the rotation of the side wall around the plastic hinge which develops in the lower part of the window pillars. To reproduce that in the simulations the nodes around the holes of the side plate at the bottom of the seat leg (figure 12) were rigidly constrained to the inertial reference system.

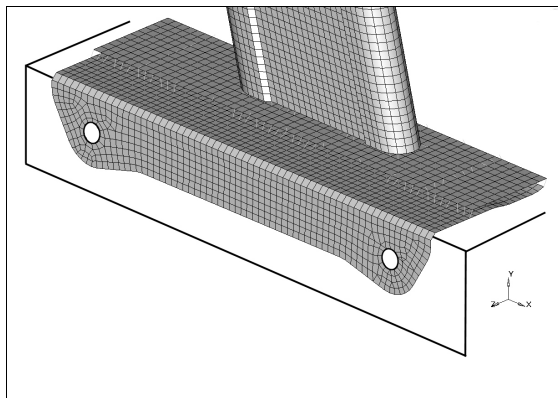


**Figure 12. FE model boundary conditions: seat leg.**

Furthermore the nodes belonging to the horizontal plate at the bottom of the leg (figure 12) were constrained so that they couldn't go down (negative Y direction) due to the presence of the vehicle floor.

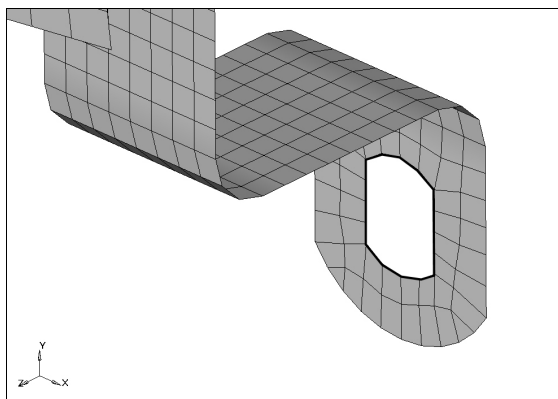


**Figure 13. FE model boundary conditions: linking element.**

The nodes around the holes in the linking element (figure 13) were constrained to a reference system rotating around the X axis.

Two different situations were simulated. A positive rotation (figure 24) to model what happens to the seat at the impact side and a negative rotation (figure 15) to simulate what happens to the seat

opposite the impact side.

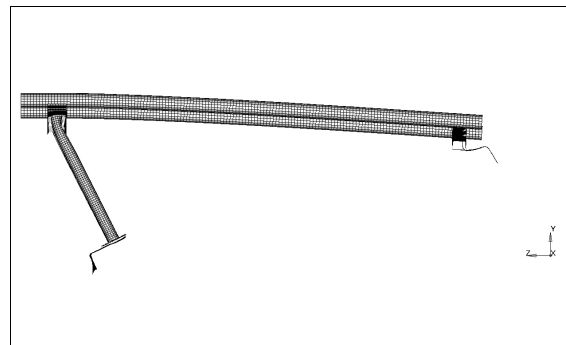


**Figure 14. Deformed shape of the seat on the impact side.**

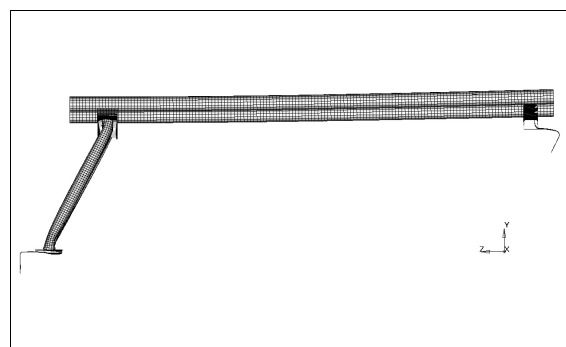


**Figure 15. Deformed shape of the seat opposite the impact side.**

For what concerns the seat on the impact side the deformed shapes obtained from the simulations are shown in figures from 16 to 18. It is possible to locate three collapse points. The first point is in the clamps of the linking element (figure 16) and the second one is at the top of the column in the seat leg (figure 17). The last point is in the side plate at the bottom of the seat leg (figure 18) which went up during the deformation process.

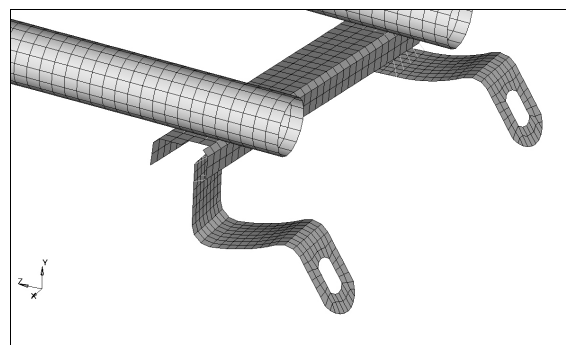


**Figure 16. Deformed shape of the linking element on the impact side.**

For the seat opposite the impact side the deformed shapes are shown in figures from 19 to 21. In this case too there are three collapse points.

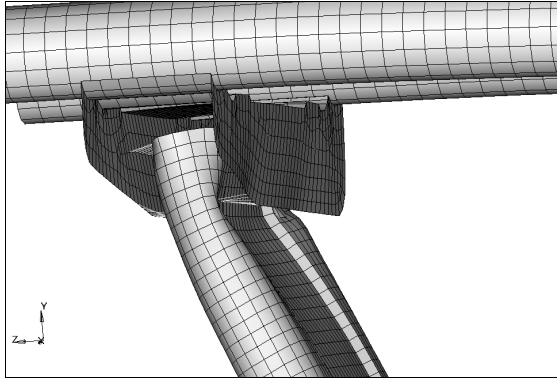


**Figure 17. Deformed shape of the upper part of the seat leg on the impact side.**

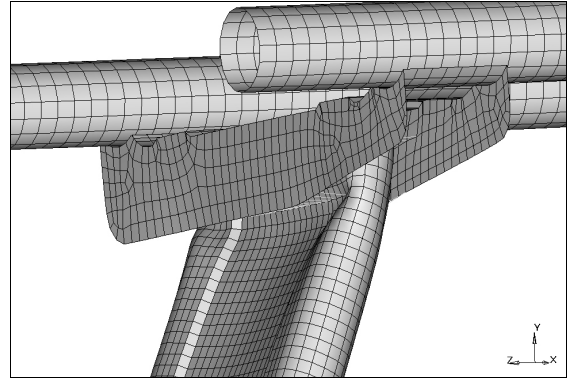


**Figure 20. Deformed shape of the upper part of the seat leg opposite the impact side.**

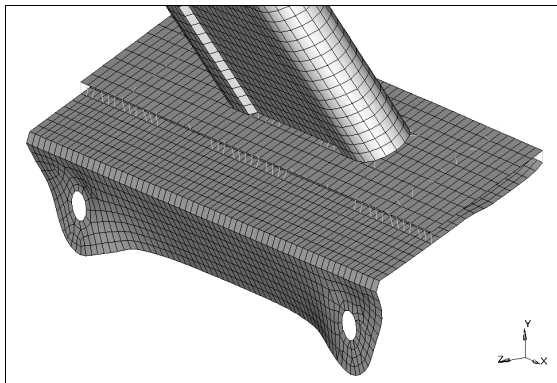


**Figure 18. Deformed shape of the lower part of the seat leg on the impact side.**

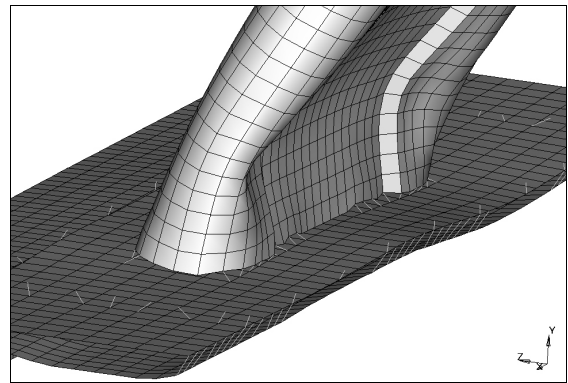


**Figure 21. Deformed shape of the lower part of the seat leg opposite the impact side.**

The first two points are similar to the ones of the seat on the impact side, i.e. in the clamps of the linking element (figure 19) and at the top of the column in the seat leg frame (figure 20). The third point developed in a different location than in the previous case. As the seat leg can't go down due to the presence of the vehicle floor, the structure collapsed in the lower part of the vertical column (figure 21).

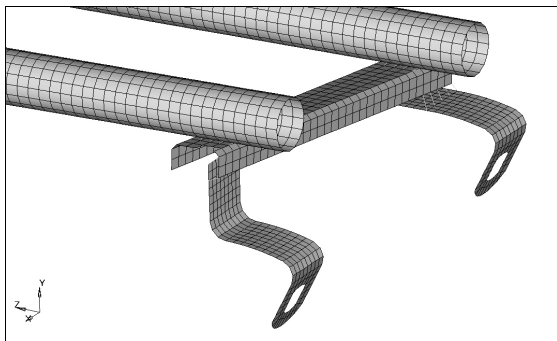


**Figure 19. Deformed shape of the linking element opposite the impact side.**

As a consequence the global behaviour of the seat frame can be described by concentrating the deformations of the structure in three points (figure 22) where the plastic hinges develop while the remaining parts of the structure can be represented as two rigid members. The non-linear strength characteristic of the seat frame in terms of resistant moment versus relative rotation of the two rigid members around point 2 is shown in figure 23. This curve was calculated from the FE simulations by an energy balance.

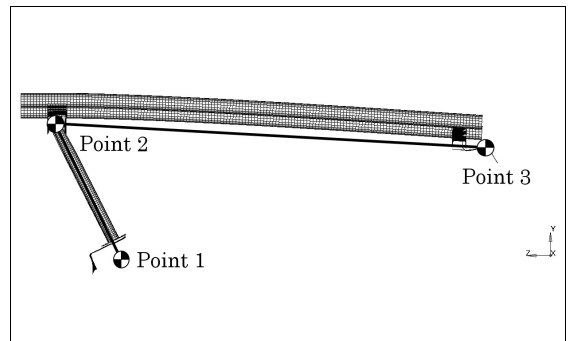


**Figure 22. Deformation points of the seat frame.**

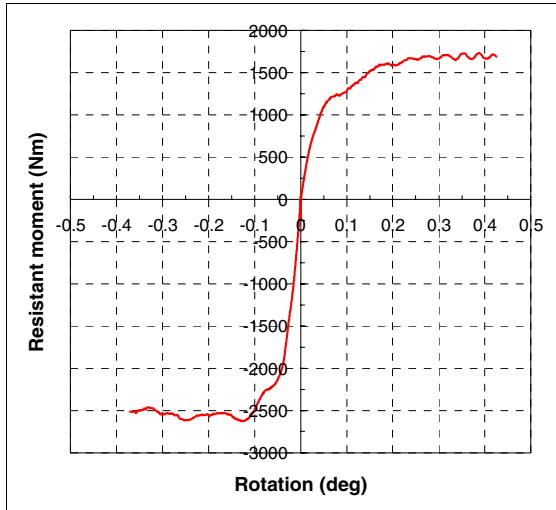


**Figure 23. Seat frame non-linear characteristic.**

**Seat MB model**

In the seat model development both techniques, MB and FE, were used. With the FE it was possible to describe the geometry of the seat in a more accurate way than with simple MB surfaces like planes, ellipsoids and cylinders. In particular the seat cushion, the seat back, the armrests, the footrests, the plastic parts in the seat back and the seat leg were modelled by shell elements (figure 24). The material used to model these components was a rigid one (NULL MATERIAL in MADYMO) without inertial properties.



**Figure 24. MB seat model with FE contact surfaces.**

The layout of the MB part of the seat model is shown in figure 25. Each seat component (seat cushion, seat back, etc.) is described by one rigid body whose inertial properties were calculated from the data provided by the seat manufacturer. The bodies are connected together by kinematic joints in an open branch chain. Joints 1 are revolute joints which allow the rotation of the seat back around the transversal axis of the seat (Y axis). The

strength characteristic of these joints were experimentally measured and provided by one the ECBOS project partners [11]. Joint 2 is a revolute joint, with the rotation axis parallel to the X direction, allowing the deformation of the seat structure in the transversal direction (Y direction). The strength characteristic of this joint was extracted from the FE simulations described in the previous section (figure 23). Each FE surface (seat cushion, seat back, etc.) is rigidly connected to the corresponding body.

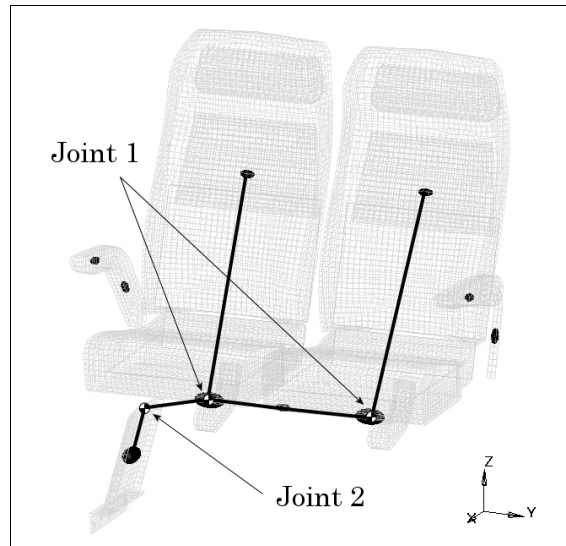


**Figure 25. Layout of the MB seat model.**

Therefore the FE components act as rigid surfaces whose role is to define the geometry for the contact interaction of the seat with other bodies like dummies, pillars, etc. The mass and the stiffness properties were described by the MB parts.

The links between the seat and the bay section structure were modelled by four point restraints, two at the window side and two at the aisle side (figures 26 and 27).

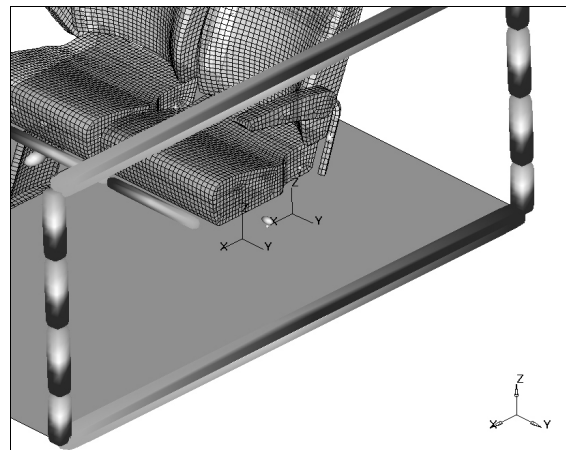


**Figure 26. Link between the seat model and the bay section mode: window side.**

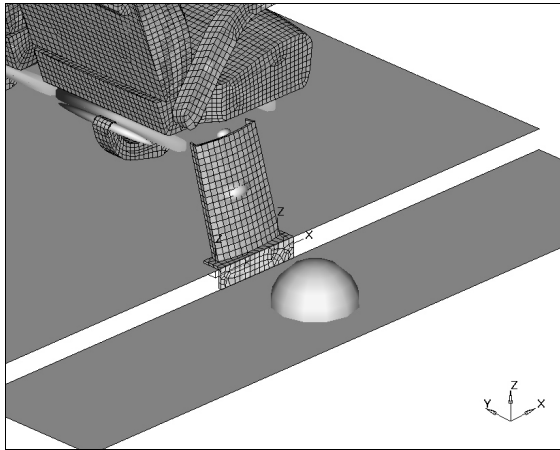


**Figure 27. Link between the seat model and the bay section mode: aisle side.**

The point restraint is a link between two points belonging to different bodies with a strength characteristic (linear or non-linear) in each principal direction (X, Y and Z). For what concern the window side (figure 26), the point restraints connect the body representing the external cushion to a body in each window pillar, while on the aisle side (figure 27) they connect the body of the seat leg to the central body of the bay section.

The strength characteristic in the X direction, corresponding to the forward and backward movement of the seat, was experimentally measured and provided by one of the ECBOS project partner [11]. In the other two directions very high strength characteristics were assigned in order to avoid, in those directions, the movement of the seat relative to the bay section structure. The values of these strength characteristics were calibrated after some test simulations.

## INTERIORS MODEL

In order to perform a realistic evaluation of the injury risk for passengers in a rollover event it is very important to correctly model the interactions between the passengers and the internal component of the vehicle. From statistical study performed within the ECBOS project the main interior components, which are cause of injury for the passengers, are the window pillar, the side window, the luggage rack and the seat [12]. For this reason, in addition to an improved seat model, in the MB bay section model some plane were added to represent the luggage racks and the side windows. To describe the contact interaction between the passengers and the interior components the following contact characteristics were assigned to the internal surface of the bay section:

- Dummy head – side window
- Dummy head – window pillar

- Dummy head – luggage rack
- Dummy – seat back
- Dummy – seat cushion

These characteristics were obtained from experimental tests carried out within the ECBOS project [11,13].

## INFLUENCE OF THE SEAT

As described above, a detailed new seat model was introduced in the MB bay section model in order to obtain a better description of the interactions between the passengers and the interior environment during the rollover.

A study was performed to evaluate how an improved description of the seat behaviour affects the results of the simulations in term of loads acting on the body of the passengers and injury parameters. To that end two rollover simulations with an EUROSID-1 dummy model seated in position 3 (near the aisle on the impact side) were carried out using the MB bay section model equipped with the improved seat model. In the first simulation the dummy was restrained with a two-point belt, while in the second one it was restrained with a three-point belt (figure 28).

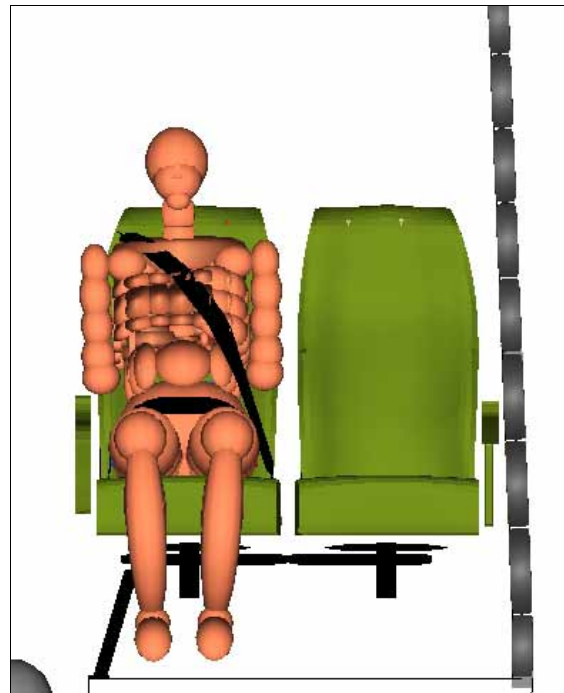


**Figure 28. Dummy model with 3-point belt.**

The loads and the injury parameters calculated in such simulations were compared with the ones obtained through the same MB bay section model equipped with a simplified seat model [5]. The comparison is reported in table 1 for a passenger restrained with a two point belt and in table 2 for a

passenger restrained with a three point belt.

**Table 1.**

**Comparison of the body loads and injury parameters for a two-point belted passenger with different seat models.**

	Simplified seat model	Detailed seat model
Head acceleration (m/s <sup>2</sup> ) (CFC1000)	1841	2619
HIC (CFC1000)	1701	2751
Force lower neck (N)	4187	5750
Moment lower neck (Nm)	142	151
Force lower lumbar (N)	7285	5340
Moment lower lumbar (Nm)	254	177
Force pubic symphysis (N)	7285	3701
Femur Left force (N)	1457	1129
Femur Right force (N)	1475	640

**Table 2.**

**Comparison of the body loads and injury parameters for a three-point belted passenger with different seat models**

	Simplified seat model	Detailed seat model
Head acceleration (m/s <sup>2</sup> ) (CFC1000)	339	567
HIC (CFC1000)	78	319
Force lower neck (N)	1776	1811
Moment lower neck (Nm)	113	135
Force lower lumbar (N)	4089	3433
Moment lower lumbar (Nm)	216	198
Force pubic symphysis (N)	4089	2500
Femur Left force (N)	1695	939
Femur Right force (N)	1624	694

The comparison of the results shows that the improved description of the seat deformation during the rollover makes it possible to simulate in a more detailed way the load distributions on the passenger. In particular the loads, and the injury parameters consequently, in the lower part of the

body (lumbar, pubic symphysis and legs) are lower with the detailed seat model than with the simplified seat model. On the contrary the loads and injury parameters on the higher part (head and neck) of the body are higher with the detailed seat model than with the simplified seat model. Furthermore with the improved seat model the loads acting on the legs are quite different while with the simplified model the loads are nearly the same. As the impact is on the left side it is reasonable to expect higher loads on the left femur as happens with the improved seat model.

## **ECE66 ROLLOVER TEST WITH PASSENGERS**

### **Effect of the additional mass**

As remarked previously, in the tests of the ECE66 regulation the presence of the passengers on board is not taken into account. As in this regulation no prescriptions are stated about restraint systems to be used on buses and coaches, the assumption behind this document is that unbelted passengers do not affect the energy absorbed by the structure during a rollover.

During a rollover only a part of the total passengers mass is coupled to the structure, this part depends on the kind of restraint system that constrains the passengers. Within the ECBOS project some studies [9] were performed to assess the mass of the occupant that is effectively coupled to the structure during the ECE66 rollover test. The results of such studies are reported in table 3.

**Table 3.**

**Mass of the occupant coupled to the structure during an ECE66 rollover test**

	mass coupled to the structure
Unrestrained passenger	20 %
2-point belted passenger	70 %
3-point belted passenger	90 %

A study was performed to evaluate how the presence of the passengers onboard affects the deformation of a bus structure in a rollover event. Using the MB bay section model, four different rollover test simulations were carried out:

- Rollover test without passengers
- Rollover test with four unrestrained passengers onboard
- Rollover test with four lap-belted passengers onboard
- Rollover test with four 3 point-belted passengers onboard

In order to simulate the presence of the passengers onboard, a ballast mass was placed on each seat and rigidly connected to it as shown in figure 29. Taking as reference a 50%ile EuroSID-1 dummy, the inertial properties of the ballast masses were assigned according to the percentage reported in table 3, while the centre of gravity of the mass was positioned in the same location of the centre of gravity of the dummy positioned on the seat.

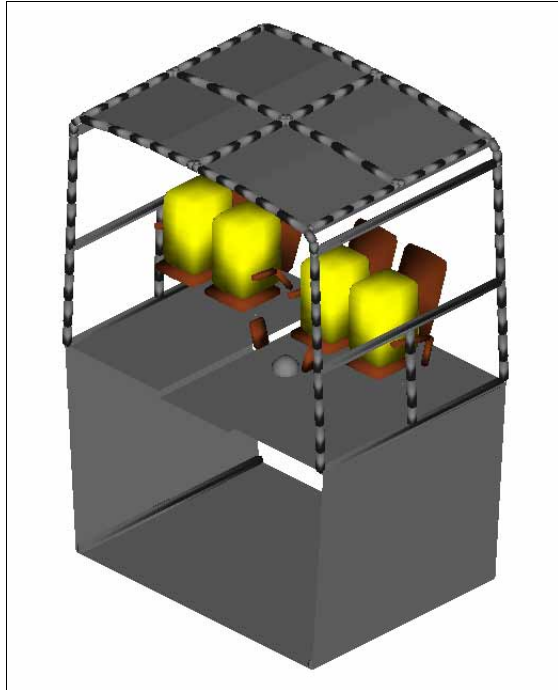


**Figure 29. MB bay section model with ballast masses.**

The rollover tests were carried out following exactly what stated in the ECE 66 regulation.

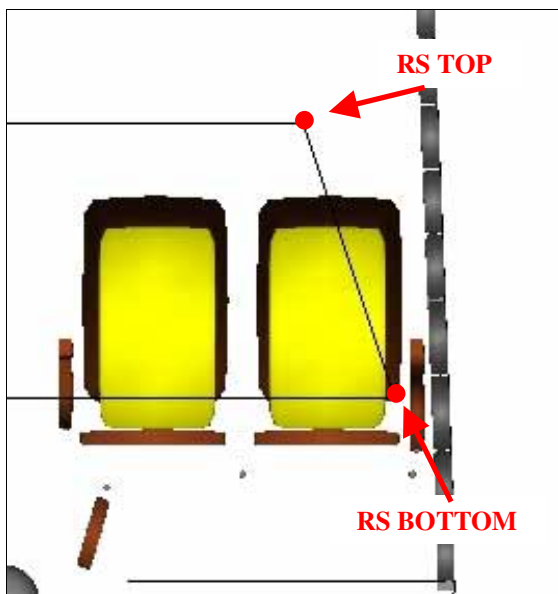


**Figure 30. Measurement points of the residual space intrusion**

During the simulations the distance between the structure and the residual space, defined as prescribed by the ECE 66 regulation, was measured in order to check if any displaced part of the structure intruded into the survival space. This distance was evaluated with respect to two different points of the residual space as shown in figure 30. The time histories of the distance between the structure and the above mentioned points of the residual space for the four tests are shown in figures 31 and 32.

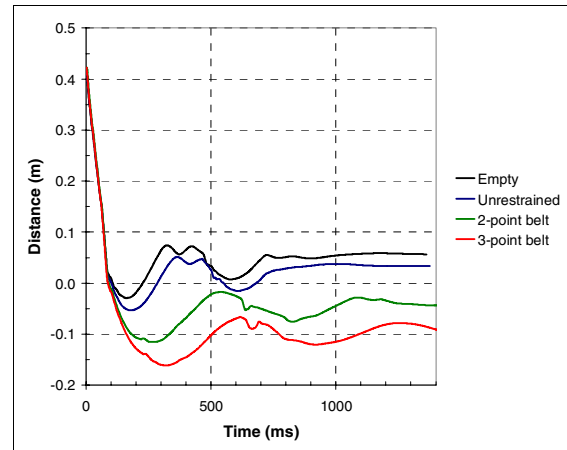


**Figure 31. RS top distance.**

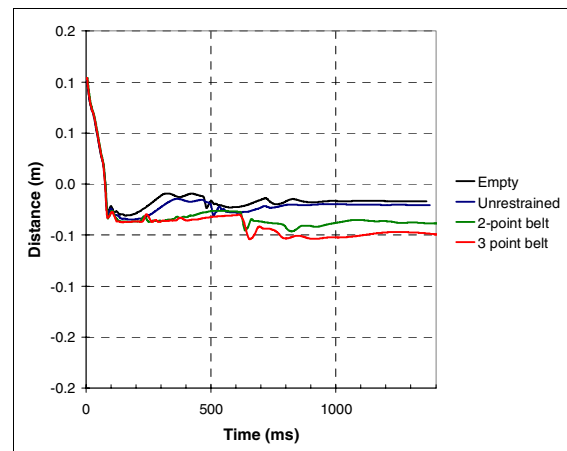


**Figure 32. RS bottom distance.**

The results reported in the figures show that the presence of the passengers on board affects the deformation level of the structure in a rollover. As expected the deformation raises by increasing the percentage of the passenger mass coupled to the structure. Even in case of unrestrained passengers, it was calculated an increment of the structural deformation.

#### **Increment of the structural strength**

Increasing the mass in the vehicle causes an increment of the structural deformation in the

rollover test. Therefore, if the presence of the passengers on board is considered in the homologation test, the energy assumed to be absorbed by the structure in order to pass the test increases. As a consequence a structure that fulfils the ECE66 rollover test requirements with no passengers on board, may not pass the same test if the presence of passengers is taken into account.

Taking as reference the rollover test carried out without passengers ('empty' plot in figures 31 and 32), the strength of the super-structure was incremented up to obtain with the passengers on board (ballast masses) the same minimum distance between the structure and the residual space as in the reference condition. To achieve an increment of the super-structure strength the window pillar strength characteristic in the MB model was multiplied by a factor greater than one.

The time history of the distance between the structure and the residual space for the three tests, empty (reference condition), belted passengers in a structure with reference strength and belted passengers in a structure with increased strength, are shown in figures 33 and 34.

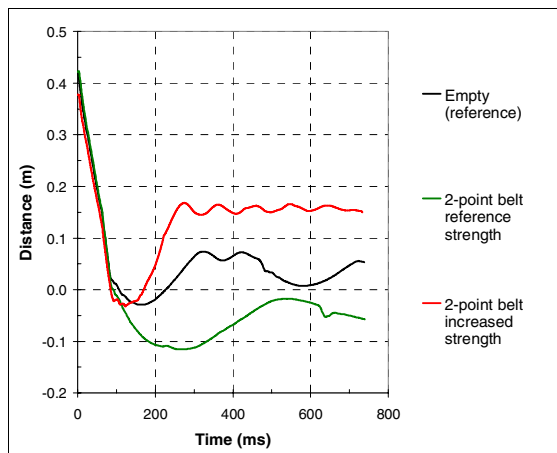


**Figure 33. Structure-residual space distance for 2-point belted passengers.**

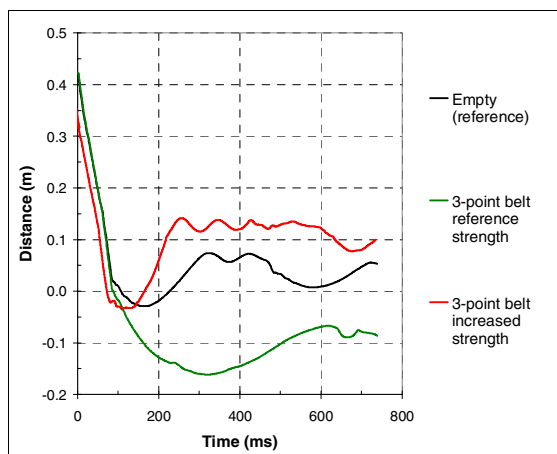


**Figure 34. Structure-residual space distance for 3-point belted passengers.**

## INJURY RISK FOR PASSENGERS

As discussed previously, if the presence of passengers on board is taken into account, it is necessary to increase the structure strength in order to obtain the same level of deformation as in the condition without passengers. Therefore a structure that fulfil the ECE66 rollover test requirements with no passengers on board, may need to be reinforced by increasing the strength characteristic of the window pillars to pass the a test with passengers on board. However a stronger structure often means a greater level of accelerations and forces on passengers. In order to evaluate the influence on the injury risk for passengers of an increment of structure strength, some simulations of an ECE66 rollover test with a passenger model on board were performed. In such simulations the ballast mass in position number 3 (near the aisle on the impact side) was replaced by the numerical model of a EUROSID-1 dummy while the other seats were still occupied by ballast masses. For each restraint system (two-point belt or three-point belt) used for the dummy, two different configurations were analysed (table 4).

**Table 4.**

**Tested configurations**

Dummy restraint system	Super-structure strength
Two-point belt	Reference
	Increased
Three-point belt	Reference
	Increased

In the first one, the reference (not reinforced) super-structure was tested, while in the second one the super-structure was reinforced so that the same maximum deformation (minimum distance between the structure and the residual space) was obtained as in the rollover test of the empty bay section.

For each simulation the most significant accelerations and loads on the passenger and injury parameters level were calculated. The results are shown in table 5 for the two-point belt condition and table 6 for the three-point belt condition

For a passenger seated in position 3 restrained with two-point belt the increment of structure strength, necessary to obtain with the passengers on board a level of deformation similar to the one of an empty bay section, yields a significant increment of the accelerations and loads on the passenger and leads to higher levels of injury parameters. The risk of injuries to head, thorax and pubic symphysis injuries rises considerably. On the other hand, for the same passenger restrained with a three-point belt the accelerations, the loads and the injury parameters are quite the same even if the strength of structure was increased. This happens because

the three-point belt better restrains the occupant to the seat avoiding, during the rollover, the impact of the passenger with the structure as discussed in [5].

**Table 5.**

**Body loads and injury parameters for a two-point belted passenger**

	Reference strength	Increased strength
Head acceleration (m/s <sup>2</sup> ) (CFC1000)	1841	<b>2873</b>
HIC (CFC1000)	1701	<b>2886</b>
Force lower neck (N)	4187	<b>7074</b>
Moment lower neck (Nm)	142	<b>175</b>
Upper rib acceleration (m/s <sup>2</sup> ) (CFC180)	650	<b>795</b>
Middle rib acceleration (m/s <sup>2</sup> ) (CFC180)	658	<b>777</b>
Lower rib acceleration (m/s <sup>2</sup> ) (CFC180)	676	<b>773</b>
TTI (FIR100)	44	43
Force lower lumbar (N)	7285	<b>8337</b>
Moment lower lumbar (Nm)	254	276
Force pubic symphysis (N)	7285	<b>8337</b>

**Table 6.**

**Body loads and injury parameters for a three-point belted passenger**

	Reference strength	Increased strength
Head acceleration (m/s <sup>2</sup> ) (CFC1000)	339	342
HIC (CFC1000)	78	91
Force lower neck (N)	1776	1745
Moment lower neck (Nm)	113	118
Upper rib acceleration (m/s <sup>2</sup> ) (CFC180)	417	375
Middle rib acceleration (m/s <sup>2</sup> ) (CFC180)	315	319
Lower rib acceleration (m/s <sup>2</sup> ) (CFC180)	294	295
TTI (FIR100)	31	32
Force lower lumbar (N)	4089	3750
Moment lower lumbar (Nm)	216	193
Force pubic symphysis (N)	4089	3750

## CONCLUSIONS

The work performed within the ECBOS project showed that the current regulation about passenger safety in the rollover an M3 class coach should be improved. The presence of passengers on board should be taken into account in the regulation. Moreover it is necessary to describe accurately the structural behaviour of the seat during the rollover as the correct description of the seat deformation is fundamental in order to evaluate properly the movement of the passenger inside the vehicle. A correct assessment of the passenger movement is necessary to evaluate properly the loads and the injury risk for passengers.

The performed simulations showed that an increment of the mass in the vehicle causes greater deformations in case of rollover. Therefore a structure that fulfils the ECE 66 rollover test requirements with no passengers on board, may not pass the same test if the presence of passengers is taken into account. That may lead to build stronger structures to fulfil the requirement of no intrusion into the survival space stated in the regulation.

The calculations showed that a more rigid structure may cause higher levels of injury on passengers if an inadequate restraint system is adopted. For this reason an improved regulation about safety in the rollover of a M3 class coach should include the adoption of restraint systems on board together with homologation tests in which the additional mass of passengers is taken into account. In particular three-point belts should be prescribed as such kind of restraint system offers, on the average, a good level of protection in rollover events.

As general outcome of this work and of the work performed within the ECBOS project, it is very important to highlight the necessity to update the safety levels of coaches and buses to the ones reached in the automotive field. Therefore, also for buses and coaches, dynamic tests with dummies on board should adopted to evaluate the safety level of the vehicles. Moreover, not only a limit to the structure deformations (survival space), but also restrictions to the loads and the accelerations (injury parameters) on occupants should be prescribed to obtain the vehicle homologation

## REFERENCES

- [1] F. Aparicio, A. Garcia, T. Vicente, V. Martinez, J. Paez, L. Martines, G. Fernandez, ECBOS Workpackage 4 Task 4.1 "Suggestion for new regulations and written standards" Final Report, European Union, June 2003.
- [2] [1] A. Kirk, R. Grant, ECBOS Workpackage 1 Task 1.1 "Statistical collection" Final Report, European Union, 2001.

- [3] ECE 66 Regulation “Uniform provisions concerning the approval of large passenger vehicles with regard to the strength of their super-structure” Economic Commission for Europe, Geneva 1986.
- [4] Directive 2001/85/EC “Special provisions for vehicles used for the carriage of passengers comprising more than eight seats in addition to the driver's seat”, European Union, 2001
- [5] G. Belingardi, D. Gastaldin, P. Martella, L. Peroni, “Multibody analysis of M3 bus rollover: structural behaviour and passenger injury risk” Proceeding of 18th International Technical Conference on the Enhanced Safety of Vehicles (ESV), Nagoya (Japan), 2003.
- [6] P. Martella, “The multibody approach in crash analysis. Study of the passive safety in the rollover of an M3 coach” Ph.D Thesis, April 2004
- [7] M. Matolcsy “Plastic hinge theory to analyse the structural strength and energy absorption of bus structures”, Proc. Int. Conf. Science and Motor Vehicles, Belgrade, 1987.
- [8] J.C. Anderson, “Rollover crashworthiness of a new coach structure”, Cranfield impact centre Ltd., Truck and Bus Meeting and Exposition, Portland (Oregon), 4-6 December 2000.
- [9] J.C. Anderson, ECBOS Workpackage 3 Task 3.3.1 “Full-scale test methods; extended rollover test” Final Report, European Union, 2002.
- [10] J. Ambrósio, M. Pereira, “Multibody Dynamics Tools for crashworthiness and impact”, Crashworthiness of transportation systems: structural impact and occupant protection, NATO Advanced Study Institute, vol. 1, pp. 437-484, Tróia (Portugal), 7th-19th July 1996
- [11] D. Twisk, C.G. Huijskens, ECBOS Workpackage 2 Task 2.1 “Seat Component and Frontal Impact Baseline Testing” Final Report, European Union, 2001.
- [12] ECBOS Workpackage 2 Task 2.5 “Cause of injury summary” Final Report, European Union, 2002.
- [13] J.C. Anderson, ECBOS Workpackage 2 Task 2.1 “Free Motion Headform Testing on Interior Components of Coaches, City-buses and Minibuses” Final Report, European Union, 2001.